AN EVALUATION OF SPECTRUM-COMPATIBLE ACCELEROGRAMS FOR NONLINEAR ANALYSIS OF SHORT-PERIOD STRUCTURES LOCATED IN EASTERN CANADA

A Thesis presented to the

Department of Civil Engineering and Applied Mechanics

McGILL University

for the Partial Fulfillment of the

Degree of Master of Engineering

by

Abdelkader Kamel TAYEBI

February 1994

ISBN 0-315-99985-3

To My Very Dear and Beloved Parents

Abstract

Smooth design spectra are generally used to describe the seismic excitation provided by the maximum design earthquake for safety evaluation of critical facilities located in Eastern Canada. However, a comprehensive study of the inelastic behaviour of critical structural systems requires step-by-step inelastic analysis in the time domain.

This thesis presents a study of inelastic seismic analysis of short-period structures subjected to ground motion acceleration time histories compatible with Eastern Canadian conditions and defined (i) from historical records scaled to the smooth design spectrum intensity, (ii) from spectrum-compatible accelerograms generated by random vibration theory, and (iii) from the modification of the Fourier Spectrum coefficients of historical records while preserving the original phase angles. The ductility demand, the input energy, the hysteretic energy, the number of yield events, and other performance indices, are examined in parametric analyses to identify the type of earthquake motions that is critical for earthquake resistant design of ductile short-period structures. The linear and cracking responses of concrete gravity dams of three different heights (90m, 45m, and 22.5m), that exhibit a brittle response to strong ground shaking, are also examined for the different types of sprectrum-compatible accelerograms. It is generally concluded that in the absence of suitable spectrum-compatible historical accelerograms, either historical records with modified Fourier spectra or synthetic records can be used to evaluate the linear structural response. For nonlinear analysis, historical records with modified Fourier amplitude spectra tend to produce closer results to those obtained from real earthquakes for cumulative damage indices, as compared to the results computed from synthetic accelerograms.

Résumé

Des spectres de dimensionnement lissés sont généralement utilisés pour décrire l'excitation sismique produite par le tremblement de terre maximum pour l'évaluation de la sécurité d'aménagements critiques situés dans l'est du Canada. Cependant une étude approfondie du comportement inélastique de systèmes structuraux critiques demande une analyse inélastique pas-à-pas dans le domaine du temps. Cette thèse présente une étude du comportement inélastique de structures ayant de courtes périodes soumises à des secousses sismiques compatibles avec les conditions rencontrées dans l'est du Canada et obtenues (i) à partir de tremblements de terre historiques étalonnés sur l'intensité spectrale du spectre de dimensionnement, (ii) à partir d'accélérogrammes obtenus de vibrations aléatoires et compatibles avec le spectre de dimensionnement, et (iii) à partir de la modification des coefficients du spectre de Fourier de tremblements de terre historiques tout en préservant les angles de phase. La demande en ductilité, l'énergie d'excitation, le nombre d'évènements de plastification et d'autres indices de performance, sont examinés dans des études paramétriques afin d'identifier le genre de secousses sismiques qui est critique pour la conception parasismique des structures ductiles avec de courtes périodes. Les réponses linéaires et la fissuration de barrages poids en béton de trois hauteurs différentes (90m, 45m et 22.5m) qui démontrent un comportement fragile sous des secousses sismiques intenses sont aussi examiées pour les différents types d'accélérogrammes compatible avec le spectre de dimmensionnement.

Il a été généralement conclu qu'en l'absence d'accélérogrammes historiques adéquatement compatible avec le spectre, on peut soit utiliser des enregistrements historiques avec spectre de Fourier modifiés, ou des accélérogrammes synthétiques, afin d'évaluer la réponse structurale linéaire. Pour les analyses nonlinéaires, des enregistrements historiques avec spectres de Fourier modifiés tendent à produire des résultats qui sont plus proches de ceux obtenus de tremblements de terre réels pour les indices cumulatifs d'endommagement, en comparaison avec les résultats calculés à partir d'accélérogrammes synthétiques.

Aknowledgements

The author wishes to thank Professor Pierre LÉGER for his countinuous help and encouragement, and his valuable suggestions and advices without which this report would not have been completed. The author also thanks : Mr. Arshad Khan and Mr. Sudip Bhattacharjee for their very friendly help, and for the very good time the author had with them. Professor Patrick Paultre is also thanked for his helpful comments. The author is very thankful and grateful to his parents who supported him by all possible means in all aspects of his life. Finally, the author wishes to thank the Algerian Ministry for higher education for their financial support for the prepared degree, as well the staff of the Algerian Embassy at Ottawa for their services.

Contents

List of Figures

List of Tables

Chapter 1

Introduction

1.1 Overview and previous work

Although critical facilities with relatively stiff structural systems such as nuclear containment structures and concrete dams have an excellent historical seismic safety record, only a few of these structures have actually experienced significant shaking, and none has been actually subjected to the maximum conceivable design earthquake ground motion. Thus, the seismic performance of existing, as well as new, short-period critical facilities built in active seismic regions must be evaluated to ensure an adequate response under the maximum ground motion that may occur at the site. The basic steps to be considered in the seismic evaluation procedure are:

(i) the definition of the expected seismic excitation at the site,

(ii) the evaluation of the structural response under the prescribed seismic excitation,

(iii) the comparison of the predicted structural response with suitable performance criteria characterising the strength and deformation capacity of the structure.

The expected seismic excitation at a site is generally defined in terms of a smooth design spectra. Since the structural systems are expected to respond in the inelastic range

under the maximum credible earthquake, ground motion acceleration time histories must be specified as input if a comprehensive seismic safety evaluation is to be performed using step-by-step nonlinear analyses in the time domain. Due to the sensitivity of the structural response to the details of the ground acceleration time histories, and the inability for a single record to induce the dynamic response amplification corresponding to the level assumed in the design over all significant frequencies, a suite of suitable input accelerograms should be considered to determine an average response. The input accelerograms can be defined from proper historical records scaled to the smooth design spectrum intensity, or from generated spectrum-compatible accelerograms. These are the time domain equivalent to the smooth design spectra. Different procedures could be used to construct spectrum-compatible input accelerograms for nonlinear seismic analyses.

A first approach consists in starting from a real acceleration time history, convert it to the frequency domain to adjust some of the Fourier amplitudes while preserving the original phase angles. This procedure is used to correct for the observed spectral deficiencies in matching the smooth spectra in the frequency range of interest. The inverse Fourier transform is then used to obtain the spectrum-compatible acceleration time history. However, the seismological significance of the resulting ground acceleration is questionable since it is no longer related to a real earthquake. Alternatively, stochastic acceleration time histories can be developed using unfiltered, filtered, stationary, and nonstationary white noise signals from random vibration, or seismological source models techniques. Stochastic time histories, that are generally able to provide very good spectrum-compatibility, have been found to often exhibit excessive numbers of acceleration pulses and unrealistic phase relationships (Christian 1988, USCOLD 1985, Shaw et al. 1975). Several authors do not recommend to use them for nonlinear analysis. Christian (1988) argued that they do not include the aspects of ground motion, such as the changes of the frequency content over time, that cannot be described by random vibration theory, especially in the computation of cumulative sliding displacement. He also added that the generated spectrum is generally higher than the target spectrum, which leads to some conservatism, and that the spectral shape is an artificial one resulting from statistical analysis, that is impossible to match for all frequencies and for all values of damping equally. The USCOLD 1985 does not recommend to use stochastic accelerograms for any

type of nonlinear analysis, however it says that concrete dams, for example, are less sensitive to them than embankment dams which sensitive to the number of induced stress cycles rather than peak stress values. However, other researchers have used stochastic time histories for inelastic analysis and report satisfactory results in terms of maximum ductility demand and hysteretic energy dissipation (Barenberg, 1989; Pal et al. 1987). Vanmarcke and Gasparini (SIMQKE, 1976) say that stochastic models of ground motion are sufficiently accurate for the purpose of seismic response prediction, for all but certain nonlinear systems. Penzien and Ruiz (PSEQGN, 1969) reported satisfactory results after using stochastic input motions in nonlinear analysis of a low-rise shear type building. FEMA (1985) prefers the use of real earthquakes to the use of synthetic time histories, however it says that the modified ground motions (wether the modification is made by adjustment of the Fourier amplitude spectrum or by the connection of segments of selected historical records) are the most commonly used sources of ground motion time histories for dynamic analyses, especially when there is a lack of recorded data. Chopra and Lopez (1979) showed that the stochastic motions led to maximum displacements as far as twice those resulting from real records, and have dissimilar average response spectra.

Thus, there is a controversy in the selection and definition of appropriate input accelerograms to investigate the inelastic seismic response of structural systems.

1.2 Objectives

The objectives of this thesis is to compare the inelastic response of short-period structures, with elastic fundamental periods, T_1, smaller than 0.5 sec, subjected to real and spectrum-compatible earthquakes rich in high frequency motion which is a characteristic of Eastern North America earthquakes (ENA). This study will thus permit to investigate the influence of either historical, Fourier modified, or synthetic accelerograms on the seismic response of ENA structures. The spectrum-compatible accelerograms are generated (i) by scaling historical records, (ii) from actual records by adjusting the Fourier amplitude spectra, or (iii) by using filtered white noise. It is assumed that the short- period structures are located in Quebec, where the recent 1988 Saguenay earthquake of magnitude M=5.9, with peak ground acceleration of the order of 10% g near the epicentre, was found to contain high

energy in the period range of relatively stiff structural systems (0.1 sec to 0.3 sec). Stiffness degrading and bilinear hysteresis models of single-degree-of-freedom systems (SDOF) with different strength have been selected to represent the short-period structures considered in this study. Several indicators such as the ductility demand, indexes related to the amount of energy dissipation, and the number of zero crossings and yield excursions, have been computed to characterize the structural response. Various scaling methods (SM) have been investigated to minimize the difference between the elastic response spectra of the historical records and the target spectrum. Also the deficiency of Western earthquakes in high frequency motion as compared to Eastern earthquakes was investigated, as well as the validity of the use of Western records to analyze or design Eastern sites.

1.3 Scope of the present study

The present study is divided in four sections. In a first section (Chapter 2), general rules of assessment of seismic hazard are described as well as the most important ground motion parameters affecting the structural response. A credible scenario for short period structures in Eastern Canada is also defined, this definition includes the choice of suitable attenuation functions for the region and the definition of peak ground motion values and response spectrum. In a second section (Chapter 3), a set of historical records compatible with the credible scenario, is selected, and various scaling methods are investigated. Methods of generating spectrum-compatible time histories are discussed, and a number of artificial records are generated and their properties discussed. In a third section (Chapter 4), the response of SDOF systems to the selected and generated records is investigated and some conclusions are made. In a fourth section (Chapter 5), a special case of short period structures, concrete gravity dams, is studied and observations are made on some overall response to the different type of accelerograms considering linear elastic behaviour and the nonlinear fracture seismic analysis.

Finally, Chapter 6 ends this thesis by summarizing the work done, and giving some conclusions and recommendations for future work.

Chapter 2

Seismicity of Eastern Canada

2.1 Causes and history of seismicity in Eastern Canada

Seismicity in Eastern Canada is characterized by plate margin earthquakes in the extreme East, and intraplate earthquakes in the South-East (St. Lawrence valley). These earthquakes are due to the continuous opening of the mid-Atlantic ridge and the slow movement of the North American plate, which activate zones of weakness and faults (Adams et al., 1989). Table 2.1 summarizes the major earthquakes that occurred in Eastern Canada. Appendix A explains the difference between the magnitude definitions reported in Table 2.1. Figure 2.1 (adapted from Tinawi et al. 1990) shows the distribution of earthquake epicenters in this region.

2.2 Seismic zonation

Seismic zonation is the key for any seismic hazard analysis. The most recent Canadian seismic zonation maps are those drawn by Basham et al. (1985) based on geological evidence and historical seismicity, and those of the Canadian Electrical Association (CEA) which are a modified version of Basham's maps, based on new interpretation of the seismicity of Eastern Canada (CEA vol. C-2 1990). Figure 2.2 shows the seismic zonation

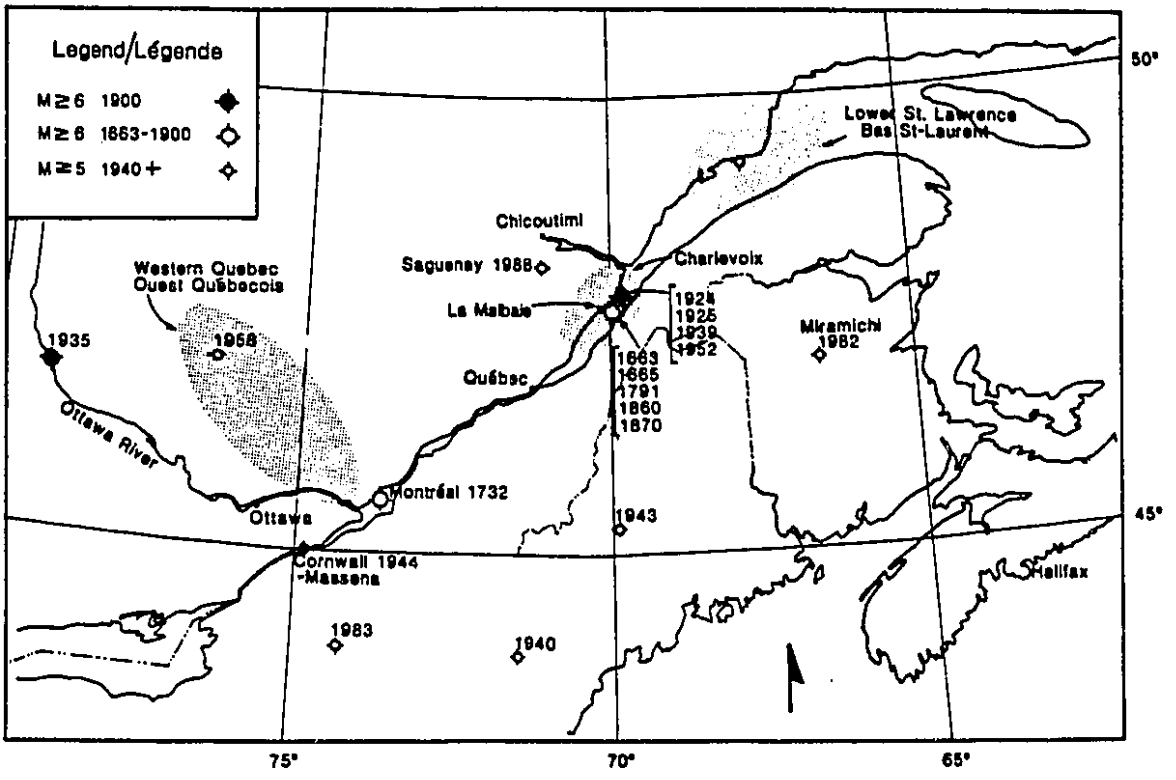

Figure 2.1: Distribution of earthquake epicenters in Eastern Canada (adapted from Tinawi et al. 1990).

used in this study as given by the CEA. Table 2.2 summarizes the earthquake magnitudes assigned to each zone.

2.3 Ground motion parameters

The seismic input to design or evaluate a structure, is defined in terms of magnitude, distance and ground motion parameters. The latter are generally the motion peak values, the frequency content, and the duration. The most commonly used parameters are the peak ground acceleration (PGA), and the peak ground velocity (PGV), however these parameters do not correlate well with the intensity of the structural response or damage potential of input motions. One of the best representation of the severity of a ground

Earthquake	Date	Magnitude			
		M	m_b	M_s	m_{bLg}
Saguenay	1988	5.9	5.9	5.7	6.5
Miramichi	1982	5.5	5.8	5.1	5.7
Cornwall	1944	5.8	4.6	5.1	5.8
Charlevoix	1939	5.3	5.4	5.8	5.6
Temiscamingue	1935	6.4	6.1	6.0	6.3
Charlevoix	1925	6.8	6.7	6.4	6.6

Table 2.1: Historical Eastern Canadian earthquakes (adapted from North et al. 1989).

Zone	Mn	Mx
Zonation 1 (Fig. 2.2a)		
CHV-CHARLEVOIX	4.0	7.5
WQU-WESTERN QUEBEC	4.0	7.0
LSL-LOWER ST. LAWRENCE	4.0	6.0
NAP-NORTHERN APPALACHIANS	4.0	6.0
ATT-ATTICA	4.0	6.0
EBG-EASTERN BACKGROUND	4.0	6.5
Zonation 2 (Fig. 2.2b)		
OTT-OTTAWA VALLEY	4.0	7.0
QUO-QUEBEC OUEST	4.0	7.0
STL-ST. LAWRENCE VALLEY	4.0	7.5

Mn : Minimum magnitude to be used in a risk analysis
Mx : Maximum magnitude to be used in a risk analysis

Table 2.2: Seismic zonation in Eastern Canada and corresponding minimum and maximum earthquake magnitudes (adapted from CEA vol. C-2 1990).

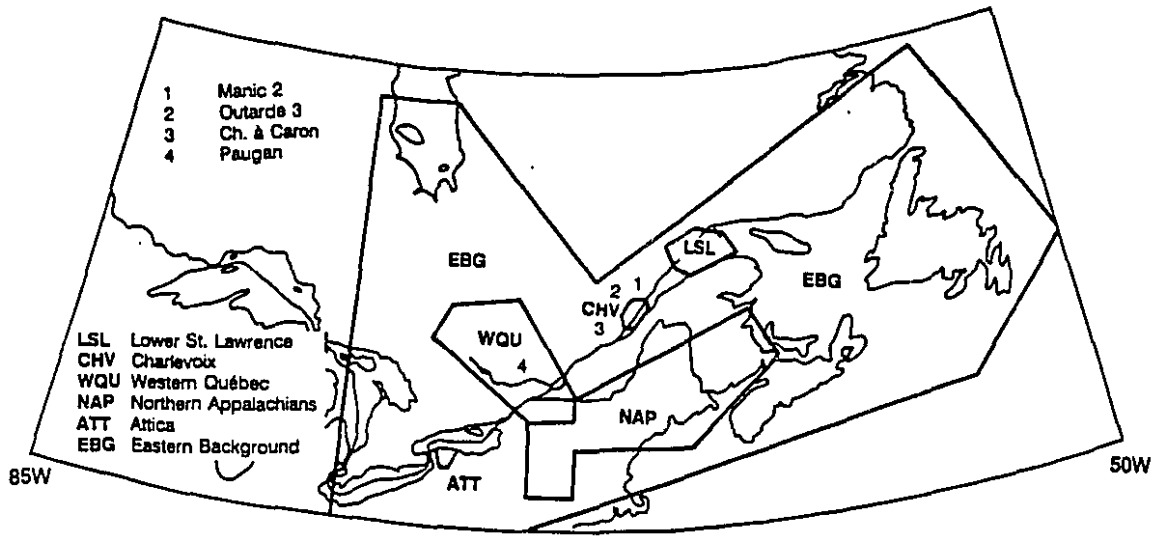

(a) Eastern Canada - Zonation 1

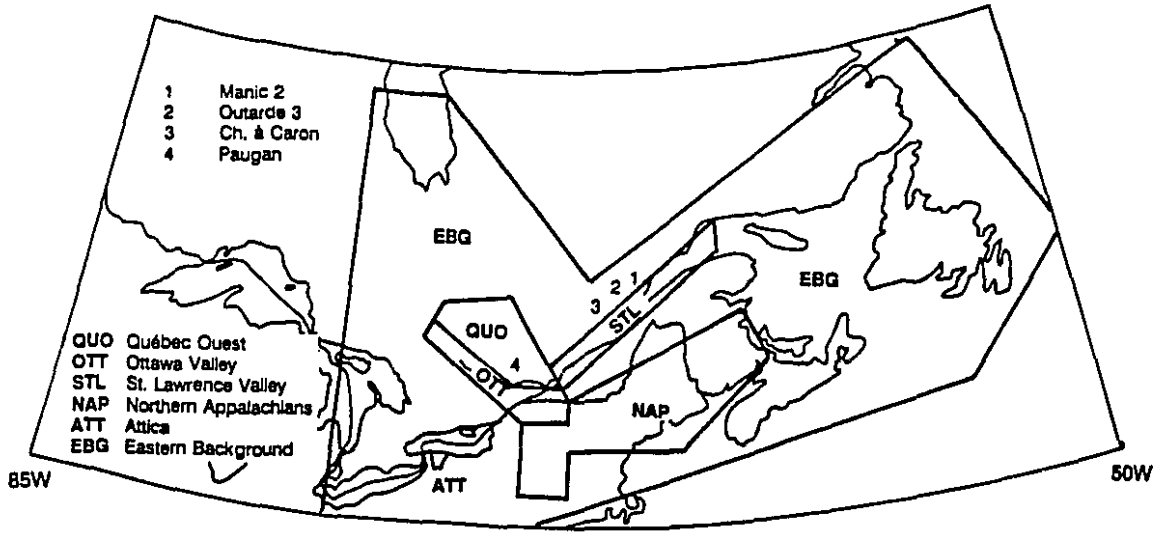

(b) Eastern Canada - Zonation 2

Figure 2.2: Seismic zonation of Eastern Canada

motion, from a structural point of view, is the response spectra.

2.4 Differences between ENA and WNA earthquakes

Due to the lack of strong motion records in the East, engineers tend to use Western records which are readily available. However, there exist many seismological differences between ENA and WNA earthquakes, but only few are of engineering interest (Nuttli 1981, 1987), they are summarized as follows:

(i) Source mechanism; the faults that cause earthquakes in the West are very well identified, in the East they are either unknown or of modest appearing.

(ii) Frequency content and attenuation of wave energy; the main characteristic of Eastern earthquakes is their richness in high frequency motions which are maintained for some hundreds of kilometers from the source region. Besides the greater attenuation at high frequencies of Western earthquakes, their source spectra are relatively deficient in high frequency motion.

(iii) Frequency of occurrence; large magnitude earthquakes occur five to ten times more often in the West than in the East.

(iv) Duration; because of differences in attenuation and in the relation between magnitude and seismic moment, Eastern earthquakes tend to be shorter than their Western counterparts for a same magnitude.

2.5 Attenuation relationships for ENA earthquakes

After assuming a credible magnitude-distance scenario, it is required to determine how the ground motion will travel from the assumed source to the site of interest, especially if a probabilistic-risk analysis is performed. This problem is solved by the use of appropriate

attenuation functions, which are mathematical expressions relating the seismic parameters to the magnitude of the earthquake and the distance to the source. Due to the small amount of strong motion records in Eastern Canada, most of these relationships have been built upon theoretical models and checked with the available data (mostly compiled from minor or moderate earthquakes). For Eastern Canada the following attenuation functions may be applicable :

(i) Hasegawa et al. (1981) ; these relations are derived from Western U.S data and intensity data from Eastern and Western Canada. These relations give PGA and PGV (Table 2.3a).

(ii) Nuttli and Hermann (1984,1987) ; these relations are derived from Eastern and central U.S data recorded on soft soil. These relations give PGA, PGV and peak ground displacement (PGD) (Table 2.3b).

(iii) McGuire (EPRI 1988) ; these relations are derived from a theoretical model (random vibration theory) and checked with available Eastern data. They give PGA and Pseudo-spectral velocity (PSV) coordinates (Table 2.3b).

(iv) Atkinson and Boore (1990) ; these relations are derived from a theoretical model (random vibration theory) and checked with available Eastern data. They give PGA, PGV and PSV ordinates (Table 2.3c).

Depending on the type of the soil at the site one may choose any of these relations. However one should pay great attention to the magnitude type (M, m_b, M_s, m_{bLg}...) and to the distance (hypocentral or epicentral). Though the Hasegawa model has been partly derived from Western data, the predicted PGA's correlate well with the mean PGA's (average of two horizontal components) of observed data obtained from the 1988 Saguenay earthquake (recorded on bedrock) for intermediate to far field epicentral distances (40-180 km, Fig. 2.3a). Nuttli and Hermann relations can be used only for sites with soft soil, however they also give a good correlation with the Saguenay earthquake (Fig. 2.3a), but in a much more conservative way for most of the sites. Compared to the Saguenay earthquake PGA's, McGuire (1988), and Atkinson and Boore (1990) relations describe poorly the attenuation of PGA of the Saguenay earthquake, however the computed response spectra

(RS) by these relations are in a pretty good agreement with the RS of real data for sites 16 (Chicoutimi- North) and 17 (St. Andre), that are the closest sites to the epicenter (Fig. 2.3b, 2.3c) in the period range of interest (short-period structures, T=0.1-0.5 sec).

From these attenuation laws one should choose the ones that best describe the parameters that influence the seismic response. Although the calibration on a single event is not enough to ensure the validity of a model, the McGuire (1988) and Atkinson and Boore (1990) models will be retained for Eastern Canadian environment for their good correlation with the observed 1988 Saguenay earthquake RS (which influences the seismic response more than the PGA). Comparing Atkinson and McGuire laws for a constant magnitude (Fig. 2.3d, Fig. 2.5, and use of equations), we observe that Atkinson parameters are higher than McGuire for very near-field distances (15 km) and vice versa beyond 20 km. Because of the uncertainties included in any attenuation law, one should use these functions in a conservative way. Therefore Atkinson laws may be used for distances closer than 20 km and McGuire laws for distance beyond that limit.

2.6 Spectrum Intensity

To characterize the intensity of the response spectrum obtained either from historical record, attenuation function, or artificial accelerograms, the spectrum intensity was defined by Housner as the area under the pseudo-velocity spectrum for 40% of critical viscous damping, between the periods of 0.1 and 2.5 seconds. Other definitions have been used depending on the frequency range and the damping of interest. For short-period structures, such as concrete dams, Tarbox (1979) and Von Thun et al. (1988) suggested that a good indicator of the potential severity of the seismic structural response can be defined in terms of an acceleration spectrum intensity, $SI_{a(.10)}$, computed from the area under the pseudo- acceleration spectrum between the periods 0.1 and 0.5 seconds for 5% damping. Figures 2.4 (adapted from Von Thun et al. 1988) and 2.5 show the relationship between $SI_{a(.10)}$ and the causative fault distance for several historical events recorded on rock in the United States and Europe, as well as some data related to the Nahanni earthquake (1985), an event retained to be representative of Eastern Canadian seismo-tectonic environment (Heidebrecht and Naumoski, 1988), and data derived from the McGuire (EPRI 1988), and

Hasegawa et al. (1981)

PGA (cm sec^{-2})=3.4 exp(1.3 M) $R^{-1.1}$
PGV (cm sec^{-1})=0.00018 exp(2.3 M) $R^{-1.0}$
M = m_b, R = hypocentral distance

Table 2.3a : Hasegawa et al. attenuation relationships for Eastern Canada (1981)

Nuttli and Hermann (1987), McGuire and Toro (1988)

$Ln(y) = a + b\, m_{bLg} + c\, Ln(R) + d\, R$
M = m_{bLg}
R = hypocentral distance
y = seismic parameter

y	a	b	c	d
Nuttli and Hermann:				
PGA	1.31	1.15	-0.83	-0.0028
PGV	-8.29	2.30	-0.83	-0.0012
PGD	-15.66	3.45	-0.83	-0.0005
McGuire and Toro				
PGA	2.55	1.00	-1.00	-0.0046
PSV (25 Hz)	-1.63	0.98	-1.00	-0.0053
PSV (10 Hz)	-1.55	1.05	-1.00	-0.0039
PSV (5 Hz)	-2.11	1.20	-1.00	-0.0031
PSV (2 Hz)	-4.65	1.63	-1.00	-0.0023
PSV (1 Hz)	-7.95	2.14	-1.00	-0.0018

Table 2.3b : Nuttli and Hermann, and McGuire and Toro attenuation relationships for ENA (1988).

Atkinson and Boore (1990)

$\log y = a + b\,(M-6) + c\,(M-6)^2 - \log r + k\, r$
y = seismic parameter
M = m_{bLg} $4.5 < M < 7.5$
r = epicentral distance $10 < r < 400$ km

y	a	b	c	k
PGA	3.49	0.54	0.00	-0.00281
PGV	1.91	0.85	0.04	-0.001131
PSV (0.2 Hz)	1.36	1.21	0.09	-0.00034
PSV (0.5 Hz)	1.83	1.17	-0.18	-0.00037
PSV (1.0 Hz)	2.04	0.93	-0.16	-0.00064
PSV (2.0 Hz)	2.10	0.71	-0.08	-0.00102
PSV (5.0 Hz)	2.04	0.58	0.01	-0.00170
PSV (10.0 Hz)	1.95	0.54	0.01	-0.00250
PSV (20.0 Hz)	1.81	0.53	0.01	-0.00350

Table 2.3c : Atkinson and Boore attenuation relationships for ENA (1990).

Table 2.3: Numerical expressions of the attenuation laws

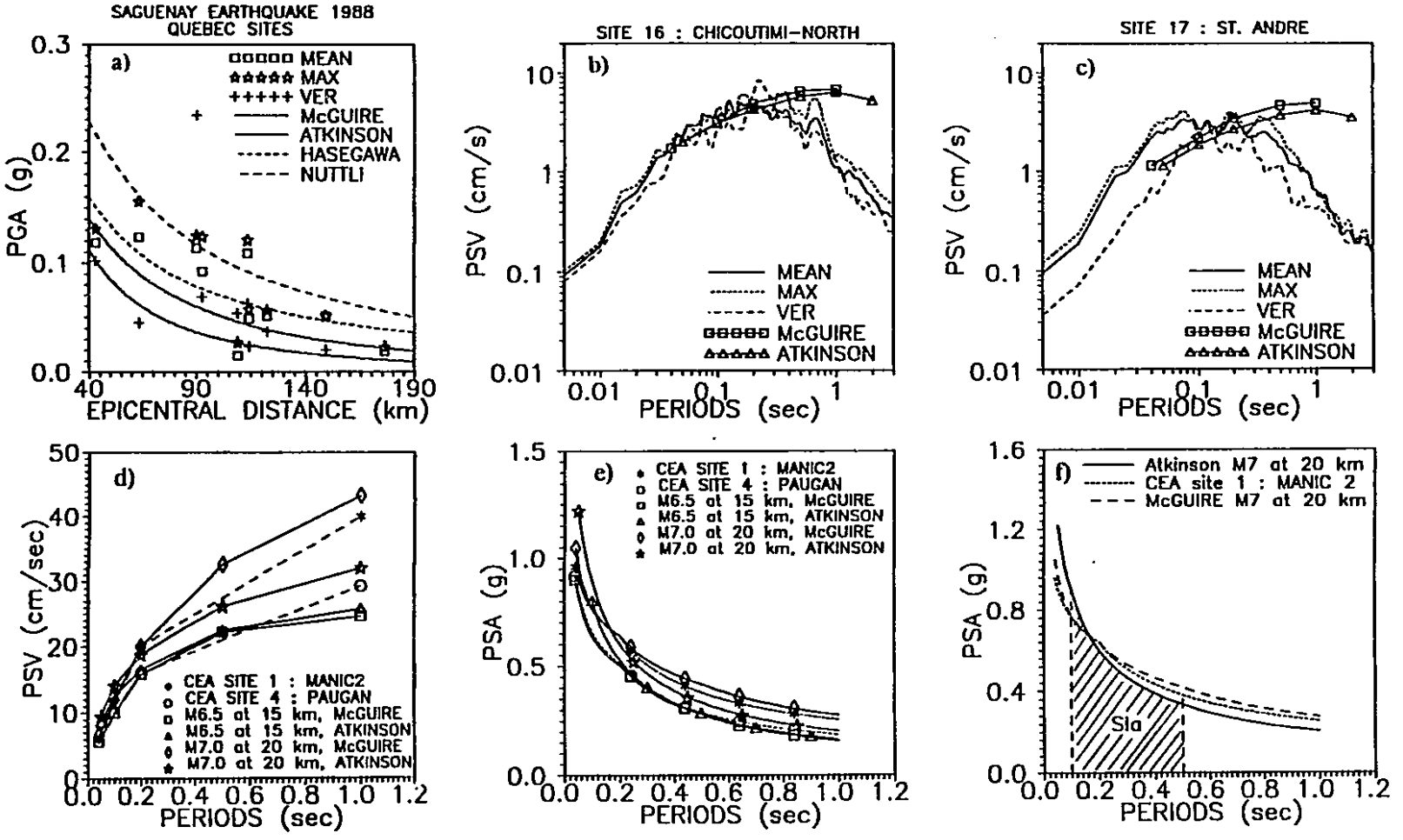

Figure 2.3: Practical use of attenuation laws

Atkinson and Boore (1990), attenuation relationships for Eastern north America (ENA). The $SI_{a(.10)}$ attenuation curves drawn by Von Thun et al. (1988) are upper bounds estimates rather than actual attenuation laws, and they may be too conservative. The attenuation relationships for magnitudes 7.0 and 7.5 are not based on any data and cannot be relied on. Overall, the added data satisfies well below the upper bounds lines drawn by Von Thun et al. (1988), except the Atkinson laws which tend to be higher for distances less than 15 km. Eastern earthquakes are richer in high frequency motions than their Western counterparts, and a significant portion of the area under the PSA spectrum is located between $T = 0.04$ sec and $T = 0.1$ sec, and therefore is neglected in the evaluation of the $SI_{a(.10)}$. To show the importance of the high frequency portion of the Eastern spectra, the lower integration limit of the integral in the SI_a was lowered to T=0.04 sec to obtain $SI_{a(.04)}$ (generally the spectrum starts decreasing towards the PGA value at a frequency close to 0.033 sec). This new definition was applied to the former Eastern attenuation laws as well as to a Western attenuation law from Crous et al. (Joyner and Boore 1988), since these laws are the only ones giving spectral values for periods lower than 0.1 sec, all others start at 0.1 sec. These attenuation functions are derived from southern Californian earthquakes recorded on soil deposits of 60 m depth and are compared to modified McGuire laws for similar soil conditions, and to some historical Eastern and Western records. Table 2.4 shows the minimum and maximum percentage of increase in the $SI_{a(.04)}$ value. Seven sets of records and attenuation functions were analyzed, The first set included all bedrock Saguenay records, the second one included all Nahanni main event records, the third one included some U.S. West coast records (Loma Prieta 1989, San Fernando 1971: Lake Hughes and Pacoima, El Centro 1940, and Taft 1952), and the rest are attenuation functions for magnitudes ranging from 5.5 to 7.5, and for epicentral distances ranging from 10 to 30 km (it has to be noted that Atkinson laws start at 0.05 sec, therefore integration started at 0.05 sec instead of 0.04sec, but this does not affect the results and conclusions). Since Eastern records are rich in high frequency motion, it is therefore recommended, that for short period structures in ENA, the lower integral limit in the SI_a be lowered to 0.04 sec to obtain $SI_{a(.04)}$.

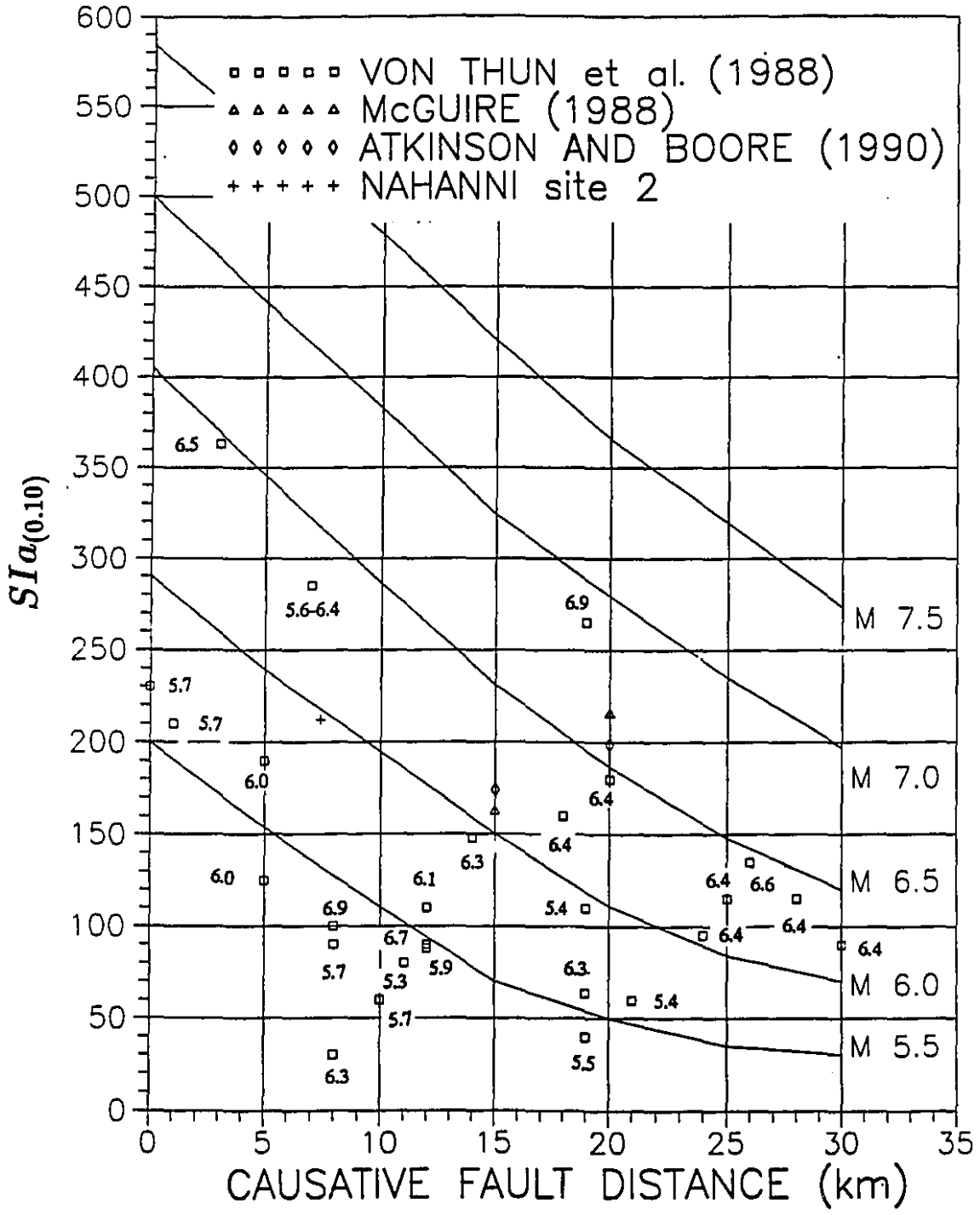

Figure 2.4: Von Thun et al. (1988) spectrum intensity attenuation laws.

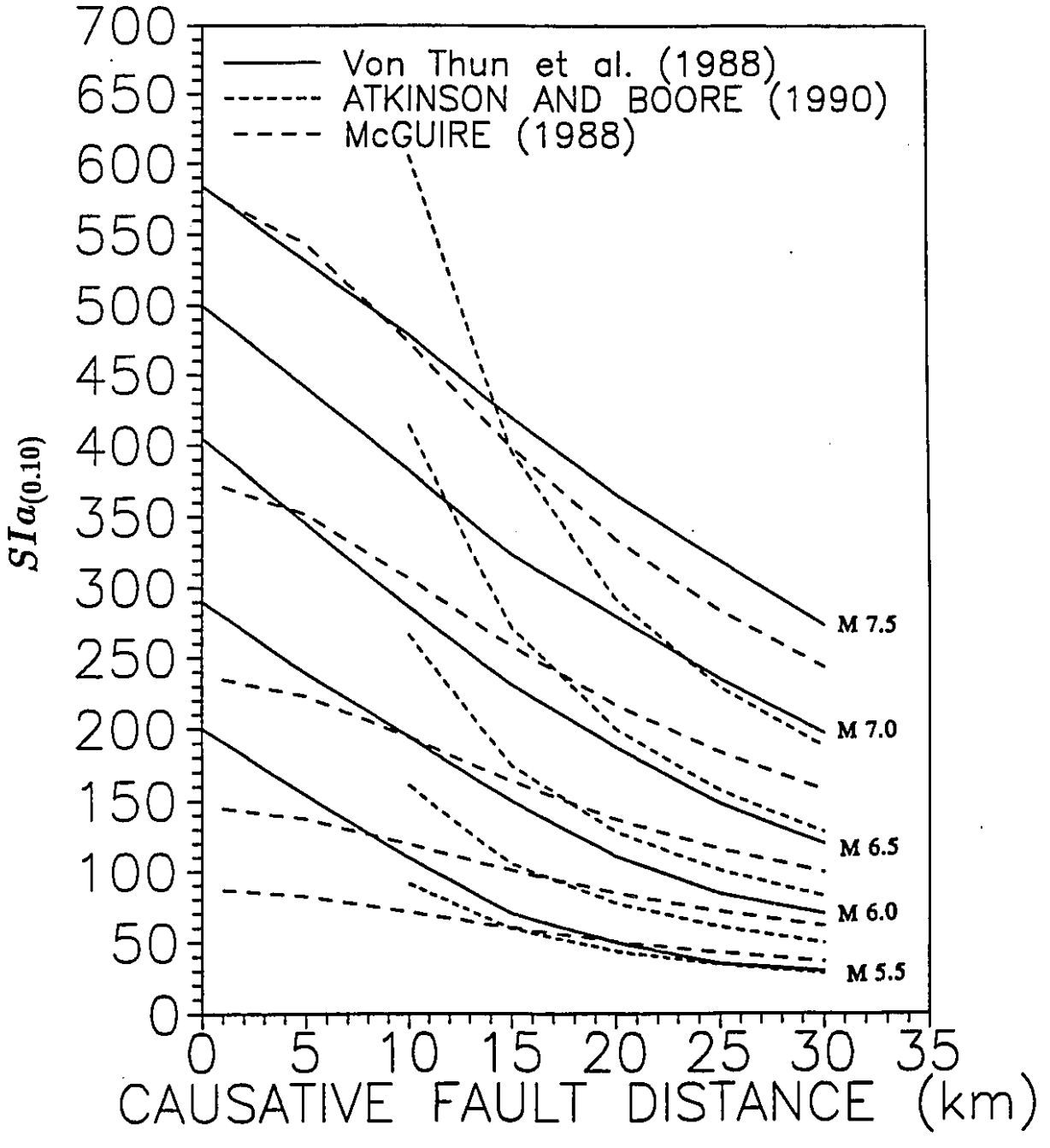

Figure 2.5: Comparison of Von Thun et al. (1988) spectrum intensity attenuation laws with equivalent ENA laws.

Set	Min increase (%)	case	Max increase (%)	case -
Saguenay records	16	Site 20 Long.	64	Site 17 Long.
Nahanni records	19	Site 1 Long.	48	Site 3 Long.
U.S. West cost records	07	Loma Prieta	14	San Fernando
McGUIRE laws	21	M=7.5 at 30 km	34	M=5.5 at 5 km
Atkinson laws	25	M=7.5 at 30 km	30	M=5.5 at 5 km
Crous et al. laws	08	M=7.5 at 30 km	12	M=5.5 at 5 km
McGuire laws for soft soil sites	18	M=7.5 at 30 km	38	M=5.5 at 5 km -

Table 2.4: Minimum and Maximum increases in SI_a value when the first integral limit is lowered from 0.1 sec. to 0.04 sec.

2.7 Duration

Another parameter of great importance is the duration of strong shaking, especially if a nonlinear analysis is performed and if materials sensitive to low-cycle fatigue are used. In this case, the damage potential is directly related to the number of yield cycles and thus to the duration. Many definitions have been proposed for the duration; three of them have been retained in this study, as given by Bolt (1973), Trifunac and Brady (1975), and McCann and Shah (1979) (Appendix B gives the detailed definition of each duration). There also exist empirical relationships relating duration to magnitude and distance, these relationships can give idea on the duration to be expected. For instance Dobry et al. (1978), based on Californian data, proposed the following relationship :

$$logD = 0.43M - 1.83 \tag{2.1}$$

with a standard deviation of 0.13, D being the duration and M the earthquake moment magnitude ($4.5 < M < 7.6$). Another empirical formula more applicable for ENA is :

$$D = M + 0.5R \tag{2.2}$$

where R is the epicentral distance in km (Atkinson personal communication, 1992).

2.8 Definition of ground motion parameters from seismic environment

The estimation of the ground motion that will occur at a specific site is a difficult task that requires the contribution of several specialists, such as geologists, geophysicists, seismologists, geotechnical and structural engineers. The first step to study is the regional geologic setting of the site. For a critical facility the area to be considered may have a radius of 100 to 300 km. This may include the identification of the tectonic zone where the site is located, the geologic history of the area, location of major folds, fractures, faults and their capability to generate earthquakes. The second step is the compilation of the seismic history of the region, by collecting all the available data with as much details as possible (epicenter, magnitude, date, type of faulting, etc..). This can be complemented by the determination of the rate of seismic activity. The third step is the processing of the local geological setting which includes the study of rocks and soil deposits, the assessment of location and chronology of nearby faults, determination of hydrogeological conditions and potential for slope failures, and precise inventory of earthquakes that occurred near the site and eventual records. After these steps, one can estimate the maximum credible earthquake (MCE) that can shake the area (which can be larger than the maximum historical events, if the period of time for which the historical seismicity is known, is shorter than the return period of the MCE), and the maximum design earthquake for which the critical facility has to be evaluated or designed. After deciding for the magnitude and distance of the maximum or design earthquake, it is required to assess the ground motion parameters of these events. This can be done in either a deterministic-statistical procedure, a semi-probabilistic procedure, or probabilistic-risk procedure.

2.8.1 Deterministic-statistical procedure

In this method, the seismic parameters are determined by the attenuation functions (that can be derived theoretically or empirically) that relate the seismic parameters to the magnitude and distance from the candidate causative fault; the combination of the magnitude and distance constitutes a credible scenario. Some attenuation relationships give only peak

ground values, others (generally most of the recent ones) give directly spectral ordinates, that can be used to compute the spectrum and choose the appropriate time histories. However the available attenuation functions include a large amount of uncertainties and may lead to conservative estimate of ground motion parameters in some cases. Alternatively, a set of records selected from a worldwide database, and satisfying magnitude (within ± 0.5), epicentral distance (within $\pm 10km$), and the geological conditions, is selected and a mean, or a mean plus one standard deviation, spectrum can be calculated, finally some of the time histories, that best fit this spectra and the peak values, are selected.

2.8.2 Semi-probabilistic (seismotectonic) procedure

In many regions earthquakes cannot be related to faults, which adds another degree of uncertainty in estimating the epicentral distance. This method requires the knowledge of seismic zones and microzones of the region. A maximum credible earthquake is defined for each microzone (this event may well exceed the maximum historical event), and then the methodology described for the deterministic method is applied.

2.8.3 Probabilistic-risk procedure

This procedure combines the seismic hazard with the probability of exceedence of certain seismic parameters, at a specific site, during a specified interval of time (annual probability of exceedence). This method has the particularity of accounting for the frequency of occurrence of earthquakes and dealing with uncertainties by assigning them adequate probabilities. In this procedure, seismic sources may be modeled by known active faults or seismically active point sources or seismic zones or microzones where the seismic activity is assumed to be randomly distributed. Attenuation relationships are required, and earthquakes are assigned an equal probability of occurrence at any location in a zone and at any time which allows the use of the Poisson's model. The probability distribution of earthquake magnitude is based on the well known Gutenberg-Richter magnitude-recurrence relationship :

$$logN(m) = a - bm \tag{2.3}$$

where $N(m)$ is the number of earthquakes in a given time interval having magnitudes greater than m, 10^a is the number of earthquakes above the magnitude zero, and b is the relative rate of occurrence of earthquakes with different magnitudes.

The annual probability of exceedence is the product of three main probabilities :

(i) The probability that a particular event of a certain magnitude will occur in a specified period of time;

(ii) the probability that the source of that event will be located at the specified epicentral distance;

(iii) the probability that the ground motion parameter of that event (magnitude and distance) will exceed a certain level.

For instance, assume that the site will be shaken by an earthquake of magnitude M higher than 6, at an epicentral distance less than 20 km, having a PGA exceeding 0.5 g and having an annual probability of exceedence of 10^{-4} pa. This does not mean that the event is the maximum one that will occur in 10000 years, but rather it is an event associated with the following possible probabilities :

(i) Probability that magnitude $M = 6$ is reached in 100 years : $p1 = 0.01$;

(ii) probability that the epicentral distance will be less than 20 km : $p2 = 0.02$;

(iii) probability that the PGA will exceed 0.5 g : $p3 = 0.5$;

The annual probability of exceedence is $pa = p1 * p2 * p3 = 10^{-4}$.

The probabilistic-risk analysis shows many advantages compared to the deterministic approach:

(i) Contribution of all possible earthquakes from different sources and of different magnitudes;

(ii) the seismic hazard may be estimated at many sites after a unique calculation.

Figures 2.6a and 2.6b show the general procedure for constructing a scaled shape spectrum and a uniform hazard spectrum from a probabilistic-risk analysis.

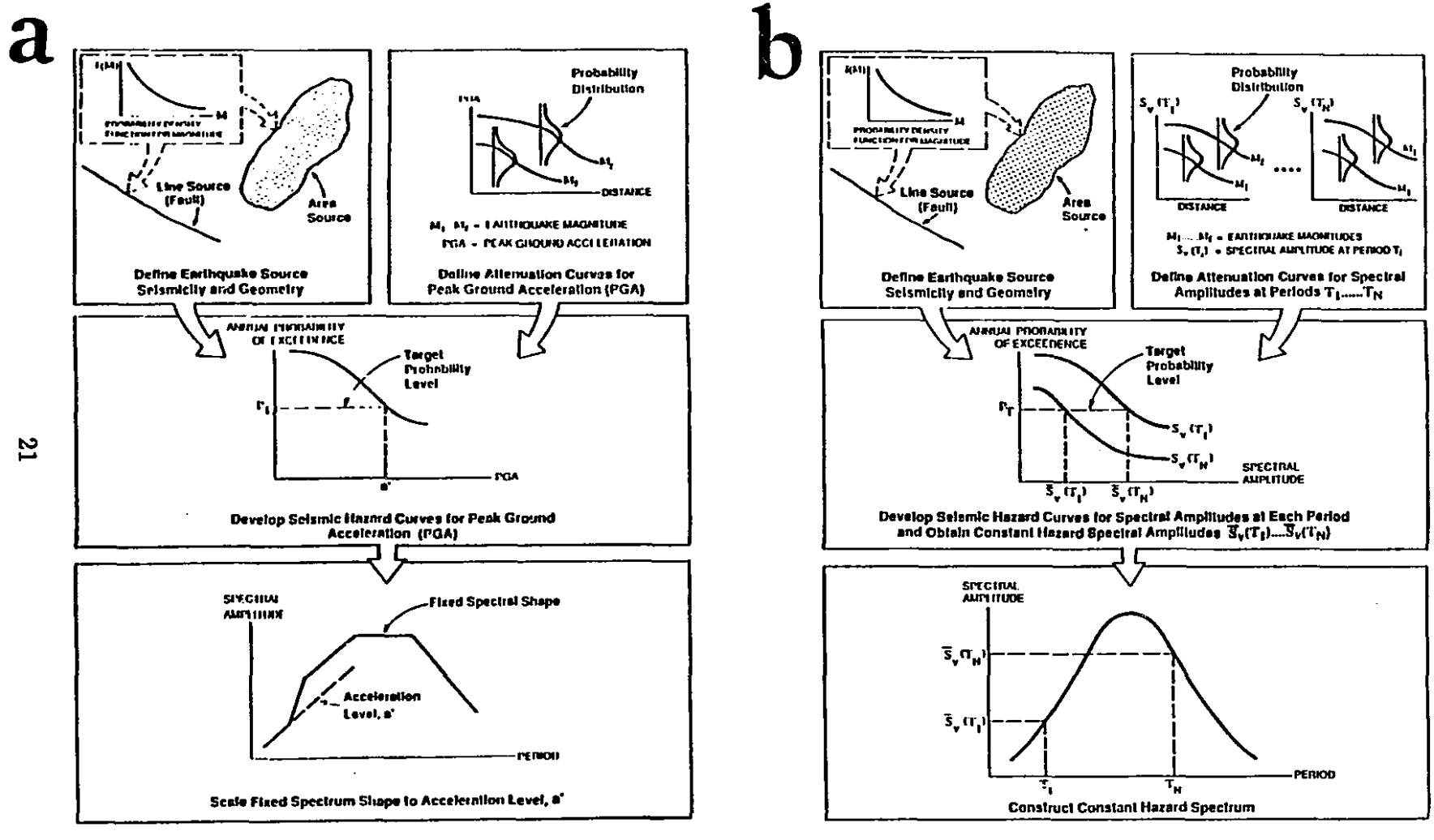

Figure 2.6: Construction of probabilistic response spectra (adapted from EERI committee on seismic risk, 1989).

2.9 Smooth design spectra for low probability events

From a structural point of view, a progressive approach is generally adopted in the seismic verification procedures of critical facilities assuming first, linear elastic behaviour with the response spectra method, and then introducing significant nonlinear response mechanisms to determine the ultimate resistance, and identify modes of failure of the structure. Therefore the structural engineer needs a time history. It is practically impossible to find a time history that answers all the conditions of a site. Therefore the engineer is provided with a smooth response spectra that best reflects the site conditions. There are five ways of obtaining a site specific smooth response spectrum (Dunbar 1991a, 1991b):

(i) Scaling spectral shapes by peak ground parameters (Newmark and Hall, 1973, 1982) that can be determined either by the use of seismic hazard maps for a specified annual probability of exceedence (Fig. 2.6a), or by the direct use of attenuation relationships for the specified magnitude, distance and site conditions.

(ii) Direct use of attenuation functions giving spectral ordinates for specific magnitude and distance of the maximum credible earthquake (MCE) scenario.

(iii) Constructing uniform hazard spectra through the use of uniform hazard maps or computer programs, for a specified annual probability of exceedence (Fig. 2.6b).

(iv) Search of available database of recorded accelerograms of events meeting the MCE scenario, to construct, from statistical analyses (Median or 84^{th} percentile), a site-specific response spectrum.

(v) Source and wave propagation modelling of representative earthquake fault rupture mechanisms to obtain a suite of synthetic time histories and related median and 84th percentile response spectra.

Since the source mechanisms in Eastern Canada are not very well known, only the first four methods can be successfully used in this region. The first method is the well known

Newmark-Hall spectrum method and has been extensively used for the two past decades. The second approach is purely deterministic and simple to implement when the credible scenario is defined. The third has been gaining a lot of interest in the seismological media this past decade, in example of this procedure; the CEA (vol. b 1990) published a series of seismic hazard maps for annual probabilities of exceedence of 10^{-3} and 10^{-4} . These maps give PGA, PGV and spectral ordinates for a specific SDOF period of vibration such that a low probability design response spectrum can be drawn for any specific site in Canada. In example of the fourth procedure, Smith et al. (1991) have derived a site specific spectrum obtained from sites located in the U.S., Canada, and Europe, from historical records, for a local near-site shallow earthquake of magnitude 6.5 at 10 km, likely to occur in the north shore mountains near Vancouver without reference to any specific fault. The records had magnitudes varying from 6.1 to 7.0, and epicentral distances ranging from 7.4 to 24 km. It is clear that this range of records suits well a credible scenario of M6.5 at 15 km. The related spectra are shown in Fig. 2.7. Due to the lack of data in ENA, the second and third methods appear to be the most appropriate for the construction of a design spectrum. The McGuire (1988) and Atkinson and Boore (1990) attenuation functions can be used to construct the spectrum and to define the peak ground parameters.

2.10 Maximum design earthquake scenarios

Using low-probability seismic hazard maps (CEA, vol. B 1990), seismic zonation maps and underlying seismological investigations in conjunction with seismic response indicators such as the spectrum intensity and the PGA, one can work backward to define credible magnitude-distance scenarios for specific regions. Except the region of Charlevoix, where a magnitude 7 to 7.5 event can occur, the St. Lawrence valley can easily be shaken by a magnitude 6.5 to 7 earthquake (Table 2.2). Generally the epicentral distance is related to the geographic location of faults. In the East, causative faults are rarely known. Therefore seismologists recommend to adopt an epicentral distance between 0 and 30 km, with 15 to 20 km being a good average distance, and a focal depth of 15 km to 25 km (Nuttli 1981, Dunbar 1991, CEA vol B.1990, Adams et al 1989). Figure 2.3d shows the uniform hazard response spectra of a low-probability event (10^{-4} pa) derived from CEA uniform

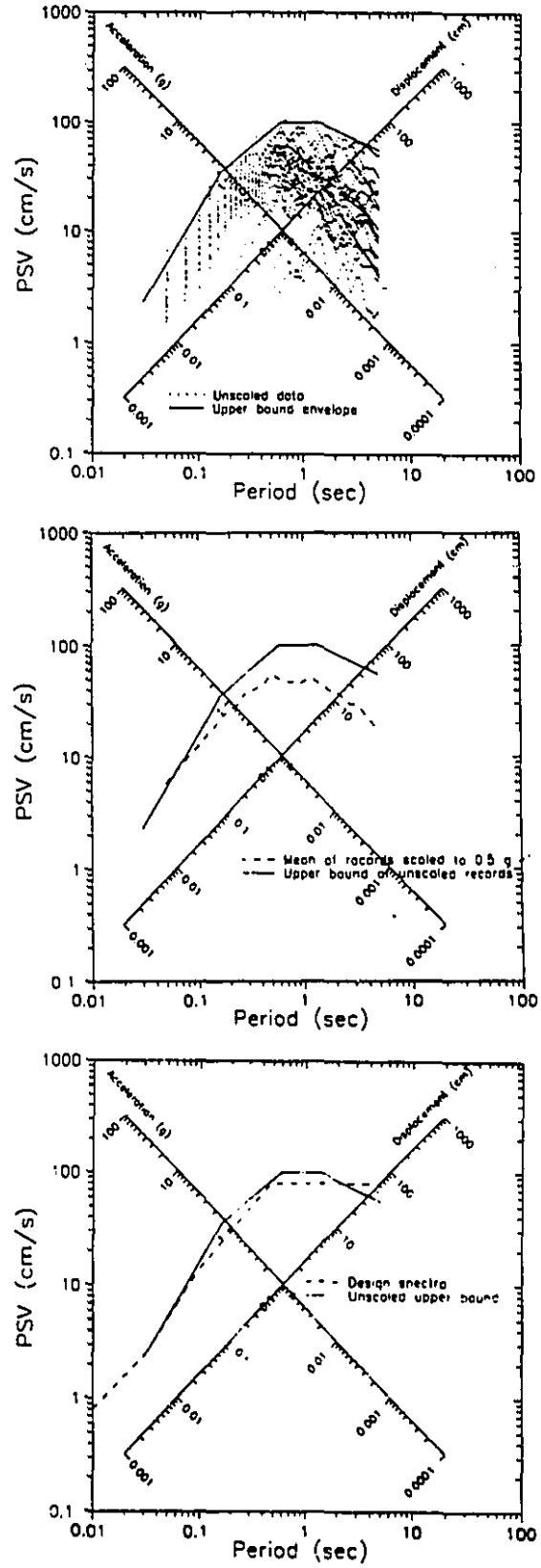

Figure 2.7: Example of a site specific spectrum for Western Canada (adapted from Smith et al., 1991).

hazard maps (1990) at site 1 (Manic2) located in the lower St. Lawrence valley, and site 4 (Paugan) located in Western Quebec, and the spectra derived from attenuation functions for magnitudes $M = 6.5$ and $M = 7.0$, and epicentral distances (ED) $ED = 15km$ and $ED = 20km$. From the figure, we observe that the McGuire and Atkinson $M = 6.5$ at $ED = 15km$ are very similar and describe well the Paugan site spectrum, the Manic2 site spectrum is located between the McGuire M=7 at ED=20 km spectrum (upper side) and the Atkinson M=7 at ED=20 km spectrum (lower side). Table 2.5 shows the PGA's and SI_a's computed from the attenuation relationships of McGuire and Atkinson for M=7 at 20 km and M=6.5 at 15 km events, with the corresponding SI_a's from Fig 2.4, as well as those computed, through a uniform hazard analysis (contribution of all possible earthquakes of magnitude 4.0 to 7.0), for different sites in the Quebec region. It is observed that the McGuire and Atkinson models for M=6.5 at 15 km and M=7.0 at 20 km encompass well all the data for different sites and different zonations; Von Thun et al. (1988) SI_a's ($SI_{a(0.10)}$) being upper bounds for all computed SI_a's.

In this study an M= 7.0 at 20 km is selected as a principal scenario and an M6.5 at 15 km as another credible scenario. Since the Manic2 spectrum is derived from a risk analysis and is, in overall, closer to the Atkinson spectrum, especially for short periods (0.1-0.5 sec), and since the McGuire spectrum is found to an upper bound for these two spectra for the M=7 at 20 km event, it is concluded that the Atkinson spectrum gives a good and not overly conservative estimate of the spectrum of ground motion in that region, for a deterministic seismic analysis based on an M=7 at 20 km credible scenario. The Atkinson M=7 at 20 km spectrum will be used as a target and design spectrum, and will serve to generate spectrum-compatible time histories, and to scale historical records.

Elastic Response Spectrum		PGA (g)	$SIa_{(.10)}$ (cm/sec)	$SIa_{(.04)}$ (cm/sec)
McGUIRE,	M7.0 at 20 km	0.51	216	268
McGUIRE,	M6.5 at 15 km	0.44	163	207
ATKINSON,	M7.0 at 20 km	0.49	199	250
ATKINSON,	M6.5 at 15 km	0.44	174	220
Manic2,	CEA zone 1	0.30	97	124
Outarde 3,	CEA zone 1	0.26	79	101
Chute à Caron,	CEA zone 1	0.36	168	206
Paugan,	CEA zone 1	0.50	16	47
Manic2,	CEA zone 2	0.45	209	259
Outarde 3,	CEA zone 2	0.29	178	212
Chute à Caron,	CEA zone 2	0.24	115	137
Paugan,	CEA zone 2	0.46	166	211

Table 2.5: PGA and SI_a from uniform hazard analysis and attenuation laws.

Chapter 3

Generation of Spectrum-Compatible Earthquakes

3.1 Introduction

There are two basic approaches to generate an artificial earthquake. The first approach is the generation of a signal directly related to the site conditions, either through geological modelling of source mechanisms (Tsai et al. 1990, Wald et al. 1988), or using parametric time series (Ellis et al.,1990), or constructing site-dependent critical signals (Wang et al. 1979). However these methods requires the availability of data and source mechanisms, which are not yet available in Eastern Canada. The second approach is the generation of spectrum-compatible time-histories. Here also various methods are available, the most common ones use a stationary or nonstationary Gaussian white noise, or a real record, in combination with an intensity function, and modify its Fourier amplitude spectra (the phase angle spectra may also be modified) or its power spectral density function until matching the target spectrum. Another alternative is to use a combination of segments of historical records to simulate a specified seismological event (Seed-Idriss 1968). In this study, spectrum-compatible time histories of ground motions suitable for severe ground

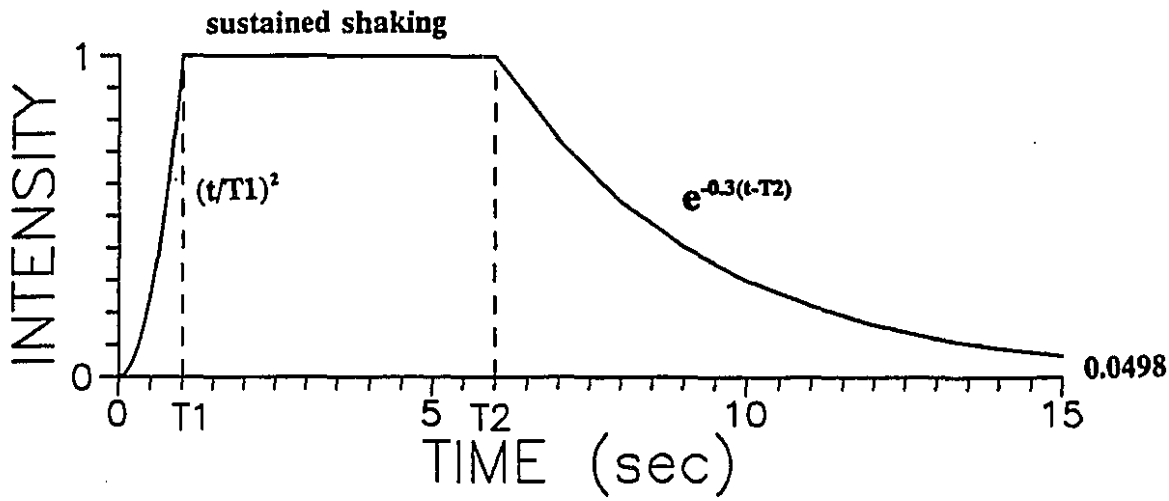

Figure 3.1: Intensity envelope.

shaking in Eastern Canada have been generated from filtered white noise and by modification of the Fourier amplitude spectra of real records. The target spectrum being derived from Atkinson attenuation laws for an M=7 at 20 km event.

3.2 Spectrum-compatible time histories generated from filtered white noise

In this method, a filtered white noise is generated and combined with the intensity envelope shown in Fig. 3.1. Some iterations are allowed until reaching an acceptable compatibility between the specified target spectrum and the spectrum of the computed artificial accelerogram (SIMQKE 1976).

This procedure is based on the fact that any periodic function Z(t) can be resolved into a series of sinusoidal waves of the form

$$Z(t) = \sum_n A_n sin(w_n t + \phi_n) \qquad (3.1)$$

Where A_n, w_n, and ϕ_n are the amplitude, the frequency, and phase angle of the nth contributing sinusoid. The array of amplitudes is fixed, and different arrays of phase angles are generated by a random number generator. The spectral density of the generated white noise is derived from the target spectrum and depends on the level of damping, the duration and the probability of exceedence of the spectral values (SIMQKE 1976). The amplitudes are related to the spectral density function as follows :

$$G(w_n)\Delta w = \frac{{A_n}^2}{2} \tag{3.2}$$

Where Δw is the frequency increment. To simulate the transient character of real earthquakes, the steady-state generated motions are combined with a deterministic intensity envelope function I(t). The artificial time history Z(t) becomes :

$$Z(t) = I(t)\sum_n A_n sin(w_n t + \phi_n) \tag{3.3}$$

The result is a motion stationary in frequency content, characterized by a peak acceleration very close to the target one. After the motion is generated the response spectrum is computed and is smoothed through some iteration in order to improve the matching with the target spectrum. At each iteration, and for each specified frequency, the ratio of the target to the computed spectra is obtained and the power spectral density is modified in proportion to the square of this ratio as follows (for cycle i+1) :

$$G(w)_{i+1} = G(w)_i[\frac{S_v(w)}{S_{vi}(w)}]^2 \tag{3.4}$$

where S_v is the target spectral value and S_{vi} is the computed spectral value at cycle i. From the modified spectral density function a new time history is generated and a new response spectrum is computed. Generally four cycles are enough to obtain acceptable results.

3.3 Spectrum-compatible time histories generated from historical records

Many researchers argued that the motions generated by the previous method have phase angles that are not compatible with those of real earthquakes and lead to undesirable

pulses that may affect the response of structures (Christian et al. 1988, Chopra and Lopez 1979). Because of that, some authors proposed that real records be used, keeping their phase angles and modifying their Fourier amplitudes until acceptable matching between the target and computed spectra, is reached. This is done in the following steps (Liou and Penzien et al. 1988, FEMA 1985, Shaw et al. 1975) :

(i) Compute the response spectrum, RS(f), and the Fourier amplitude spectrum, FAS(f), using the fast Fourier algorithm, for the current record at similar frequencies, f (for the first iteration, the current record is the historical record),

(ii) using the current RS(f) normalize the FAS(f) to the target response spectrum, TRS(f), ie :

$$FAS(f) = FAS(f)\frac{TRS(f)}{RS(f)} \tag{3.5}$$

(iii) generate a new time history by performing an inverse Fourier transform with the modified Fourier spectrum combined with the original phase angle spectrum,

(iv) compute the response spectrum of the generated signal and compare it to the target spectrum, iterate until an acceptable compatibility is obtained.

Some points of the spectrum of the generated time history may fall under the target spectrum. For example the regulatory norm related to the Design Procedures for Seismic Qualifications of CANDU Nuclear Power Plants (CSA CAN-N3-N289.3-M81), requires that :

" no more than 6% of the total number of points used to generate the spectrum from time history shall fall below the target spectrum, but by no more than 10% at any point ".

3.4 Base line correction

Simulated ground motion are signals similar to recorded ones, and therefore need to be corrected before any use in structural evaluation or design, because these signals have to satisfy some boundary conditions. The simplest form of base line correction (BLC) is the

satisfaction of zero mean value. However in a more general case the following boundary conditions have to be satisfied (Rainer, 1986):

(i) Zero mean acceleration, velocity and displacement;

(ii) Zero initial and final displacement, velocity, and acceleration.

The first condition is implied by the second one. There are many procedures of BLC either in the time domain, or in the frequency domain. However no procedure is able to entirely eliminate the drifts caused by the recording instrument or by the numerical generation. A basic procedure is to satisfy a zero final displacement or velocity by subtracting a very small constant term to the acceleration record as described below :

(i) **Zero final velocity :** If v_0 is the final integrated velocity and t is the total length of the record, then the quantity $a_0 = \frac{v_0}{t}$ is subtracted from the acceleration record.

(ii) **Zero final displacement :** If d_0 is the final integrated displacement, and t is the total length of the record, then the quantity $a_0 = \frac{2d_0}{t^2}$ is subtracted from the acceleration record: $\bar{a}(t) = a(t) - a_0$

(iii) **Zero mean velocity :** A parabolic acceleration correction $a_0(t)$ is added to the initial record such that the mean square velocity over the duration of the record is minimized.

$$a(t) = a(t) + a_0(t), \quad 0 < t < T \tag{3.6}$$

$$a_0(t) = C_1 + C_2(\frac{t}{T}) + C_3(\frac{t}{T})^2 \tag{3.7}$$

Where T is the total duration of the record. The algorithm to determine the coefficients C_i is given in appendix C.

To illustrate the application of BLC to an actual accelerogram, the Nahanni 1985 site 2 transversal component record obtained from Geological Survey of Canada (GSC) will be considered. Fig. 3.2a shows the corrected acceleration, velocity, and displacement records that are provided in separate files by the GSC, where relatively complex frequency

domain BLC have been carried out at the acceleration, velocity and displacement level separately. Fig. 3.2b shows the velocity and displacement time histories obtained by numerical integration of the acceleration record provided by the GSC. It is obvious that the zero final displacement, and zero final and zero mean velocity requirements are not met. Fig. 3.2c shows the ground motions obtained after the application of a base line correction to obtain zero mean velocity. Fig. 3.2d shows the ground motion corrected for zero mean velocity and adjusted for zero final displacement. Fig. 3.2e and 3.2f show the corrected record for zero final velocity and displacement, respectively, without satisfying zero mean velocity. It is clear that the zero mean velocity condition should be performed to obtain realistic representation of ground velocity and displacement from the numerical integration of a given acceleration record. It can be observed that the BLC has little influence on the acceleration time history, but its major impact is on the velocity and displacement time histories, which sometimes become meaningless without it.

3.5 Historical records

The offshore structures code, CSA M471-M1989 (1989), recommends that at least three sets of input ground motion time histories be used in seismic safety evaluation of critical facilities with $P = 10^{-4}$ pa. Four historical earthquakes have been selected for this study. Ideally they should be representative of an M=7 Eastern earthquake recorded at 20 km from the source. The M=6.9 Nahanni 1985 earthquakes that occurred in the North-West territories (Canada) represents an intraplate event having similar source mechanism as the St. Lawrence valley earthquakes, and in a broader sense similar to those that can be expected in ENA. Due to the lack of other suitable large magnitude near source Eastern records, two U.S. West coast earthquakes have been considered, one representing an M=7 at 20 km event (Loma Prieta M=6.9) and another representing an M=6.5 at 15 km event (San Fernando). The fourth selected record is the 1988 M=5.9 Saguenay earthquake which is a typical Eastern Canadian earthquake. The Saguenay earthquake having a relatively low magnitude (M=5.9) is treated separately. The nearest recording of the M=5.9 1988 Saguenay earthquake is 42 km from the source. Although this earthquake does not correspond to the selected earthquake scenario, it has been included in the parametric analysis

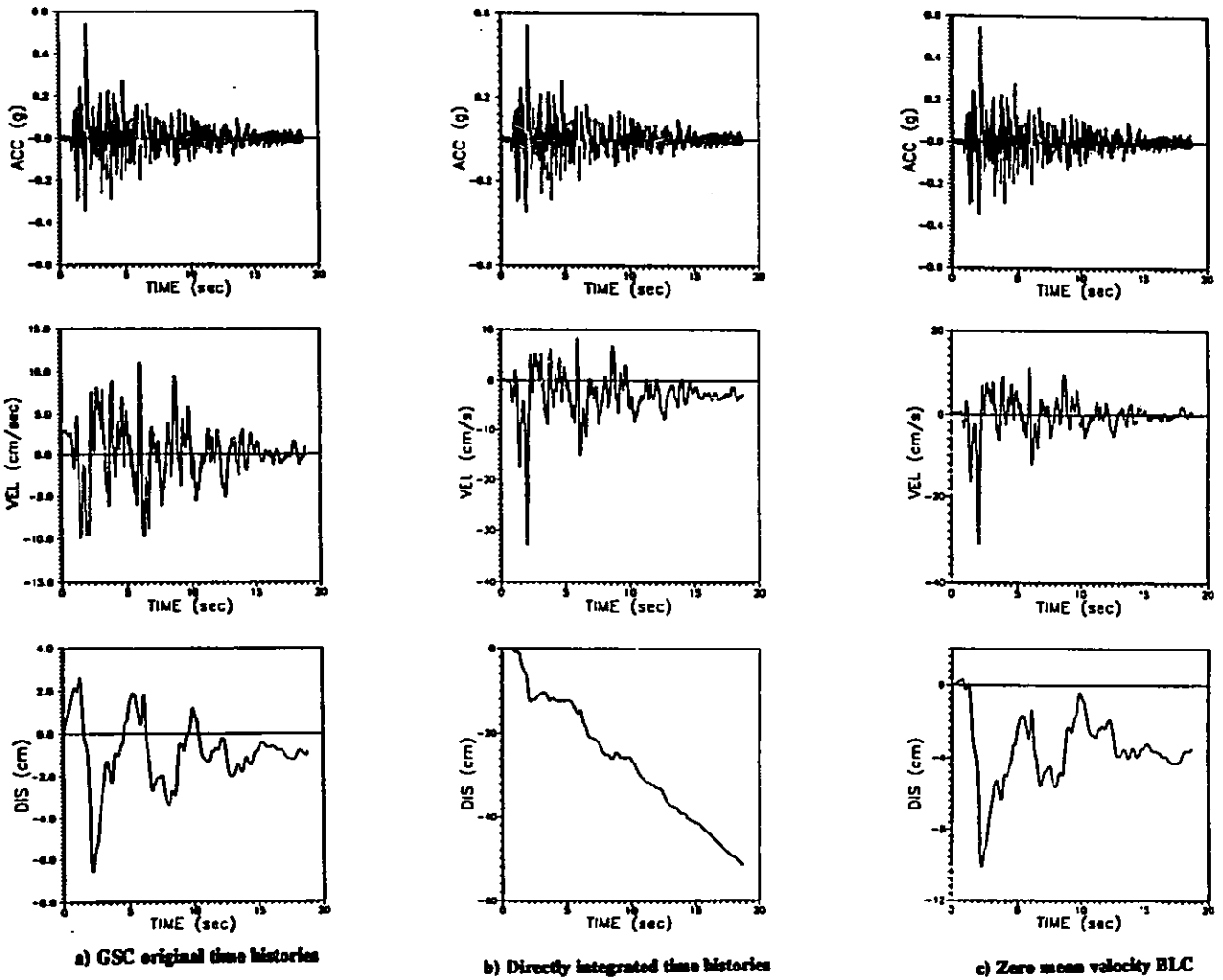

Figure 3.2 : BASE LINE CORRECTION (BLC, a, b, c).

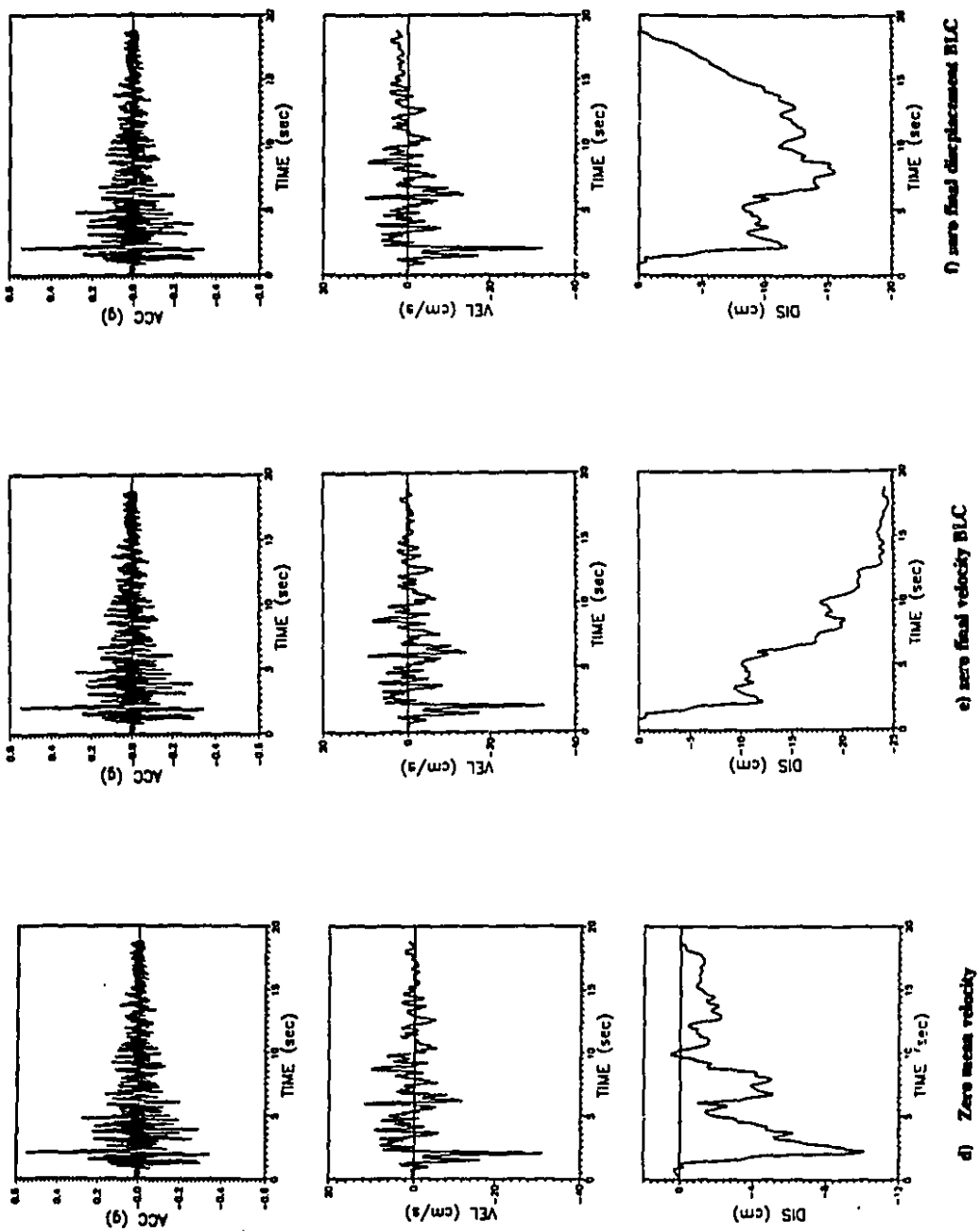

Figure 3.2 : BASE LINE CORRECTION (B.L.C. d, e, f).

since it is a recent strong Eastern earthquake from which good records are available, Table 3.1 shows the characteristics of the 1988 Saguenay records at ten recording stations on bedrock, Fig. 3.3 shows the RS at different recording stations compared to RS given by Atkinson an Boore (1990) and McGuire (1988) for the same magnitude and epicentral distance. The characteristics of the selected records are summarized in Table 3.2. These accelerograms have to be scaled to match as well as possible, the acceleration spectrum intensity of the target spectrum. It has been shown by many authors (Nau and Hall 1984, Barenberg 1989) that the scaling by spectrum intensity leads to the least dispersion in the structural response. The following scaling methods (SM) have been investigated to minimize the difference among the elastic response spectra of the historical records and the target spectrum:

(i) SM1: scale the historical record to obtain the same SI_a as defined by the target spectrum (for this method two SI_a's have been used: $SI_{a(.10)}$ and $SI_{a(.04)}$),

(ii) SM2: Scale the historical record to obtain the same PGA (0.5 g for a M=7 at 20 km) as defined by the attenuation function,

(iii) SM3: scale the historical records to obtain the same pseudo-spectral velocity spectrum intensity, SI_v, defined as the area under the pseudo-velocity spectrum between 0.1 sec and 2.5 sec for 5% damping, compute the average PSA, apply a scaling factor such that the SI_a of the average PSA correspond to the value defined by the target spectrum (Schiff 1988).

Table 3.3 summarizes the various scaling factors computed for each method. Table 3.4 summarizes the characteristics of the original and scaled historical records. D1 is the effective duration of strong shaking, defined by McCann and Shah (1979), which is related to the rate of arriving energy. The "bracketed duration" of the records, D2, is defined as the elapsed time between the first and last acceleration excursions greater than 0.05g (Bolt 1973). The duration D3 has been obtained from the method given by Trifunac and Brady (1975), which corresponds to the time needed for the integral of $\ddot{u}_g^2(t)$ to build up for 5% to 95% of its final value. Table 3.4 also gives values of the peak ground velocity, PGV, the peak acceleration to peak velocity ratio, $\frac{a}{v}$, the number of zero crossings, NZC,

SITE Name	SITE No	E.D Km	PGA g	PGV cm/s	PGD cm	A/V g*cm/s *100	DUR s	SIA g*s/cm	SIV cm	RMSA g *100	AI g**2*s *1000
Chicoutimi-North	16 L	43.2	0.106	1.51	0.08	7.02	17.14	3.51	2.4645	1.58	8.474
	T	43.2	0.131	2.52	0.20	5.12	17.57	5.00	5.0500	1.87	11.936
	V	43.2	0.102	1.85	0.15	5.51	20.43	4.38	3.4070	1.19	4.822
St. André	17 L	63.6	0.156	1.83	0.07	8.52	12.58	3.19	2.3371	1.78	9.016
	T	63.6	0.091	0.94	0.04	9.69	15.15	2.39	1.6534	1.49	6.297
	V	63.6	0.045	0.88	0.05	5.14	19.44	1.91	1.2995	0.79	1.768
Les Eboulements	20 L	90.4	0.125	4.40	0.32	2.85	08.55	8.13	7.6268	1.65	5.645
	T	90.4	0.102	2.65	0.18	3.86	16.17	5.15	5.6853	1.94	7.801
	V	90.4	0.234	5.01	0.43	4.68	15.72	9.33	7.1240	4.84	46.733
La Malbaie	8 L	93.0	0.124	4.65	0.41	2.67	11.05	7.88	11.0789	1.28	4.834
	T	93.0	0.060	1.33	0.12	4.50	15.47	3.23	3.8214	0.77	1.763
	V	93.0	0.068	1.72	0.11	3.94	16.28	4.47	3.8889	0.67	1.332
Tadoussac	5 L	109.2	0.027	0.58	0.11	4.63	29.35	1.27	2.0674	0.48	0.917
	T	109.2	0.002	0.14	0.04	1.56	36.33	0.06	0.6807	0.04	0.007
	V	109.2	0.053	1.05	0.15	5.07	31.65	1.73	3.2384	0.63	1.548
St. Ferreol	1 L	113.8	0.121	2.71	0.11	4.47	21.29	5.75	3.7410	1.15	6.429
	T	113.8	0.097	2.45	0.09	3.97	19.65	5.43	3.3978	1.03	5.207
	V	113.8	0.062	1.71	0.13	3.65	28.51	3.54	3.8227	0.75	2.766
Rivière-Ouelle	10 L	114.4	0.040	2.71	0.11	4.47	13.29	3.15	6.1175	0.52	0.904
	T	114.4	0.057	2.45	0.09	3.97	13.06	4.45	7.7966	0.61	1.255
	V	114.4	0.023	1.71	0.13	3.65	26.10	1.84	3.1444	0.42	0.584
St. Pascal	9 L	122.7	0.046	2.60	0.34	1.78	21.62	3.84	7.9231	0.64	1.603
	T	122.7	0.056	2.62	0.19	2.13	20.89	4.82	5.7736	0.72	2.045
	V	122.7	0.037	1.85	0.13	1.98	26.21	3.18	3.9407	0.36	0.521
Quebec City	2 L	149.3	0.050	1.50	0.21	3.33	15.64	2.79	4.0671	0.49	0.942
	T	149.3	0.051	2.16	0.16	2.36	12.32	3.89	4.6556	0.56	1.246
	V	149.3	0.020	0.96	0.14	2.08	29.33	1.75	3.4638	0.30	0.363
St. Lucie de Beau	14 L	176.2	0.014	0.64	0.04	2.16	14.98	1.24	1.5940	0.30	0.143
	T	176.2	0.023	1.03	0.19	2.26	15.05	1.52	2.6630	0.32	0.184
	V	176.2	0.023	1.23	0.23	1.90	11.45	1.63	3.1555	0.29	0.150

Table 3.1 : Seismic parameters of the 1988 Saguenay earthquake records (Quebec sites).

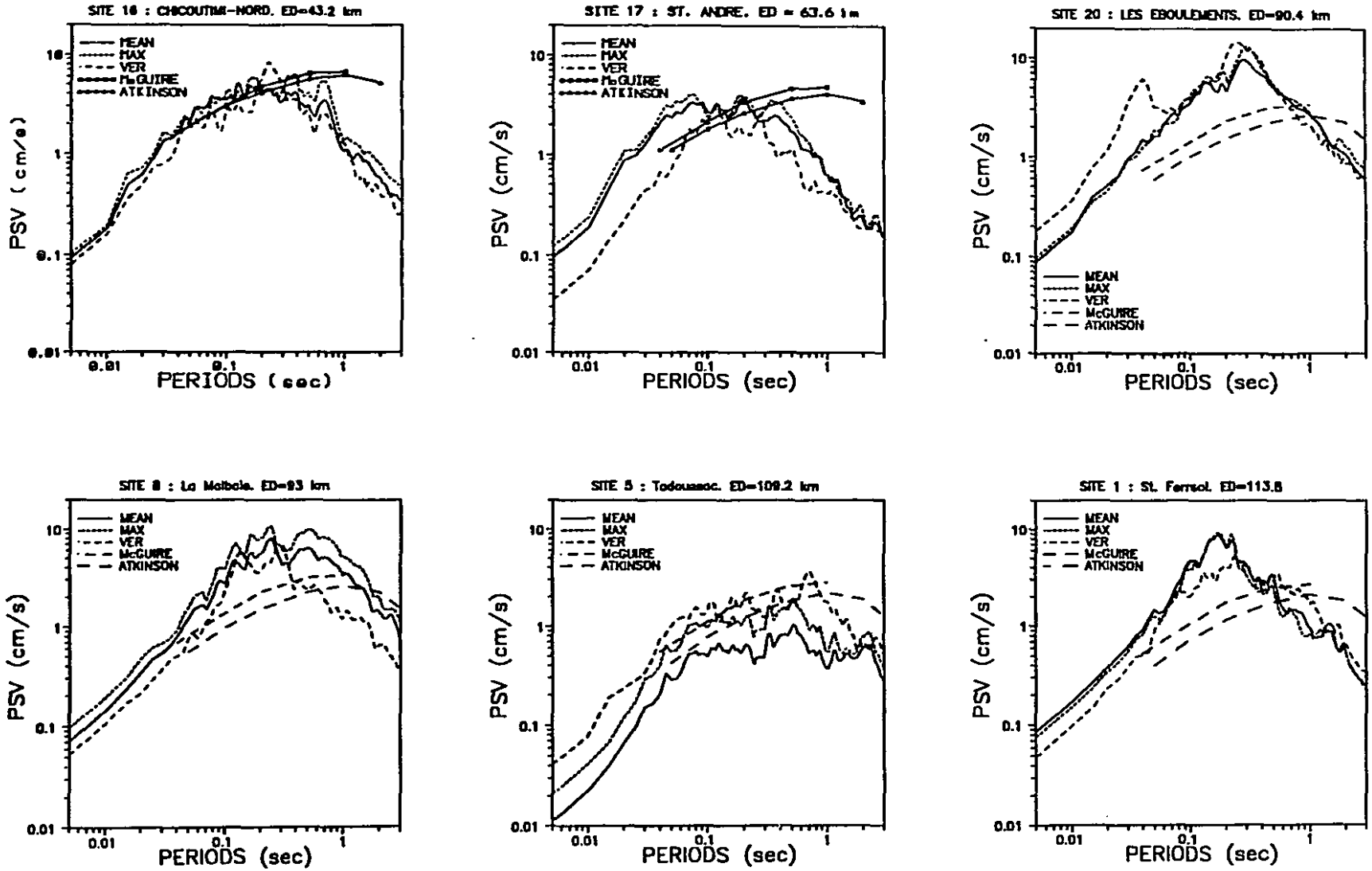

Figure 3.2a : Correlation between the 1988 Saguenay earthquake response spectra and the corresponding spectra from attenuation laws.

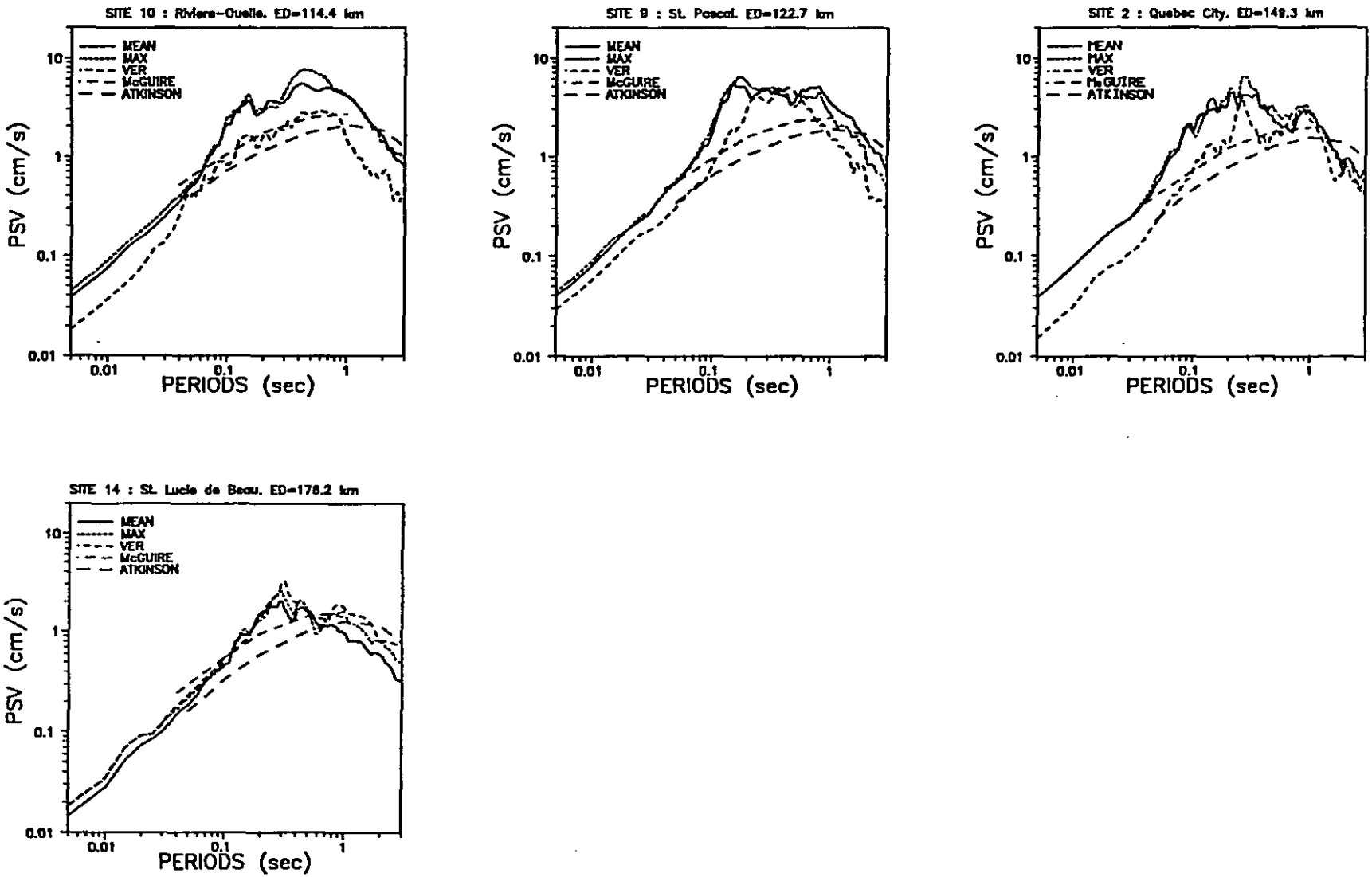

Figure 3.2b : Correlation between the 1988 Saguenay earthquake response spectra and the corresponding spectra from attenuation laws.

the predominant period of shaking, PPS, defined as the ratio of the total duration of the record, t_d, to $\frac{NZC}{2}$, the Arias intensity, and the root mean square of the accelerogram, defined respectively as,

$$AI = \int_0^{t_d} \ddot{u}_g^2(t)dt \tag{3.8}$$

$$RMSA = \sqrt{\frac{AI}{t_d}} \tag{3.9}$$

From Figure 3.4 that shows the elastic spectra of the scaled earthquake records., we observe that using the SM1, it did not make any significant difference whether to scale to $SI_{a(.10)}$ (Fig. 3.4a) or $SI_{a(.04)}$ (Fig. 3.4b) (in fact because Atkinson laws start at T=0.05 sec it is a scaling to Atkinson $SI_{a(.05)}$, we maintained the name $SI_{a(.04)}$ for compatibility with the CEA data) since the scaling factors were very similar (Table 3.2). SM1 is grouping the elastic spectra more closely around the target spectrum, than the SM3 in the period range 0.04-0.4 sec, but SM3 is better in the 0.4-0.6 sec period range. The scaling by PGA (SM2) leads to the highest level of dispersion (Fig. 3.4c) in the 0.1-0.6 sec period range, however there is a good spectrum compatibility of Eastern records at very short periods (0.04-0.06 sec for Nahanni and 0.04- 0.20 sec for Saguenay). The SM3 (Fig. 3.4d) does not allow to achieve good spectrum compatibility in the high frequency range whether from Eastern or Western records, however there is an acceptable compatibility with of Western records in the 0.2-0.6 sec period range. It is observed from Table 3.3 that the different scaling procedures do not affect the $\frac{a}{v}$ ratio, the D3 duration, the NZC, and the PPS. Except for the D1 and D2 durations, all the remaining parameters are linearly or quadratically (AI) modified by the scaling procedure.

Scaling on PGA (SM2) does not preserve the target SIa, however SM2 SIa's for Eastern records are closer to target values than for the Western records, while scaling to mean SIa (SM3) provides low PGA values. However, scaling to SIa (SM1), maintained also the PGA close to the target value (0.5 g) for Eastern records, with more closeness if scaling is done by $SI_{a(.04)}$. It has to be noted that when scaling the real earthquakes by the SM1 or SM2, only the Saguenay and Nahanni records could match the target spectrum in the periods lower than 0.1 sec, the Western records spectra were lower than the target in this period range. In Table 3.4 the mean spectral value reported initially excludes the

Event Name	Component	Date	Magnitude	Epicentral distance
Nahanni	Site 2, Trans.	1985	6.9	7.4
Loma Prieta	USCC/Lick Lab, Trans.	1989	6.9	16.0
San Fernando	Lake Hughes No. 4, Long. S69E	1971	6.4	25.0
Saguenay	Site 16, Chicoutimi-Nord, Trans.	1988	5.9	43.2

Table 3.2 : Characteristics of selected historical records

EVENT	SM1 ($SIa_{(.10)}$)	SM1 ($SIa_{(.05)}$)	SM2 (PGA)	SM3 ($SIa_{(.10)}$) mean SF1	SF2	SF
NAHANNI	0.938	0.924	0.917	1.098		0.639
LOMA PRIETA	0.468	0.547	1.136	1.000	0.582	0.582
SAN FERNANDO	1.809	1.994	2.941	3.304		1.924
SAGUENAY	4.067	3.837	3.817			

SF1 : First scaling factor to normalize to the SIv of the Loma Prieta record
SF2 : Second scaling factor to normalize the mean $SIa_{(.10)}$ to the target $SIa_{(.10)}$
SF : Final scaling factor (SF=SF1*SF2)

Table 3.3 : Scaling factors for the different scaling methods

	PGA (g)	PGV (cm/sec)	a/v (g*sec/m)	D1 (sec)	D2 (sec)	D3 (sec)	$SI_{a(0.10)}$ (cm/sec)	$SI_{a(0.05)}$ (cm/sec)	SI_v (cm)	RMSA (g) *100	AI (g^2*sec) *1000	NZC	PPS (sec)
Historical records													
Nahanni	0.545	30.26	1.8	12.8	13.8	10.1	212.8	271.2	64.4	5.86	64.4	754	0.050
Loma Prieta	0.440	21.23	2.1	10.6	16.6	9.5	426.7	457.9	70.7	6.57	172.8	396	0.202
San Fernando	0.170	5.75	2.9	6.9	5.7	12.7	110.4	125.6	21.4	1.95	10.5	585	0.127
Saguenay	0.131	2.52	5.1	14.9	11.4	17.6	49.1	65.3	5.1	1.87	11.9	2383	0.029
Scaled historical records SM1 ($SIa_{(0.10)}$)													
Nahanni	0.511	28.40	1.8	12.7	14.6	10.1	199.7	254.4	60.5	5.50	56.7	754	0.050
Loma Prieta	0.207	9.94	2.1	8.9	13.9	9.5	199.7	214.3	33.1	3.07	37.8	395	0.202
San Fernando	0.310	10.40	2.9	7.9	15.3	12.7	199.6	227.2	38.7	3.53	46.2	585	0.127
Mean spectrum							199.7	232.0	44.1				
Saguenay S16	0.533	10.25	5.1	19.9	33.7	17.6	199.3	265.6	20.5	7.62	197.4	2383	0.029
Mean spectrum							199.6	240.4	38.2				
Scaled historical records SM1 ($SIa_{(0.05)}$)													
Nahanni	0.503	27.95	1.8	12.8	13.7	10.1	196.6	250.5	60.0	5.41	55.0	754	0.050
Loma Prieta	0.241	11.61	2.1	8.9	13.7	9.5	233.4	250.5	38.9	3.59	51.7	395	0.202
San Fernando	0.342	11.47	2.9	6.6	15.1	12.7	220.1	250.5	43.0	3.89	56.2	585	0.127
Mean spectrum							216.1	250.5	47.3				
Saguenay S16	0.503	9.67	5.1	19.6	32.7	17.6	188.4	250.5	20.0	7.19	175.7	2383	0.029
Mean spectrum							209.6	250.5	40.5				
Scaled historical records SM2 (PGA)													
Nahanni	0.500	27.76	1.8	12.5	14.6	10.1	195.2	248.7	59.1	5.38	54.2	754	0.050
Loma Prieta	0.500	24.12	2.1	9.4	18.8	9.5	484.9	520.2	80.3	7.46	223.1	396	0.202
San Fernando	0.500	16.91	2.9	15.4	18.4	12.7	324.7	369.4	62.9	5.73	90.8	585	0.127
Mean spectrum							334.9	379.4	67.5				
Saguenay S16	0.500	9.62	5.1	19.4	33.5	17.6	187.4	249.2	19.5	7.14	173.3	2383	0.029
Mean spectrum							297.9	346.9	55.4				
Scaled historical records SM3 ($SIa_{(0.10)}$ mean)													
Nahanni	0.348	19.35	1.8	12.7	12.8	10.1	136.1	173.3	41.2	3.75	26.3	754	0.050
Loma Prieta	0.257	12.36	2.1	9.3	13.2	9.5	248.5	266.5	41.2	3.83	58.6	396	0.202
San Fernando	0.330	11.06	2.9	6.6	12.2	12.7	212.4	241.7	41.2	3.76	52.3	585	0.127
Mean spectrum							199.0	227.2	41.2				

Table 3.4 : seismic parameters of scaled historical records

contribution of the Saguenay earthquake record, but the second value includes it. The Saguenay record increased the mean $SI_{a(.04)}$ by 4%, illustrating the high content of ground motion in the .04-.10 sec period range. However, it has a lowering effect in the medium and long period range ($T_1 > 0.1$ sec) as shown in Fig. 3.5. More definite conclusions on the performance of any of these scaling methods can be drawn only after seismic response analysis of the SDOF to the scaled records. However, it is clear that Western earthquake records should be used with great caution to carry out seismic safety evaluation of Eastern critical facilities with period of vibration smaller than 0.1 sec.

3.5.1 Artificial earthquake generated from modified Fourier amplitudes

Using the program STARDYNE (1991) to perform the forward and inverse Fourier transforms, along with the M=7 at 20 km response spectrum, generated from Atkinson and Boore (1990) attenuation laws as a target spectrum, and the 1985 Nahanni, the 1989 Loma Prieta, the 1971 San Fernando, and the 1988 Saguenay earthquake records as the initial accelerograms, four modified accelerograms were generated and base line corrected. Figures 3.6a, 3.6b, 3.6c, and 3.6d show the initial and modified accelerograms. Figure 3.7a shows the spectrum compatibility of the modified Eastern records and Fig. 3.7b shows that of modified Western records. It is observed that there is no major change to the acceleration time history, except at the end of the Californian records. However, the velocity and displacement time histories are affected. The target spectrum-compatibility of the modified Eastern accelerograms is very good over the complete period range. On the other hand, the modified Western records, have a good spectrum compatibility for periods longer than 0.1 sec, but they could not match the target spectrum ordinates in the high frequency range because their Fourier amplitude coefficients are very close to zero in this frequency range. Therefore, the deficiency in high frequency motion of Western records is inherent in them, and cannot be compensated by modification of the Fourier amplitude spectrum, or any scaling procedure. It may be anticipated that Western records may be used for long, medium, and short period structures having natural periods longer than 0.1 sec.

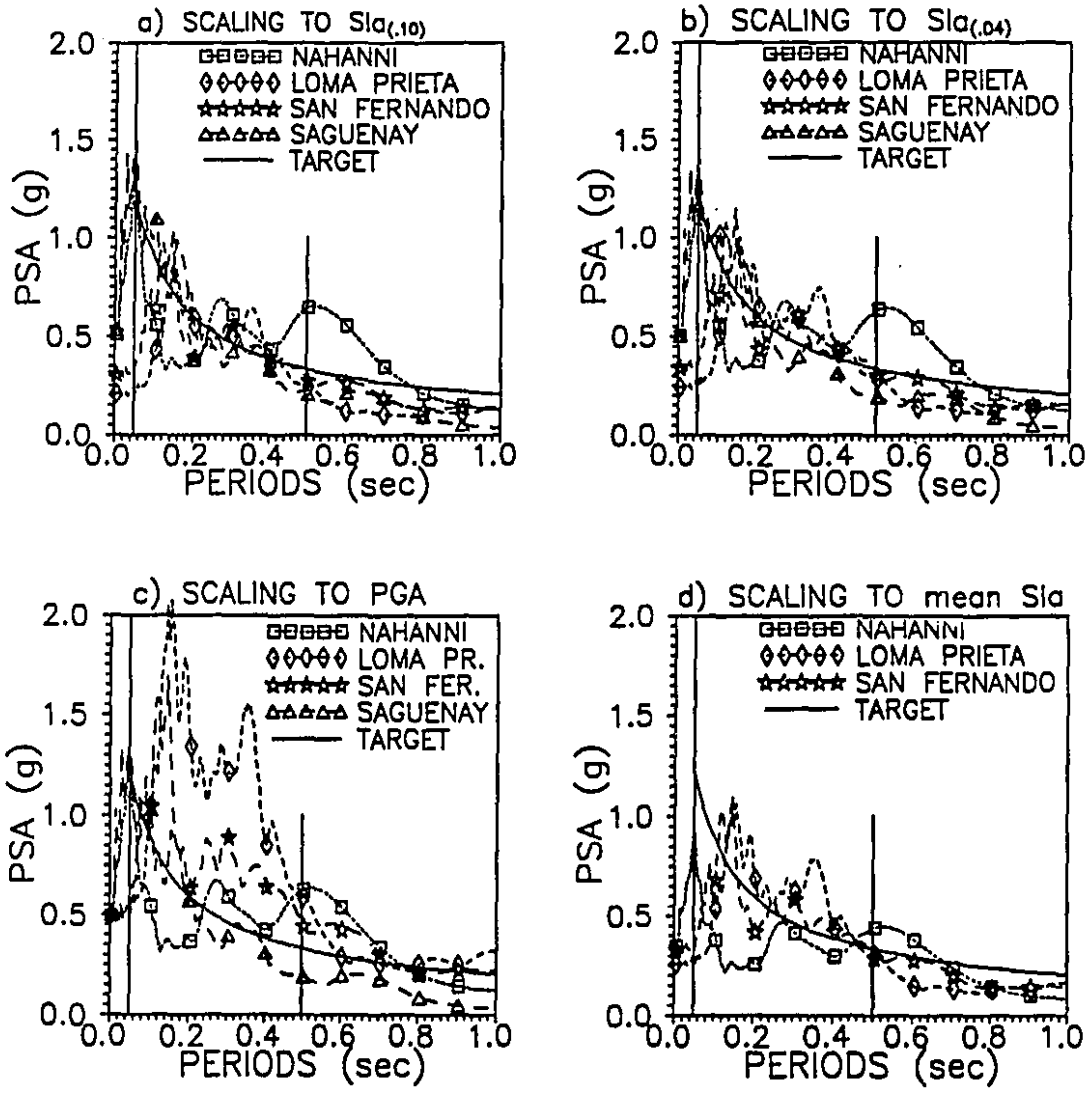

Figure 3.4: Spectra of Scaled Records.

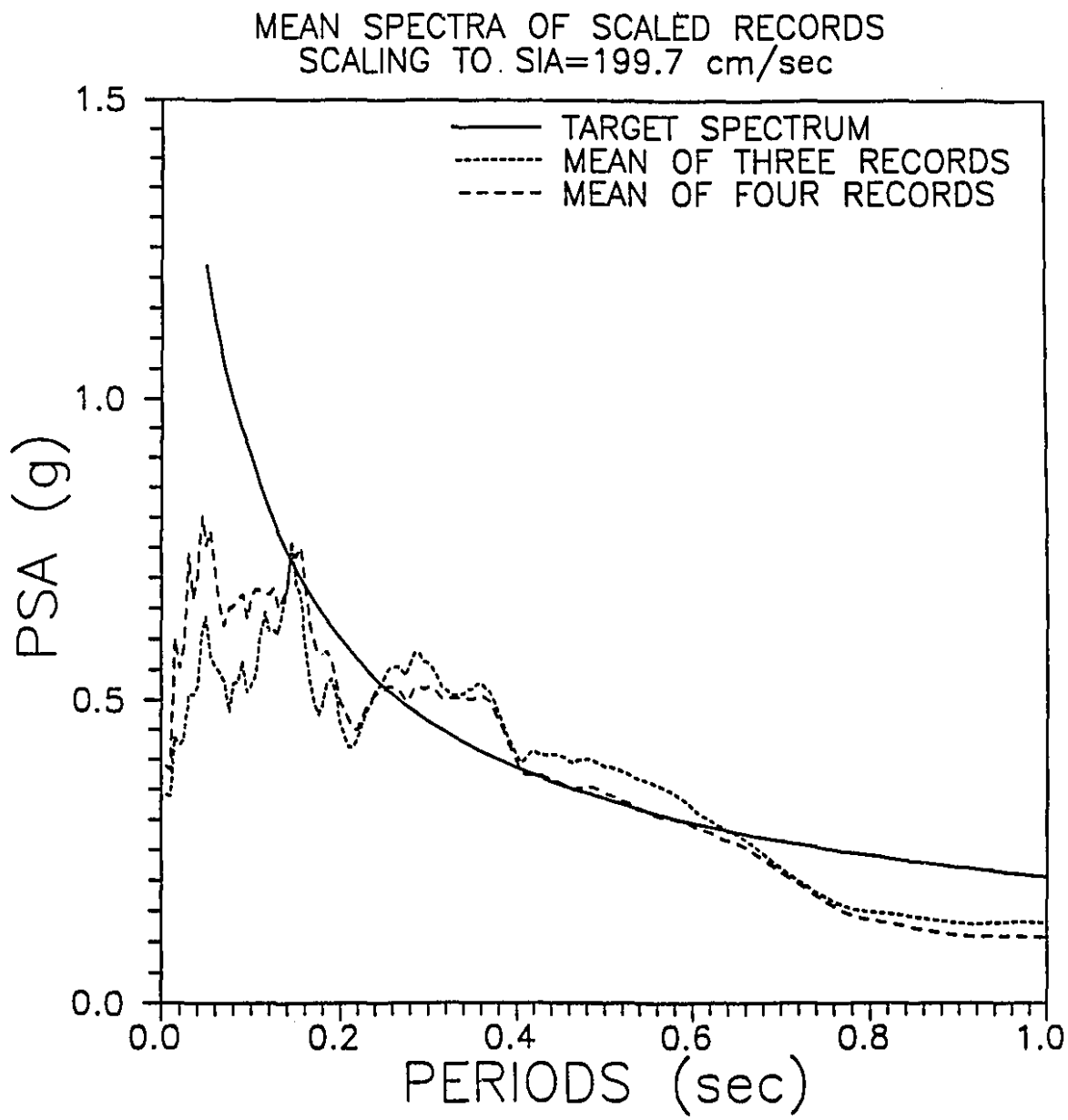

Figure 3.5: Effect of a high frequency motion on the mean spectrum of scaled records.

Figure 3.6: Time histories and spectra of modified records

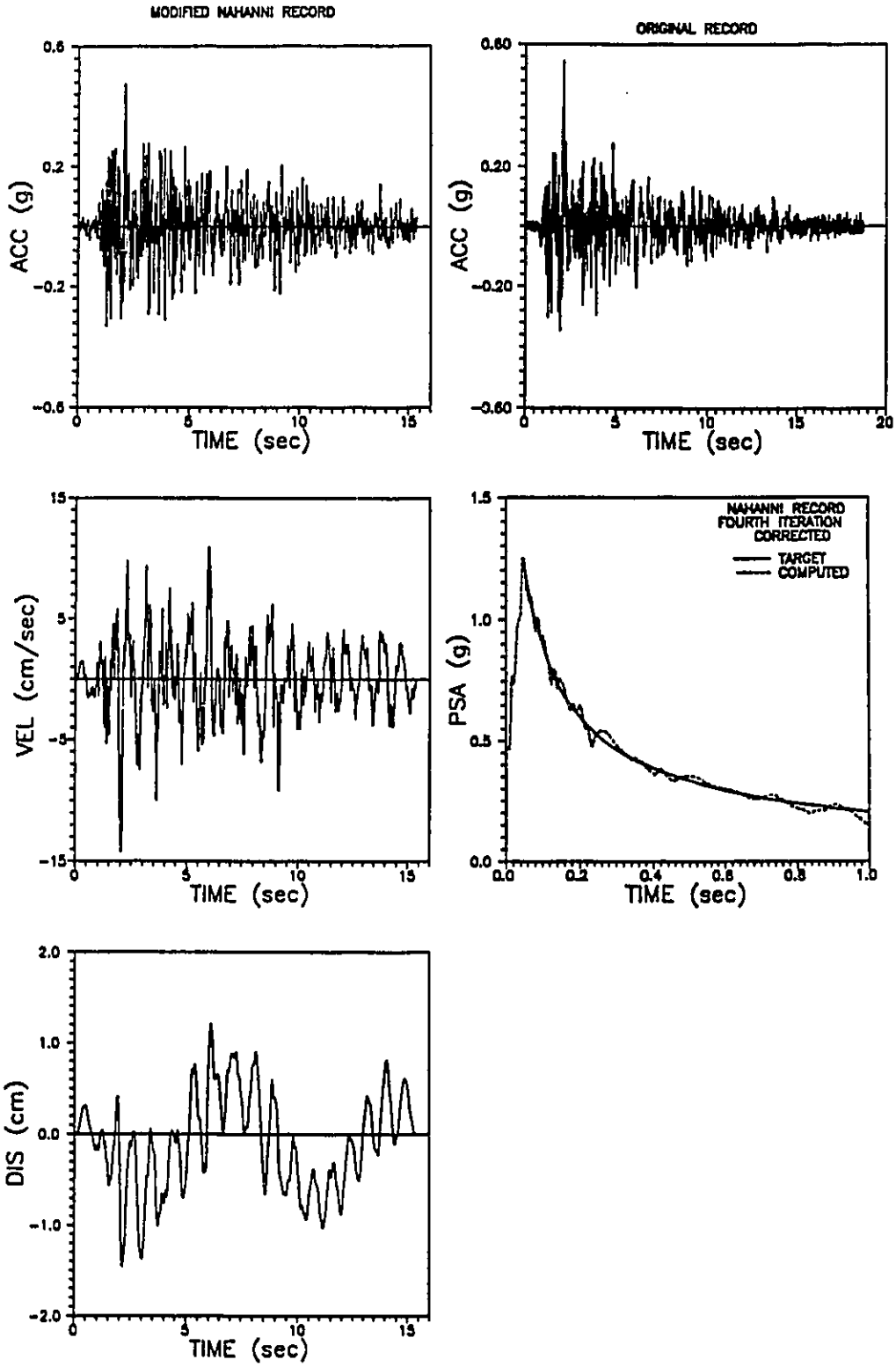

Figure 3.6a : Modified Nahanni record.

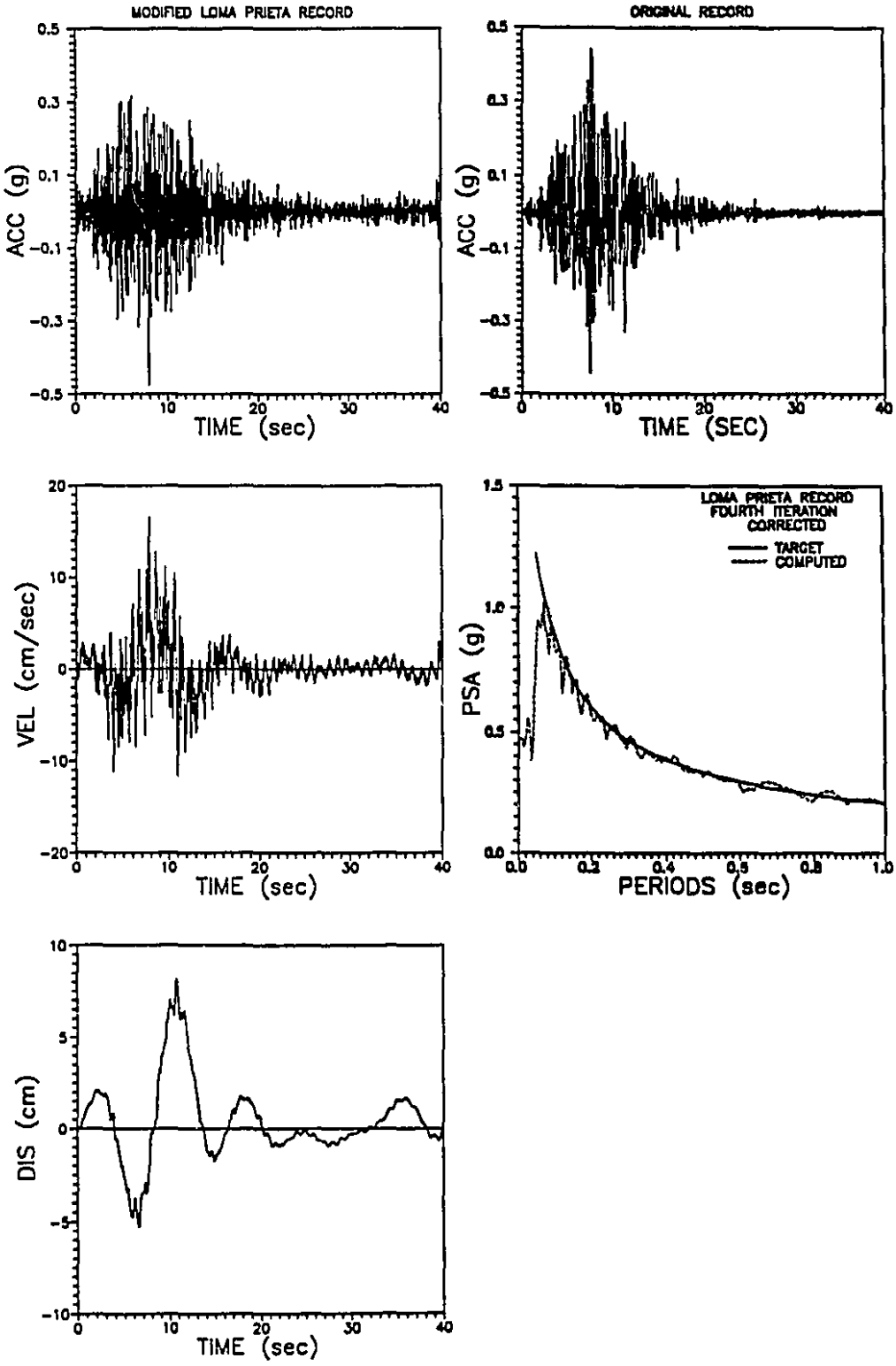

Figure 3.6b : Modified Loma Prieta record.

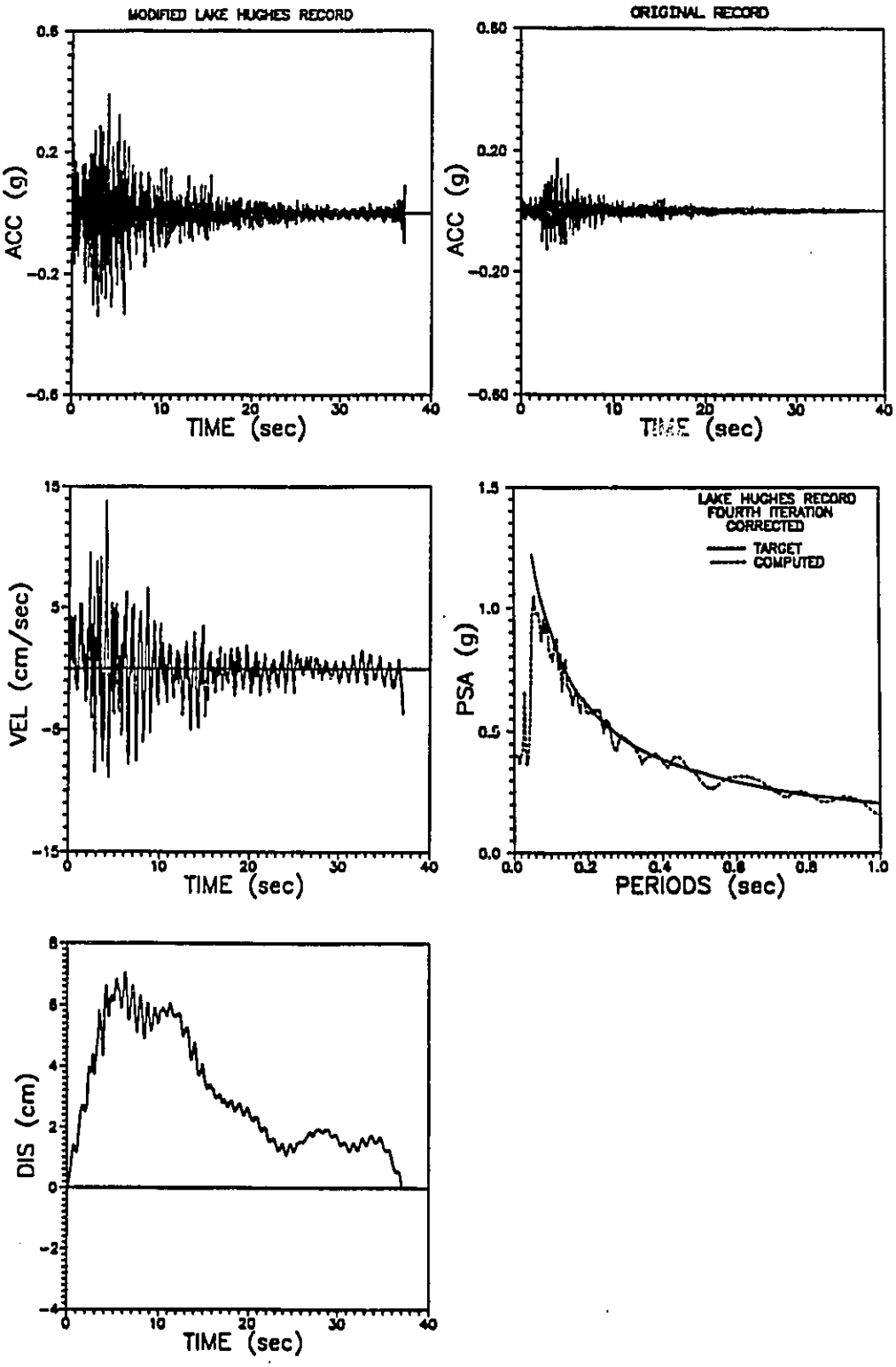

Figure 3.6c : Modified Lake Hughes record.

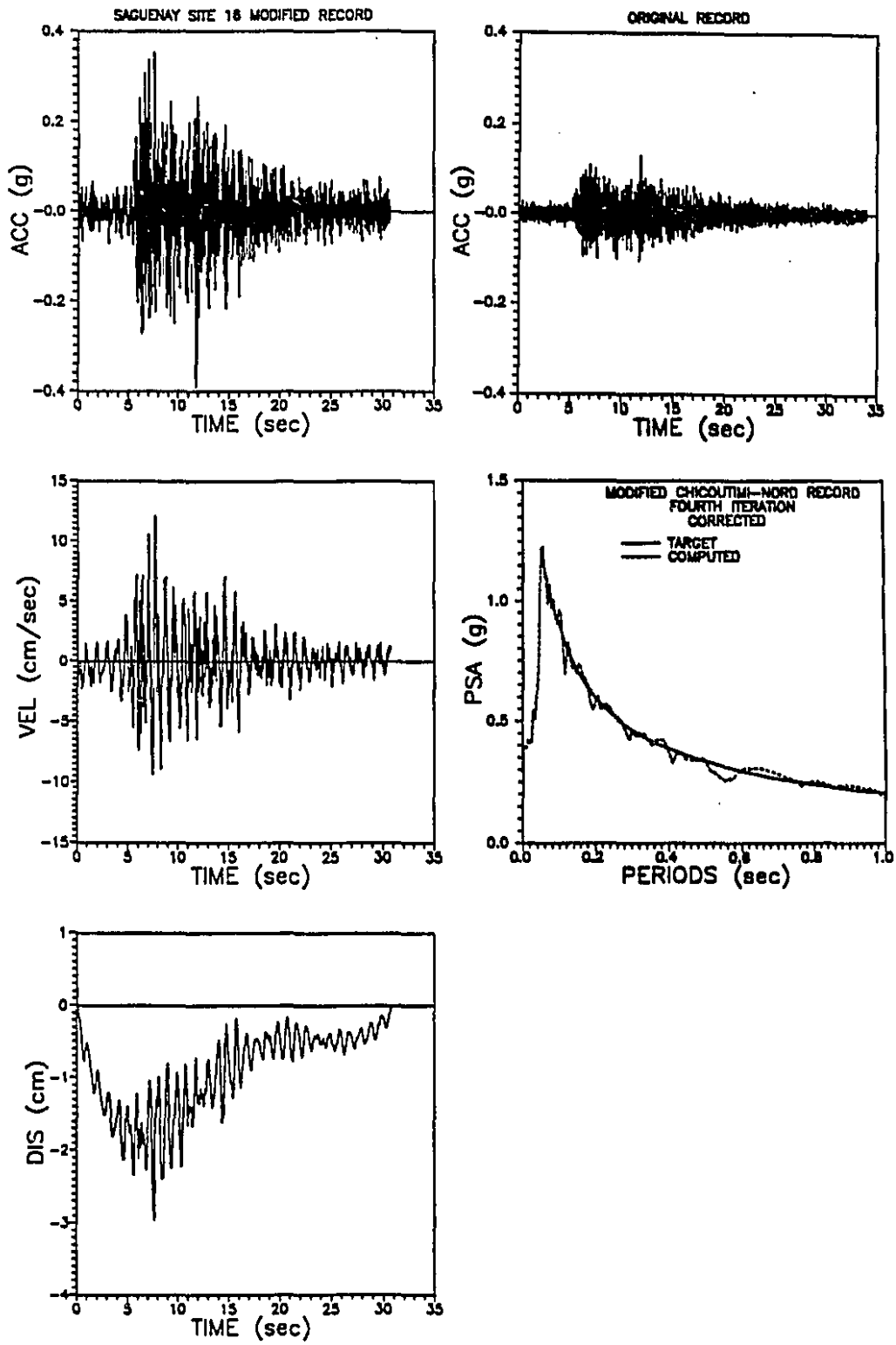

Figure 3.6d : Modified Saguenay Site 16 record.

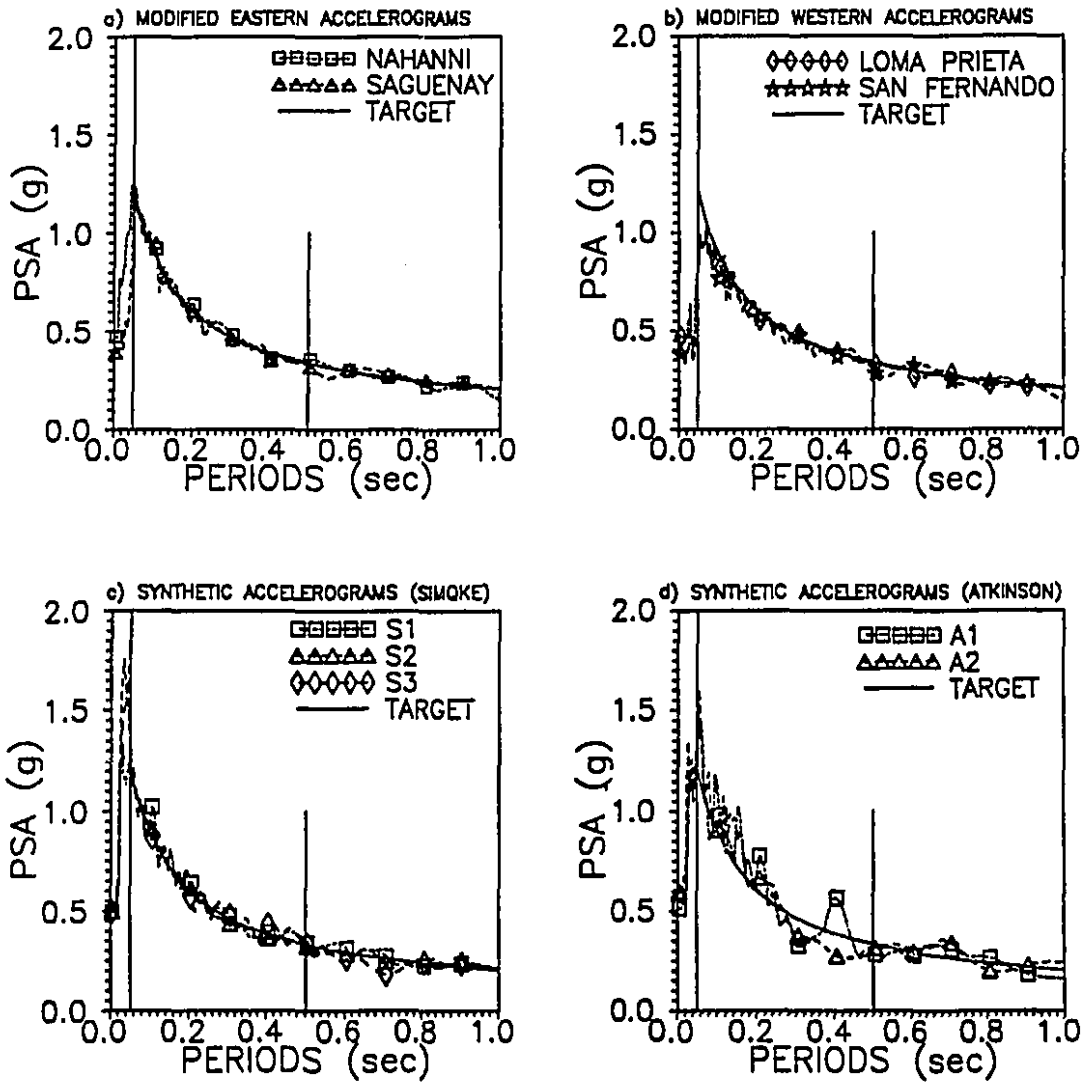

Figure 3.7: Spectra of artificial accelerograms

3.5.2 Artificial earthquakes generated from filtered white noise

Using the program SIMQKE (1976), with a duration of 15 seconds as suggested by the CSA Standard CAN-N3-N289.2-M81 (1981), a 5% damping value, the intensity envelope shown in Fig. 3.1, and the M=7 at 20 km spectrum generated from Atkinson and Boore (1990) attenuation functions, as a target spectrum, three time histories were generated and base line corrected for zero mean velocity and zero final displacement. Figures 3.8a,3.8b, and 3.8c show the acceleration velocity and displacement time histories as well as the RS and the excellent spectrum compatibility achieved by these synthetic records. The synthetic accelerograms are rich in motion in the very short period range ($T_1 < 0.10$ sec) even if the cut-off frequency spectral value is maintained down to the zero period. As shown in the previous figures, and in Fig. 3.7c, the synthetic accelerograms (random vibration) achieved an excellent spectrum compatibility. Two additional synthetic accelerograms, A1 and A2 (Figs 3.9a and 3.9b) generated from a random vibration seismological model of Eastern Canada for an M=7 at 20 km event, were provided by Atkinson (1992) for comparison purposes (Fig. 3.7d). Table 3.5 presents a summary of the ground motion parameters obtained from the historical records with modified Fourier Amplitude Spectra, the synthetic time histories generated from SIMQKE, and those provided by Atkinson (1992). The simulated records (modified and generated by SIMQKE) were generated after four iterations, and all were base line corrected. The artificial accelerograms show high values of RMSA and AI as compared to the real records. They also have a more or less constant $\frac{a}{v}$ ratio, ranging from 2.8 to 3.3. Almost all modified accelerograms have the same D3 duration, as well as for the synthetic accelerograms. The numbers of zero crossings of all artificial (modified or synthetic) accelerograms are higher than those of Western historical records, and lower than those of Eastern records.

3.5.3 Analysis of the acceleration pulses characteristics

The ground motion characteristics required to assess the inelastic dynamic response of structural systems include the severity of duration of strong shaking, and the number and characteristics of intense, relatively long acceleration pulses (Bertero 1979). Large

Figure 3.8: SIMQKE generated motions time histories and spectra

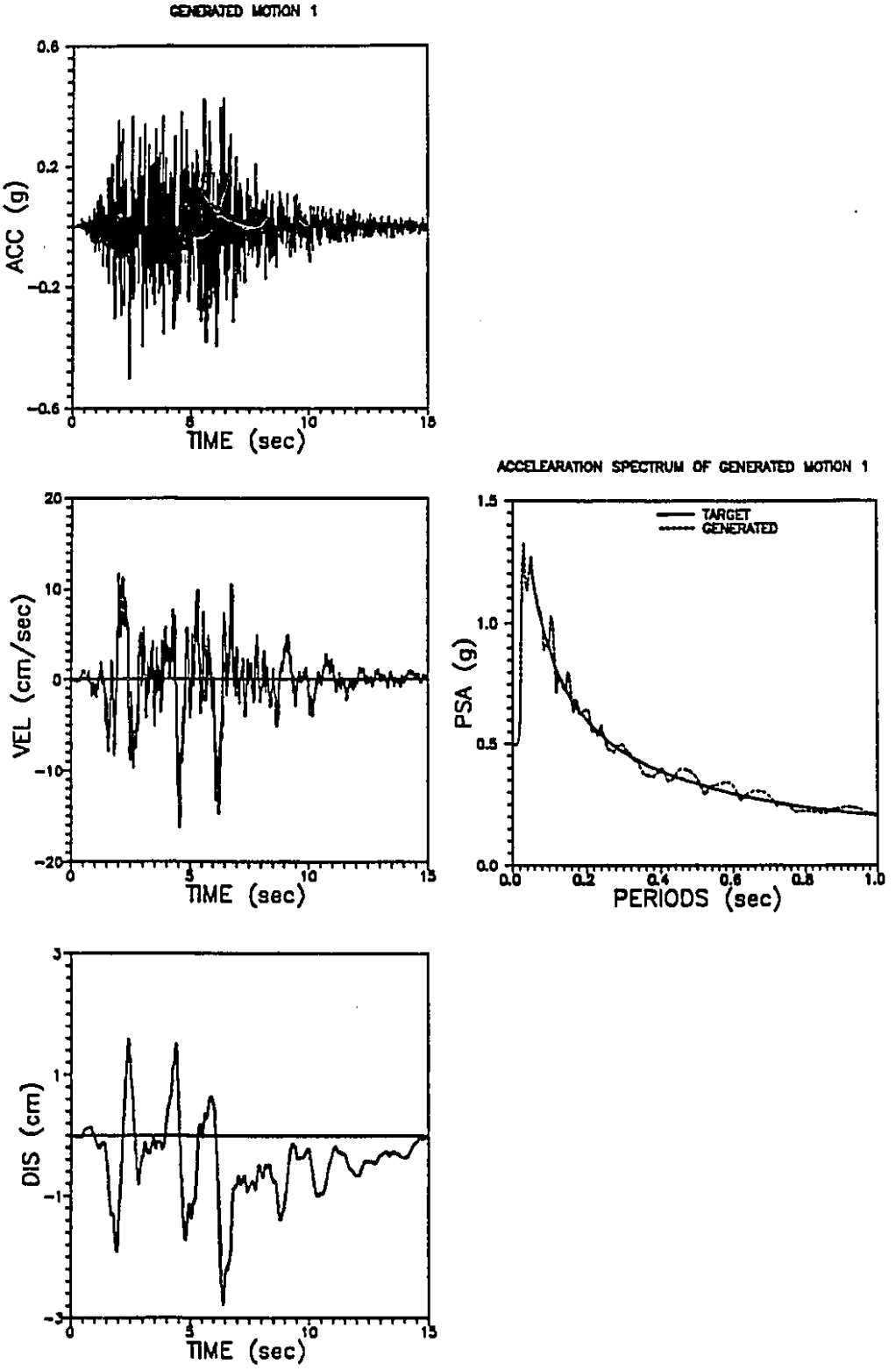

Figure 3.8a : SIMQKE generated motion S1.

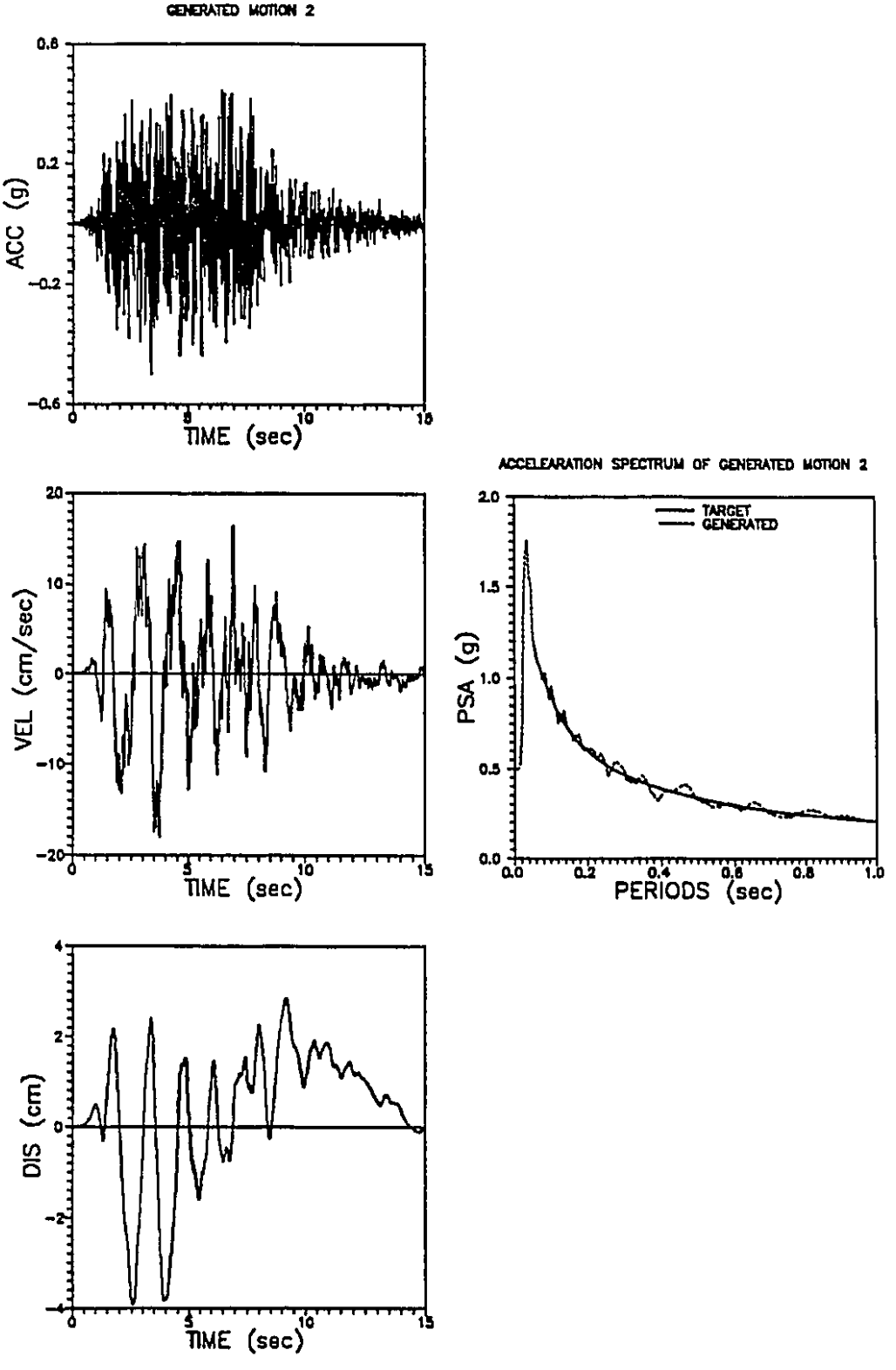

Figure 3.8b : SIMQKE generated motion S2.

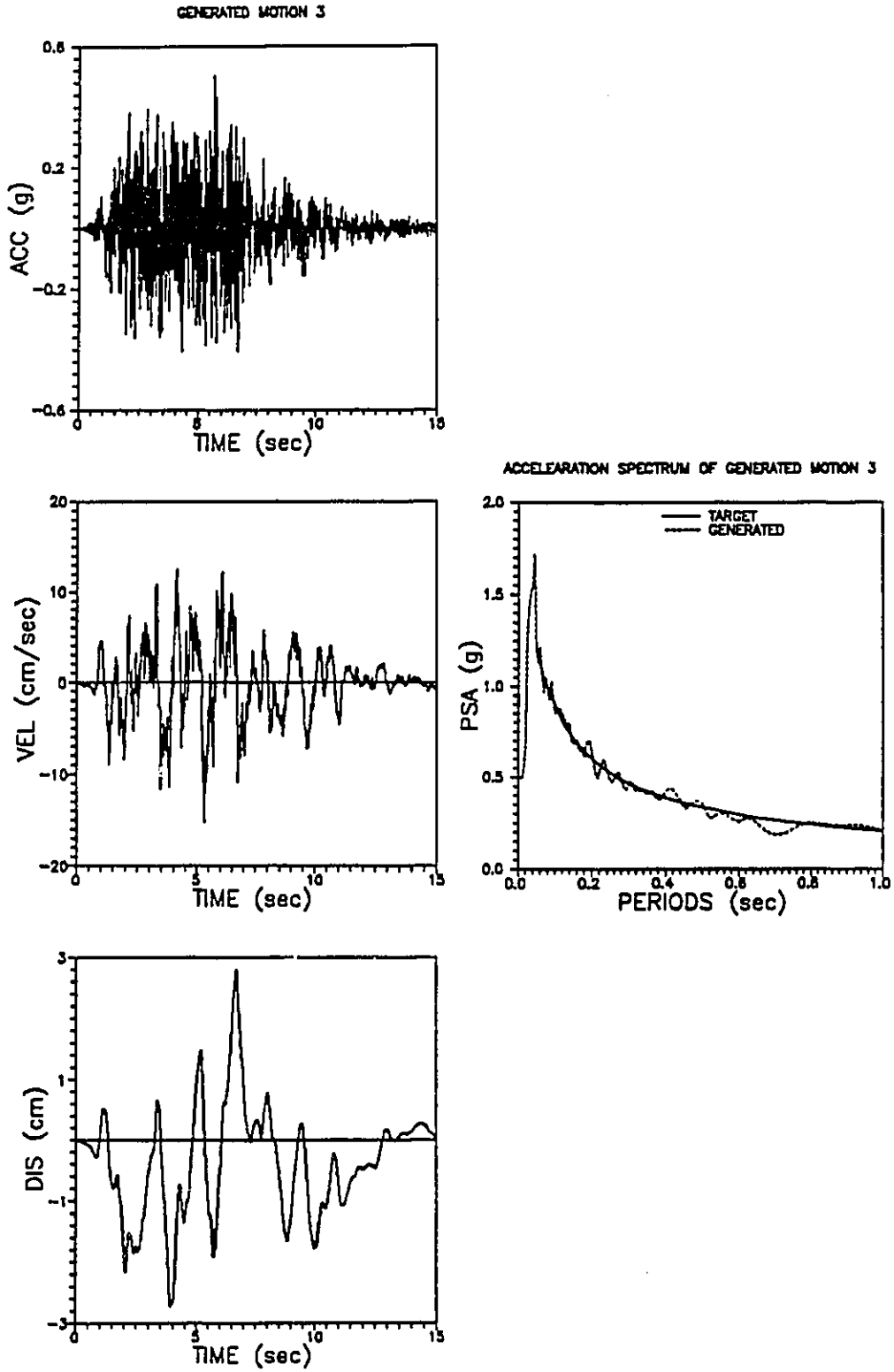

Figure 3.8c : SIMQKE generated motion S3.

Figure 3.9: Atkinson generated motions time histories and spectra

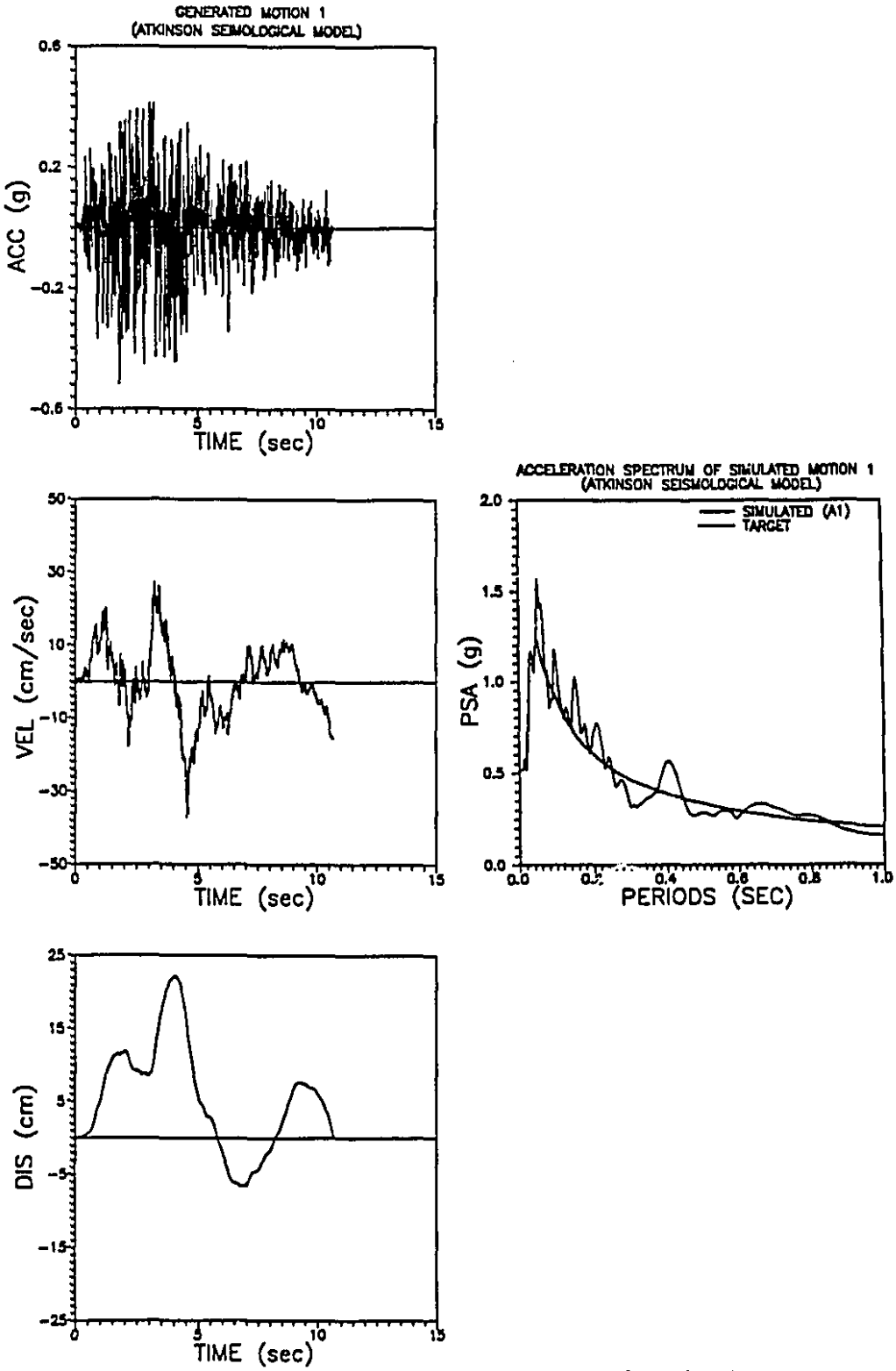

Figure 3.9a : Atkinson generated motion 1.

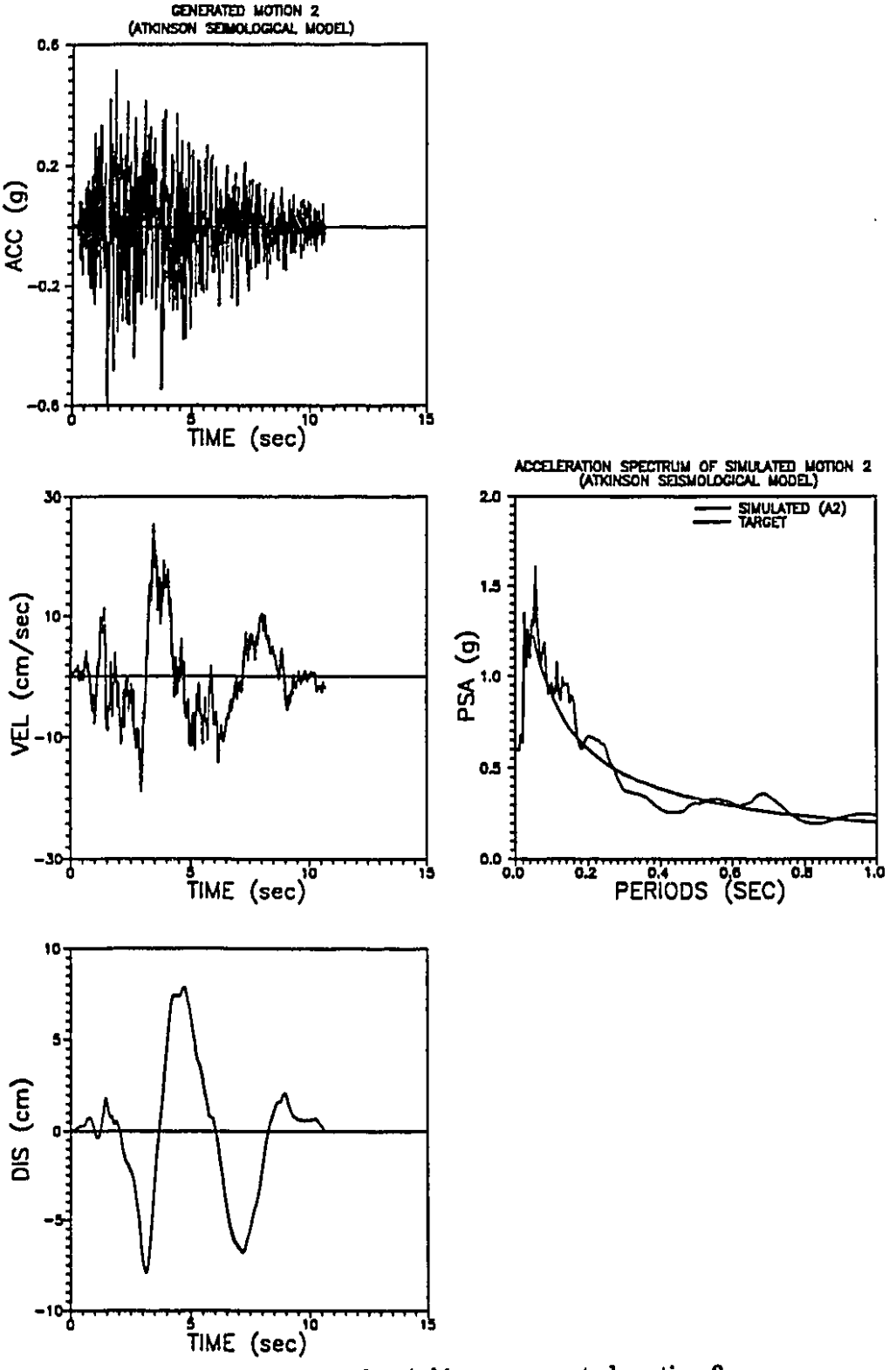

Figure 3.9b : Atkinson generated motion 2.

	PGA (g)	PGV (cm/sec)	a/v (g*sec/m)	D1 (sec)	D2 (sec)	D3 (sec)	$SI_{(0.1)}$ (cm/sec)	$SI_{(0.04)}$ (cm/sec)	SI_v (cm)	RMSA (g) *100	AI (g^2*sec) *1000	NZC	PPS (sec)
Historical records with modified Fourier amplitude spectrum													
Nahanni	0.472	14.20	3.3	13.5	14.2	10.2	205.8	269.7	31.6	7.51	86.6	488	0.063
Loma Prieta	0.474	16.45	2.9	14.1	39.0	15.2	199.6	248.8	33.2	6.44	166.3	1171	0.068
San Fernando	0.388	13.81	2.8	37.0	37.0	15.2	198.9	246.7	32.6	5.68	119.5	940	0.079
Mean spectrum							201.4	255.1	32.5				
Saguenay S16	0.391	12.09	3.2	14.9	29.4	15.4	202.7	260.3	34.0	5.91	107.3	1043	0.059
Synthetic time histories (white noise)													
S1	0.500	16.19	3.1	7.4	11.0	6.3	206.9	270.9	52.3	9.11	124.5	552	0.054
S2	0.500	18.00	2.8	8.0	12.3	7.1	207.5	276.0	82.8	11.35	193.2	680	0.044
S3	0.500	15.15	3.3	8.4	11.5	6.4	205.9	274.9	57.6	9.85	145.6	623	0.048
Synthetic time history (Random vibration seismological model)													
A1	0.520	48.88	1.2	7.8	10.2	6.8	214.2	282.1	91.3	13.0	170.6	443	0.048
A2	0.600	25.95	2.3	8.6	10.3	6.7	201.2	271.1	76.6	12.0	166.3	435	0.049

Table 3.5 : seismic parameters of artificial accelerograms.

deformations can be induced by the presence of a single pulse with an effective acceleration larger than the yield strength of the structure. Repeated application of intense long acceleration pulses can lead to low cycle fatigue and incremental collapse.

Since most researchers criticized the artificial accelerograms because of their excessive number of acceleration pulses, an analysis was made on the characteristics of these pulses for the three types of accelerograms considered in this study: (i) scaled historical records, (ii) Fourier modified records, and (iii) synthetic accelerograms. An acceleration pulse is defined as the segment of an accelerogram between any two successive zero crossing points (Chopra and Lopez 1979). Consequently the number of pulses is equal to the number of zero crossings minus one. This is presented in Table 3.6 where A is the area under the pulse (amplitude of the pulse) corresponding to the incremental ground velocity, DP is the pulse duration, TP is the time of occurrence of the pulse, I1, I5, I10, I20, and I50 are the numbers of pulses which amplitude are as follows :

$$
\begin{array}{llcccl}
(i) & I1 & : & & A \leq 1 & cm/sec \\
(ii) & I5 & : & 1 < A \leq 5 & & cm/sec \\
(iii) & I10 & : & 5 < A \leq 10 & & cm/sec \\
(iv) & I20 & : & 10 < A \leq 20 & & cm/sec \\
(v) & I50 & : & 20 < A \leq 50 & & cm/sec
\end{array}
$$

It is observed from Table 3.6 that the different scaling procedures do not affect the various indexes characterizing the pulses, and the length and time of occurrence of the largest and longest pulses, except the amplitude which varies linearly with the value of the scaling factor. It can also be inferred that the amplitude of the largest pulse follows the intensity of the ground motion (magnitude and distance), in fact the largest pulse amplitude is that of Nahanni (M=6.9 at 7.4 km), then Loma Prieta 1989 (M=6.9 at 16 km), then San Fernando (M=6.5 at 25 km), and finally Saguenay 1988 (M=5.9 at 43 km). In general the largest pulse and the longest pulse do not occur at the same time. Initially Eastern records have a higher number of pulses than the Western records, especially for the 1988 Saguenay record, and also have shorter longest pulses, and in general more small short pulses and less large long pulses than Western records. The use of modified historical records decreased the total number of acceleration pulses, ISUM, for the Eastern records,

and increased this number for the Western records. The amplitudes and durations of the largest pulses are comparable, as well as the durations of longest pulses.

Synthetic accelerograms have similar number and amplitude of pulses. The largest pulses of modified accelerograms have the same time of occurrence as the historical records. Artificial accelerograms have less number of large pulses ($A > 20$ cm/sec) than the historical records, the amplitude of the largest pulse tend also to be smaller.

	LARGEST PULSE			LONGEST PULSE					NUMBER OF PULSES			
	A cm/sec	DP sec	TP sec	A cm/sec	DP sec	TP sec	I1	I5	I10	I20	I50	ISUM
ORIGINAL HISTORICAL RECORDS												
NAHANNI	27.491	.140	2.075	23.767	.225	5.945	589	144	16	3	2	754
LOMA PRIETA	28.278	.100	7.800	3.061	.360	19.120	204	111	37	30	14	396
SAN FERNANDO	11.102	.080	3.820	.984	.260	27.680	488	89	7	1	0	585
SAGUENAY	4.215	.070	7.575	2.521	.090	7.790	2332	51	0	0	0	2383
HISTORICAL ACCELEROGRAMS, SCALING METHOD 1 ($SI_{a_{0.2}}$)												
NAHANNI	25.798	.140	2.075	22.304	.225	5.945	603	132	14	3	2	754
LOMA PRIETA	13.234	.100	7.800	1.433	.360	19.120	269	86	32	9	0	396
SAN FERNANDO	20.082	.080	3.820	1.779	.260	27.680	413	146	19	6	1	585
SAGUENAY	17.143	.070	7.575	10.252	.090	7.790	1898	457	25	3	0	2383
HISTORICAL ACCELEROGRAMS, SCALING METHOD 1 ($SI_{a_{2.0}}$)												
NAHANNI	25.394	.140	2.075	21.954	.225	5.945	603	132	14	3	2	754
LOMA PRIETA	15.470	.100	7.800	1.675	.360	19.120	260	50	30	15	0	395
SAN FERNANDO	22.142	.080	3.820	1.962	.260	27.680	394	160	22	7	1	584
SAGUENAY	16.171	.070	7.575	9.671	.090	7.790	1929	431	22	1	0	2383
HISTORICAL ACCELEROGRAMS, SCALING METHOD 2 (PGA)												
NAHANNI	25.221	.140	2.075	21.805	.225	5.945	604	133	12	3	2	754
LOMA PRIETA	32.133	.100	7.800	3.479	.360	19.120	196	112	39	32	16	395
SAN FERNANDO	32.653	.080	3.820	2.893	.260	27.680	329	209	26	15	5	585
SAGUENAY	16.087	.070	7.575	9.620	.090	7.790	1929	431	22	1	0	2383
HISTORICAL ACCELEROGRAMS, SCALING METHOD 3 (mean $SI_{a_{0.2}}$)												
NAHANNI	17.579	.140	2.075	15.198	.225	5.945	643	101	6	4	0	754
LOMA PRIETA	16.468	.100	7.800	1.783	.360	19.120	253	94	31	18	0	396
SAN FERNANDO	21.362	.080	3.820	1.893	.260	27.680	400	155	21	7	1	584
MODIFIED HISTORICAL ACCELEROGRAMS												
NAHANNI	15.283	.075	2.095	12.896	.165	5.965	284	151	47	6	0	488
LOMA PRIETA	12.439	.080	7.760	6.853	.160	6.380	789	309	67	6	0	1171
SAN FERNANDO	19.476	.080	3.880	1.026	.140	33.280	601	296	39	3	0	939
SAGUENAY	19.105	.110	7.590	5.933	.205	4.860	680	327	34	2	0	1043
SYNTHETIC ACCELEROGRAMS (RANDOM VIBRATIONS)												
S1	18.525	.135	4.365	.170	.220	.005	321	189	37	5	0	552
S2	13.826	.055	4.610	.113	.155	.005	361	263	51	5	0	680
S3	13.354	.090	3.295	4.467	.125	11.005	367	223	26	7	0	623
SYNTHETIC ACCELEROGRAMS (SEISMOLOGICAL MODEL)												
A1	16.884	.070	1.270	4.952	.110	10.480	184	197	43	9	0	433
A2	20.673	.120	1.380	1.120	.200	.010	176	216	40	6	1	439

Table 3.6 : Pulses characteristics.

Chapter 4

Inelastic Response of SDOF Systems

4.1 Systems analyzed

Two hysteretic models have been used to describe the behaviour of SDOF systems with elastic periods of vibration varying from 0.04 sec to 1 sec, the Modified Clough Stiffness Degrading model (SDM), and the Bilinear model (BM), both with a strain hardening parameter $\alpha = 10\%$ and a 5% viscous damping ratio. Figures 4.1a and 4.1b illustrate the characteristics of each hysteresis model.

A nondimensional parameter, η, is used to characterize the strength of the SDOF systems. The parameter η is expressed as the ratio of the base shear at yield, V, to the maximum effective force applied during the earthquake:

$$\eta = \frac{V}{M * PGA} \tag{4.1}$$

where M is the mass of the system ($M = 100kN.sec^2/m$ for this study) and the PGA is expressed in consistent units with the mass. A value of $\eta = 0.6$, which is typical of reinforced concrete structures, has been selected. This value will be modified in parametric analyses.

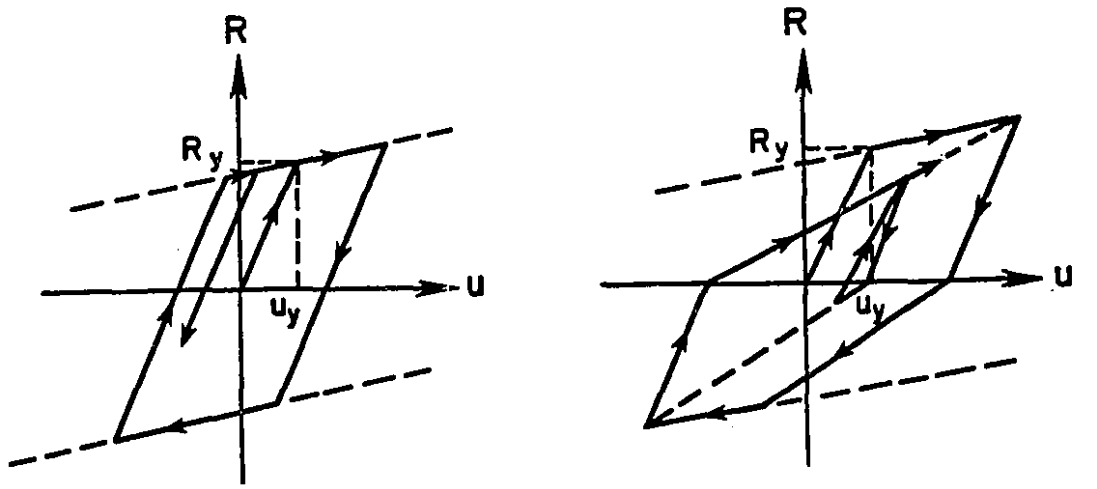

(A) Bilinear Model (B) Stiffness Degrading Model

Figure 4.1: Hysteresis models

4.2 Inelastic response indicators

To interpret the nonlinear response time-histories, that were computed using the computer program NONSPEC (Mahin and Lin 1983), several indices reflecting the inelastic performance of the structures are defined :

(i) The maximum displacement ductility, μ_{max}, which is the maximum absolute value of the displacement response normalized by the yield displacement of the system during one yield excursion,

(ii) The accumulated displacement ductility, μ_{acc}, which corresponds to the sum of the absolute values of inelastic deformations normalized by the yield displacement plus one. This ductility index gives a measure of the total amount of inelastic deformation and may be more important than peak ductility for structures susceptible to low cycle fatigue.

(iii) The number of yield events (NYE) and zero crossings (NZC). Yielding is defined as an excursion on the primary post yield envelope curve. For the stiffness degrading model a "yield event" is restricted to the primary post

yield envelope curve, and small hysteresis loops are not counted. The NZC gives an indication of the mean frequency of the response which may be altered by inelastic behaviour.

(iv) The absolute seismic input energy, E_i, and the ratio of the energy dissipated by hysteresis, E_h, to the amount of input energy, $\frac{E_h}{E_i}$. Detailed expressions for the computation of E_h and E_i can be found in Uang and Bertero (1990).

(v) The maximum relative displacement u_{max}.

A parametric study on the strain hardening ratio α, showed that for the stiffness degrading model, and for all type of selected and generated accelerograms, all the chosen response parameters were sensitive to the value of α, in the short period range 0.04-0.20 sec. This is clearly shown in Fig. 4.2. However for the bilinear model, only the maximum ductility appeared to be sensitive to strain hardening ratio. Therefore one must carefully model the strain hardening characteristics of short period structures when inelastic analyses are done.

4.3 Seismic response analysis

The results reported in this section are for SDOF with $\eta = 0.6$ with a stiffness degrading hysteresis model.

4.3.1 Influence of scaling procedures

Only absolute response parameters like E_i and u_{max} are very sensitive to different scaling procedures, the other normalized parameters as well as the NZC and the NYE, are not affected by the scaling procedure. For example Fig. 4.3 shows the E_i and μ_{max} variations for different scaling procedures. The scaling to PGA (SM2) produces a lot of dispersion in the E_i responses, especially for the Western records. For short-period structures scaling to SI_a (SM1) groups the absolute parameters (E_i and u_{max}) better than the other scaling methods. However, for periods longer than 0.4 sec, the SM3 gives a better grouping and less dispersion. It was decided to scale all historical records to $SI_{a(.10)}$ since we are interested in short- periods, and there is a mixture of Eastern and Western records.

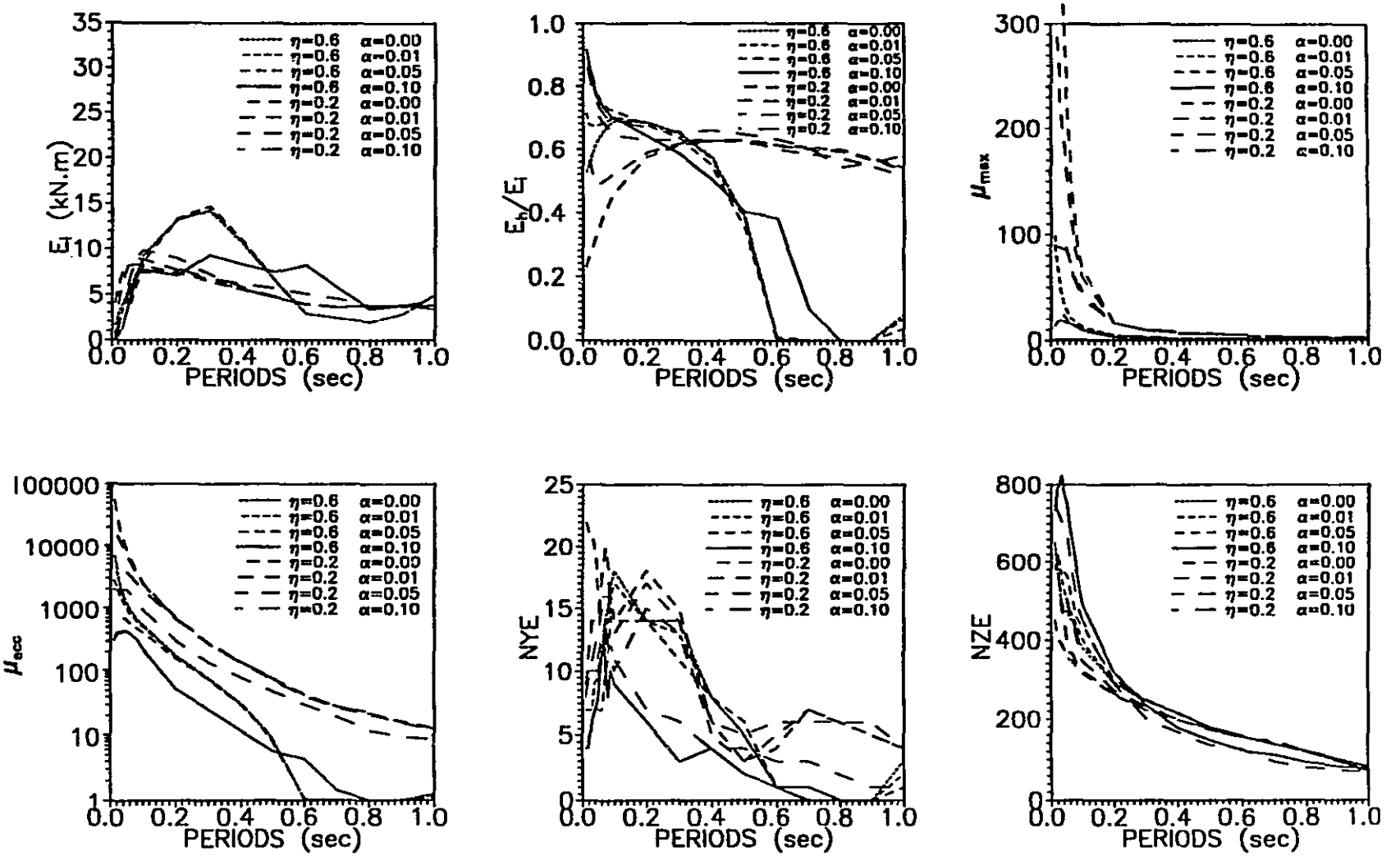

Figure 4.2 : Influence of the strain hardening ratio.

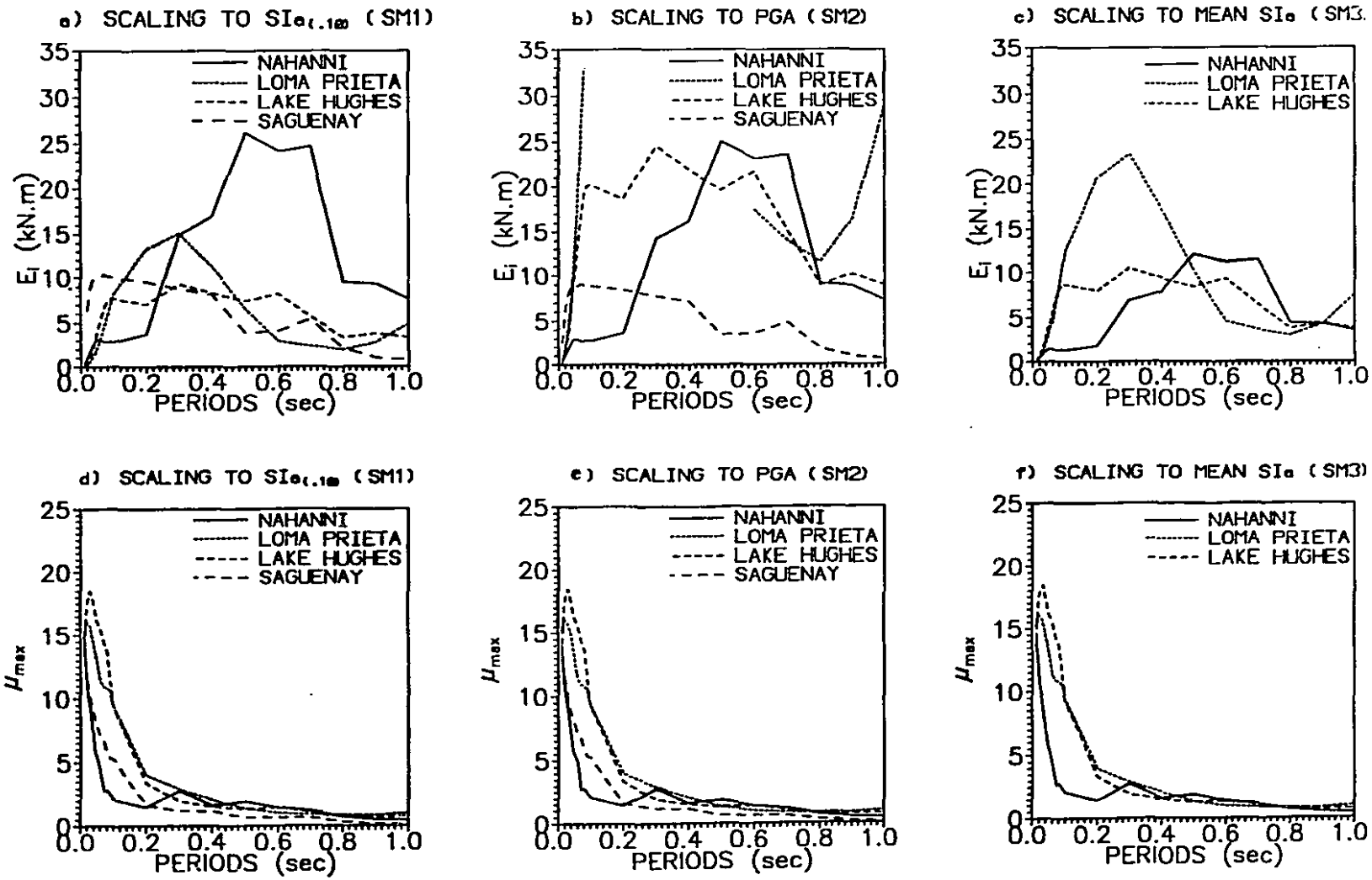

Figure 4.3 Effect of scaling procedures on E_i and μ_{max}.

4.3.2 Influence of the type of accelerograms

As shown in Figure 4.4, E_i is very sensitive to the details of the input motions. For example, three synthetic accelerograms that have excellent spectrum-compatibility, have some E_i differences after $T_1 = 0.1$ sec (Fig. 4.4c). When $T_1 < 0.1$ sec, the E_i is very similar for all artificial accelerograms (whether modified or synthetic). The least dispersion is observed in the synthetic, then among the modified, and finally in the scaled accelerograms. Overall, the E_i of artificial records is higher than the E_i of scaled historical records.

The responses to the scaled Saguenay record were not included in the computation of the average responses since it has a scaling factor of more than two. However, additional computations have shown that the inclusion of the contribution of the Saguenay record in the average response, introduces an increase in the very short-period region, and a decrease in other regions. For modified records it does not make any difference whether it is added or not. Thus, it appears acceptable to start from historical records that may have a weak intensity but a high frequency content, to generate spectrum-compatible accelerograms for Eastern conditions. In the 0.05-0.2 sec period range, the E_i of artificial accelerograms is higher than the average E_i of scaled records. This is due to the deficiency in high frequency motion of Western scaled records.

Figure 4.5 shows the single, and the average ratios of the hysteretic energy responses to the input energy. The same observations made for E_i are valid for $\frac{E_h}{E_i}$, except for the average $\frac{E_h}{E_i}$ where the scaled records have higher values than artificial accelerograms. Figure 4.5a shows that the $\frac{E_h}{E_i}$ responses tend to be grouped according to their geographical origin (either ENA or WNA), which is especially apparent for $T_1 < 0.2$ sec. Figure 4.6 and Figure 4.7 show that the ductility parameters are more closely grouped than the energy parameters, but the degree of dispersion according to the type of accelerograms is maintained. The scaled records tend to group themselves by geographical origin. Synthetic accelerograms produce the same μ_{max} for $T_1 \geq 0.1$ sec, whereas the modified are so, only for $T_1 \geq 0.2$ sec. It is also observed from the average response in Figure 4.6d, that the ductility demand is very close for the two types of artificial accelerograms, and is lower than the demand for scaled records for the whole period range of interest. Overall, μ_{max} related to Western records is decreased by the use of artificial accelerograms, however it

remains similar for Eastern records.

For μ_{acc}, the dispersion is considerable for the scaled accelerograms (Fig. 4.7a), it starts to occur at $T_1 = 0.5$ sec for the modified accelerograms, but it is minor (Fig. 4.7b). Almost no dispersion in μ_{acc} is observed for the synthetic accelerograms. When compared to scaled historical records, modified accelerograms lead to larger μ_{acc} for Eastern records for $T_1 < 0.3$ sec, and smaller μ_{acc} for Western records with $T_1 < 0.8$ sec. Except for the scaled Nahanni record for $T_1 < 0.2$ sec, all μ_{acc} responses to synthetic accelerograms fall below scaled historical records. Figure 4.7d shows that the average μ_{acc} is larger for scaled historical records than for artificial accelerograms except in the 0.05-0.08 sec period range, and μ_{acc} from modified records is larger than for the synthetic accelerograms.

As shown in Fig. 4.8a the NZC obtained from Eastern records are higher than the values obtained from Western records for $T_1 < 0.10$ sec. This reflects the deficiency of Western records in high frequency motion. The use of artificial earthquakes (modified or synthetic) reduces the NZC of Eastern records, and increases the NZC of Western records. The average NZC of scaled and modified records become similar and larger than the NZC of synthetic accelerograms for $T_1 \geq 0.2$ sec (Fig. 4.8d).

When the NYE is considered, there is also a grouping by geographical origin for $T_1 < 0.15$ sec. In the very short period range, the scaled historical Western records produce less NYE than their Eastern counterparts (Fig. 4.9a). The NYE of artificial accelerograms are larger than the NYE of the scaled Eastern records for $T_1 < 0.2$ sec, and the inverse is observed for the Western records (Fig. 4.10b and 4.10c). For $T_1 \geq 0.2$ sec, the NYE of the Western records is more than for artificial accelerograms. The NYE is a quantity very sensitive to the details of the input accelerogram as shown for the synthetic records that have an excellent spectrum-compatibility (Fig 4.10c). Artificial records lead to fairly similar trends in the NYE. The average NYE of artificial records are larger, in the 0.05-0.20 sec range than NYE obtained from scaled records, this trend is reversed for $T_1 \geq 0.2$ sec.

Figure 4.10 shows u_{max} which is very similar for the modified and synthetic accelerograms, and for scaled accelerograms for $T_1 < 0.2$ sec. For $T_1 \geq 0.2$ sec, u_{max} values computed from scaled accelerograms show a lot of dispersion.

4.3.3 Influence of the hysteresis model and the strength η

The nonlinear structural behaviour of a particular system is always difficult to generalize to other configurations. Thus, the study has been extended to bilinear hysteretic model (BM) considering three different values of strength parameter η : (i) η=5 (linear elastic), (ii) η=0.6 (moderately inelastic R=4, where R is the ductility factor used in the NBCC 1990), and (iii) η=0.2 (highly inelastic R=12). The same analyses made on the SDM with η=0.6 were repeated and all the observed trends were confirmed whether the hysteresis model or the strength η were modified. Sample results are shown in Fig. 4.11a, b, c for μ_{acc}, and Fig. 4.12d, e, f for NYE that are closely related to the degree of inelasticity and thus are very sensitive to changes in the strength and the hysteresis models. Figure 4.11d, e, f shows that the NYE of artificial accelerograms is larger than NYE for scaled records in the very short period range. There is more yielding when the strength is decreased. The SDM shows less NYE because the small hysteresis loops are ignored in the calculation of the NYE.

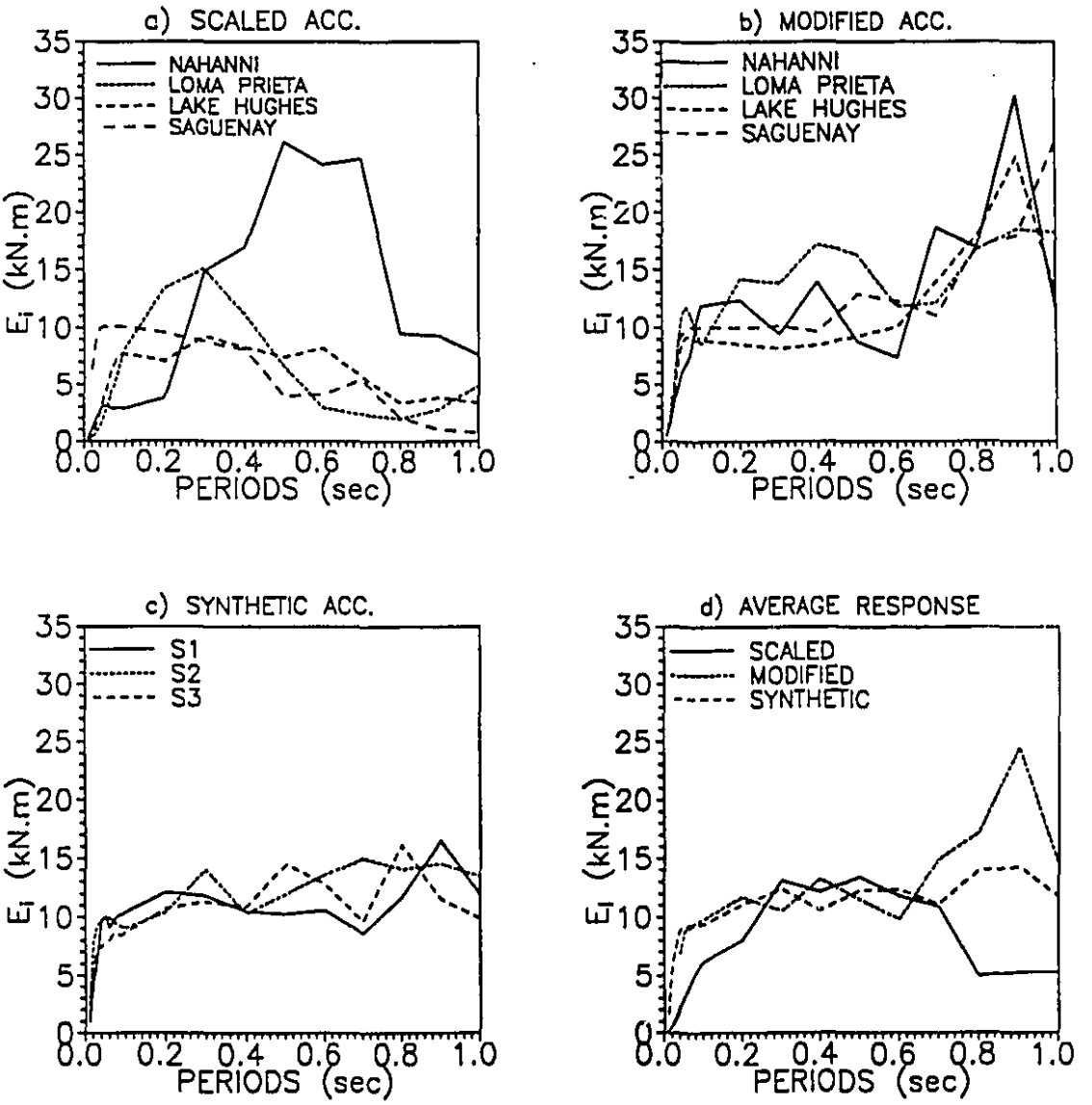

Figure 4.4: Effect of the type of accelerogram on input energy, E_i.

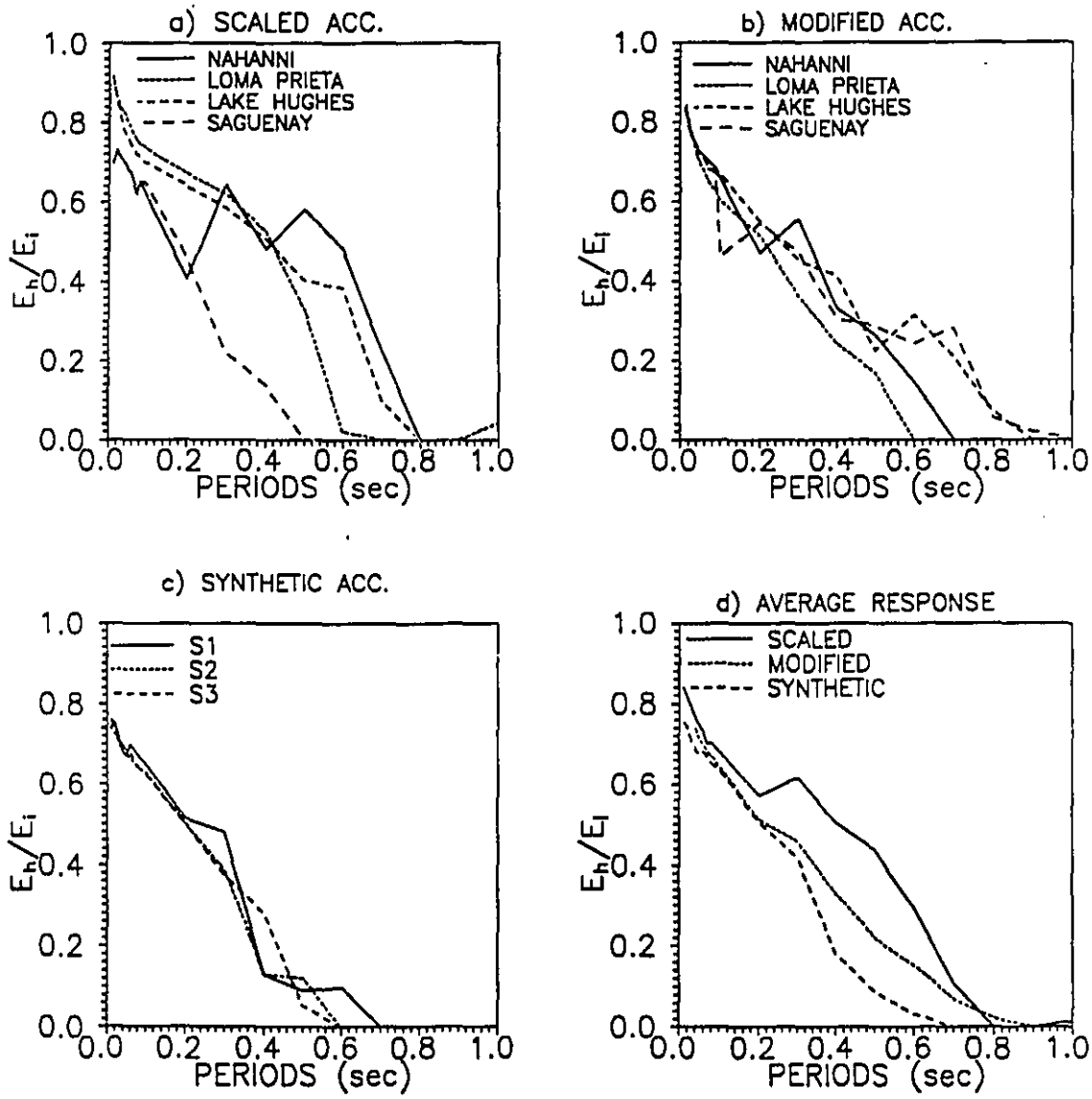

Figure 4.5: Effect of the type of accelerogram on the ratio of hysteretic to input energy, $\frac{E_h}{E_i}$.

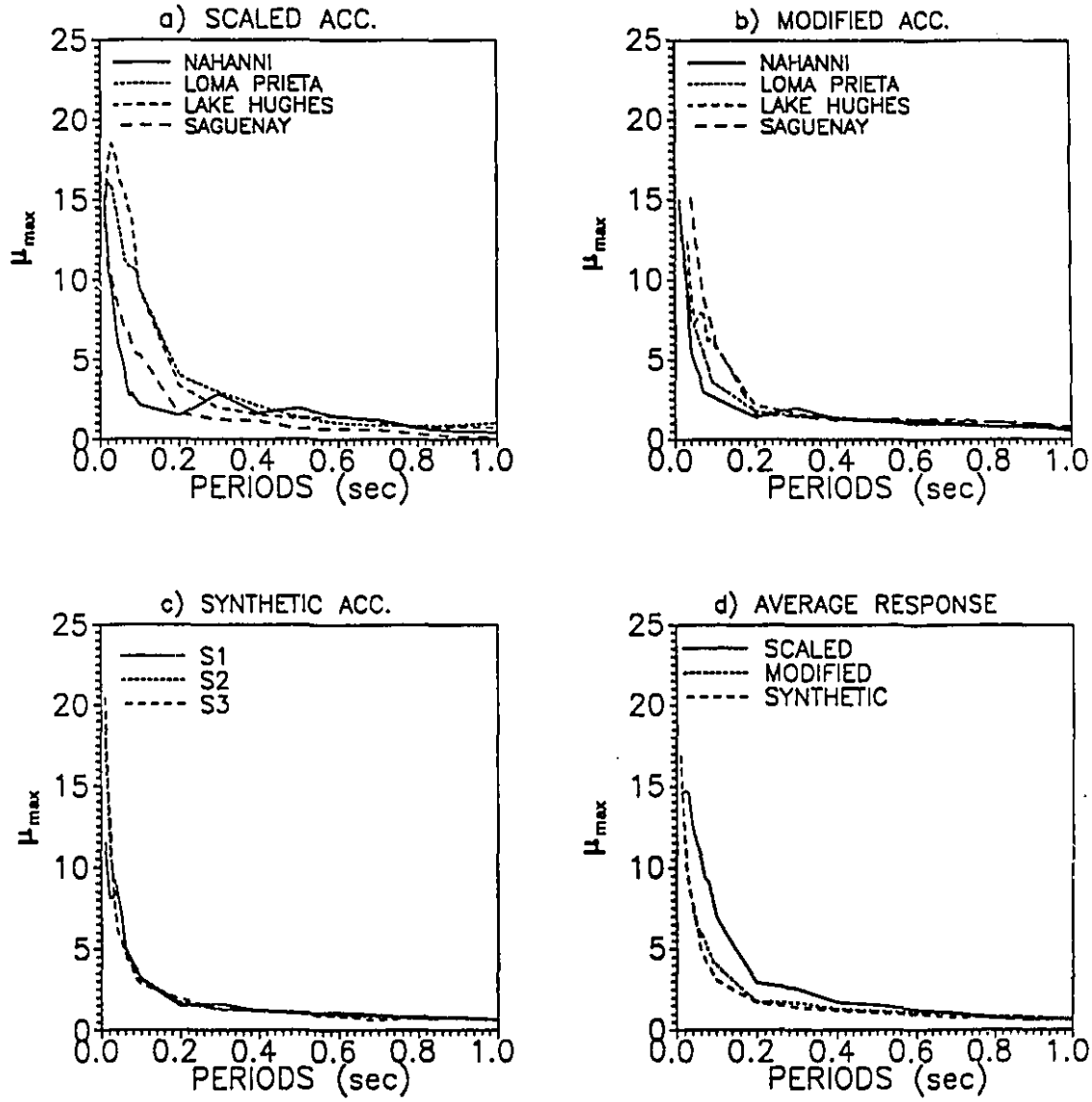

Figure 4.6: Effect of the type of accelerogram on maximum displacement ductility, μ_{max}.

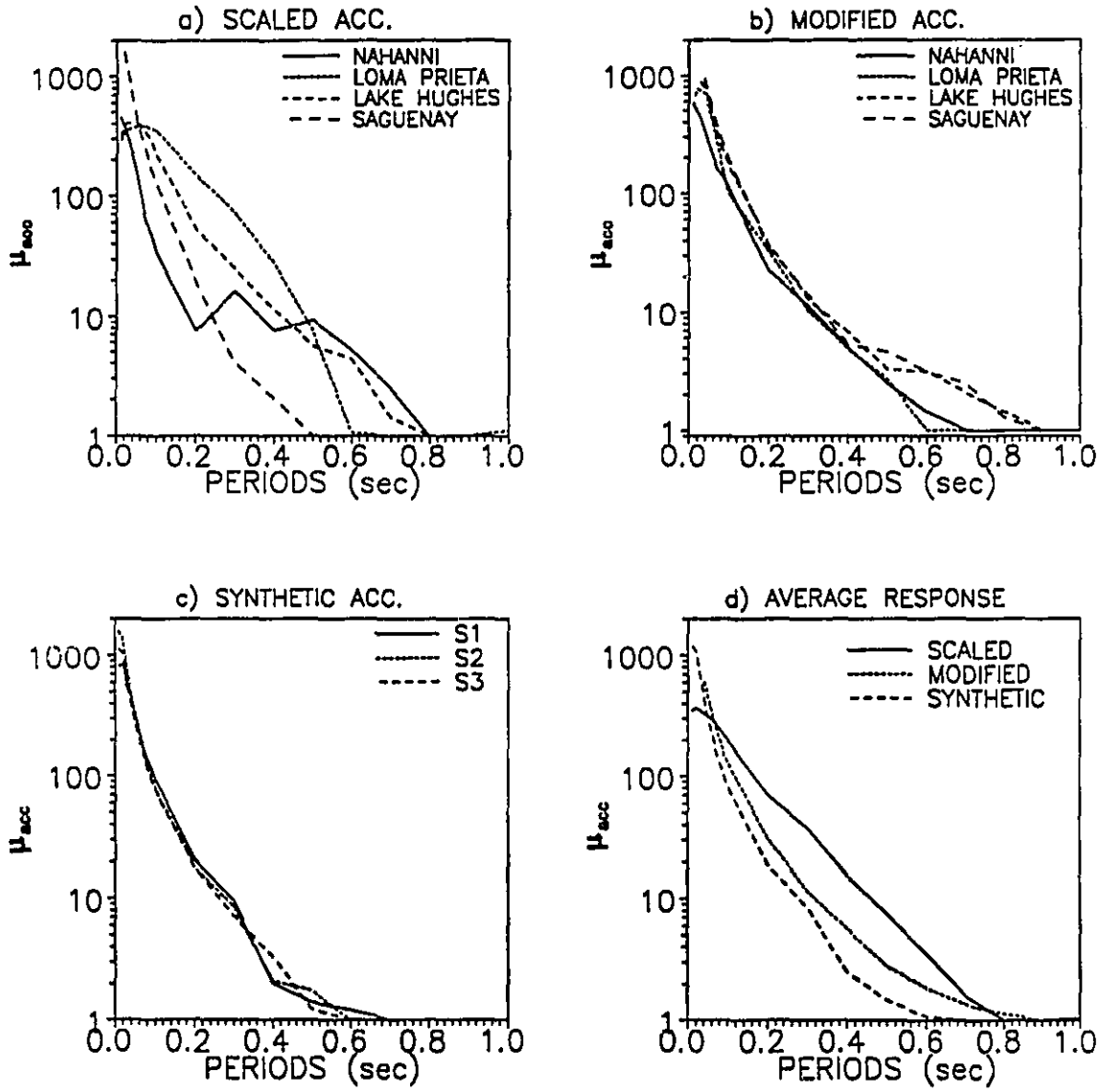

Figure 4.7: Effect of the type of accelerogram on accumulative displacement ductility, μ_{acc}.

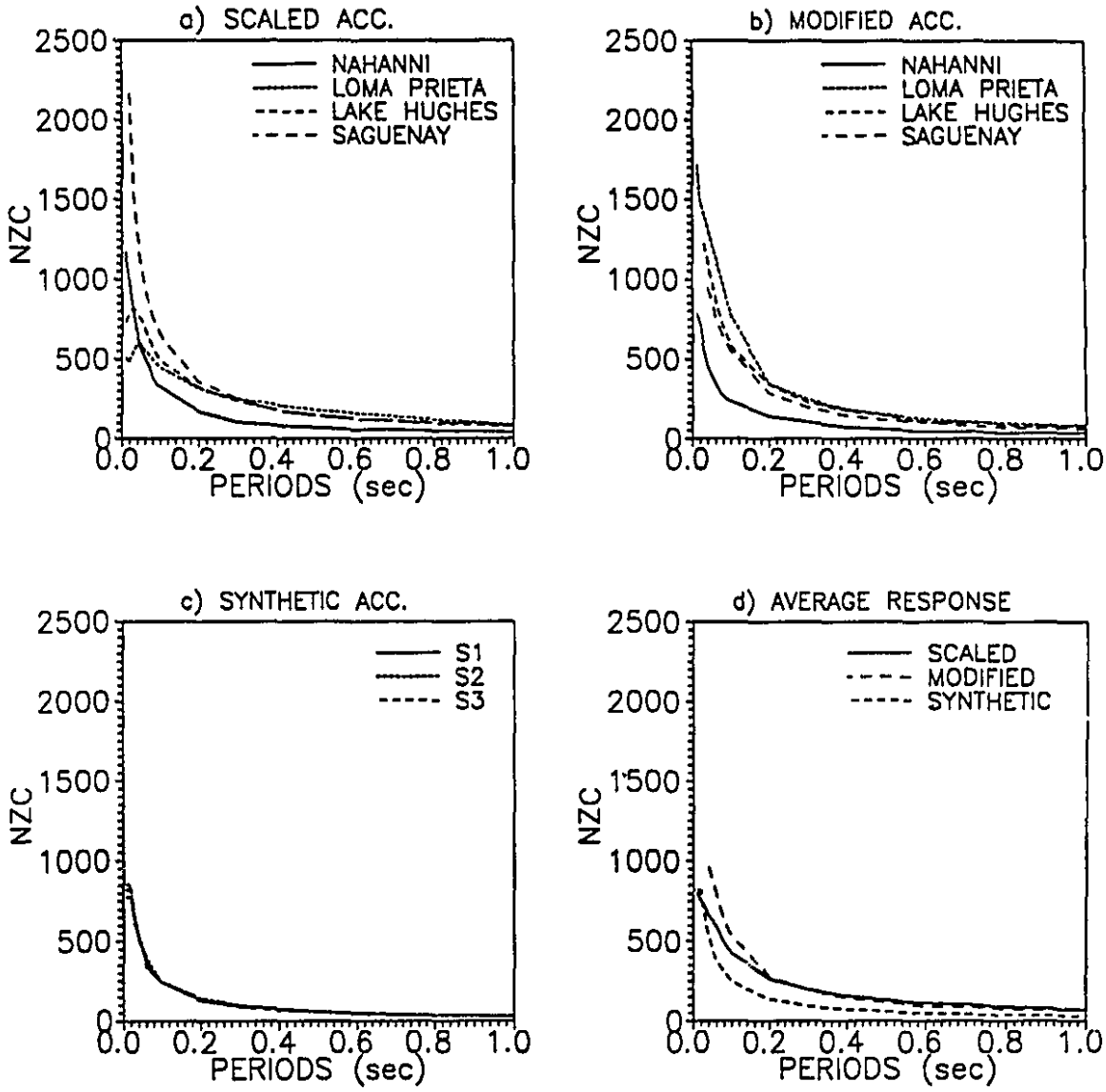

Figure 4.8: Effect of the type of accelerogram on the number of zero crossings, NZC.

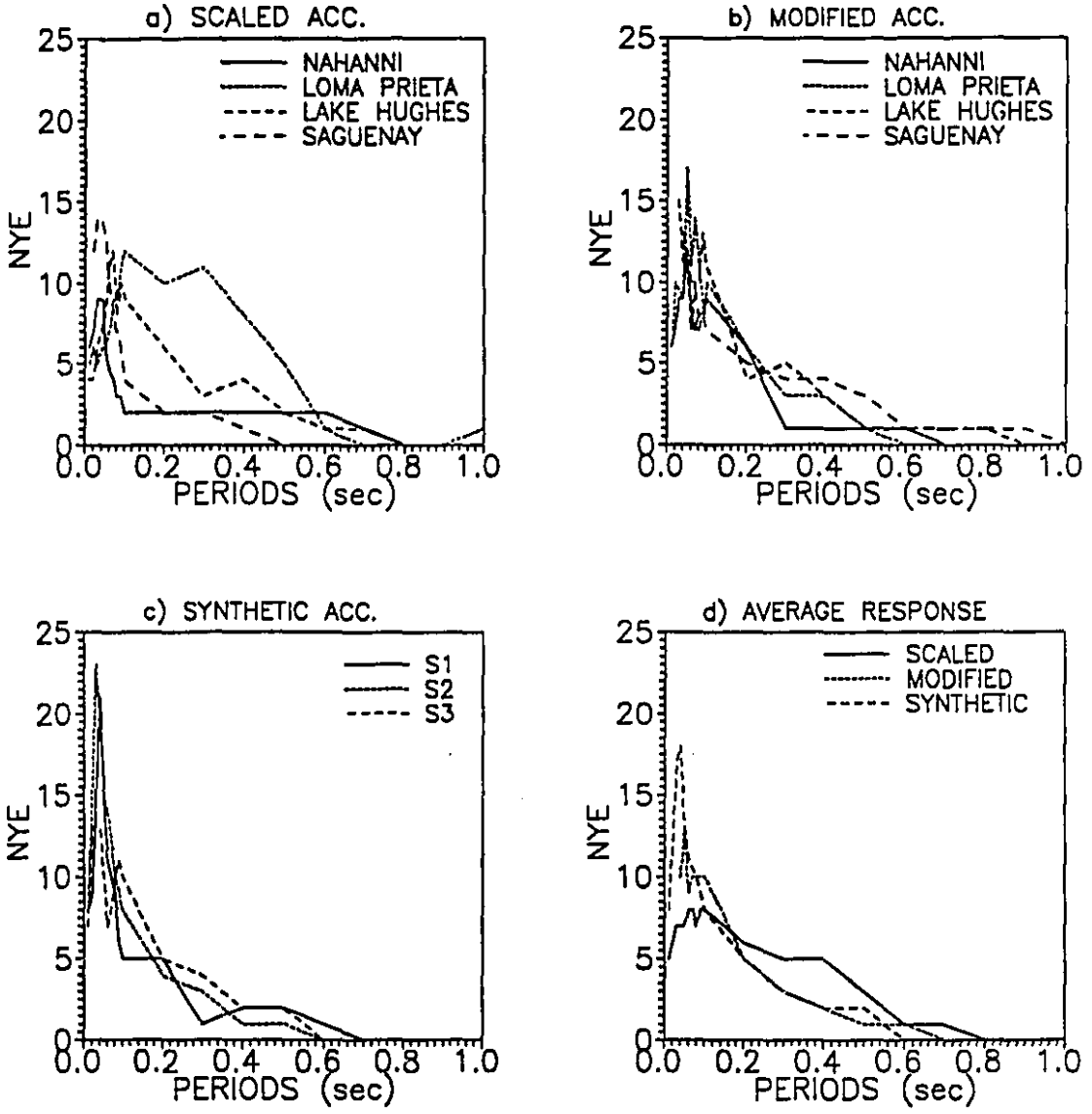

Figure 4.9: Effect of the type of accelerogram on the number of yield events, NYE.

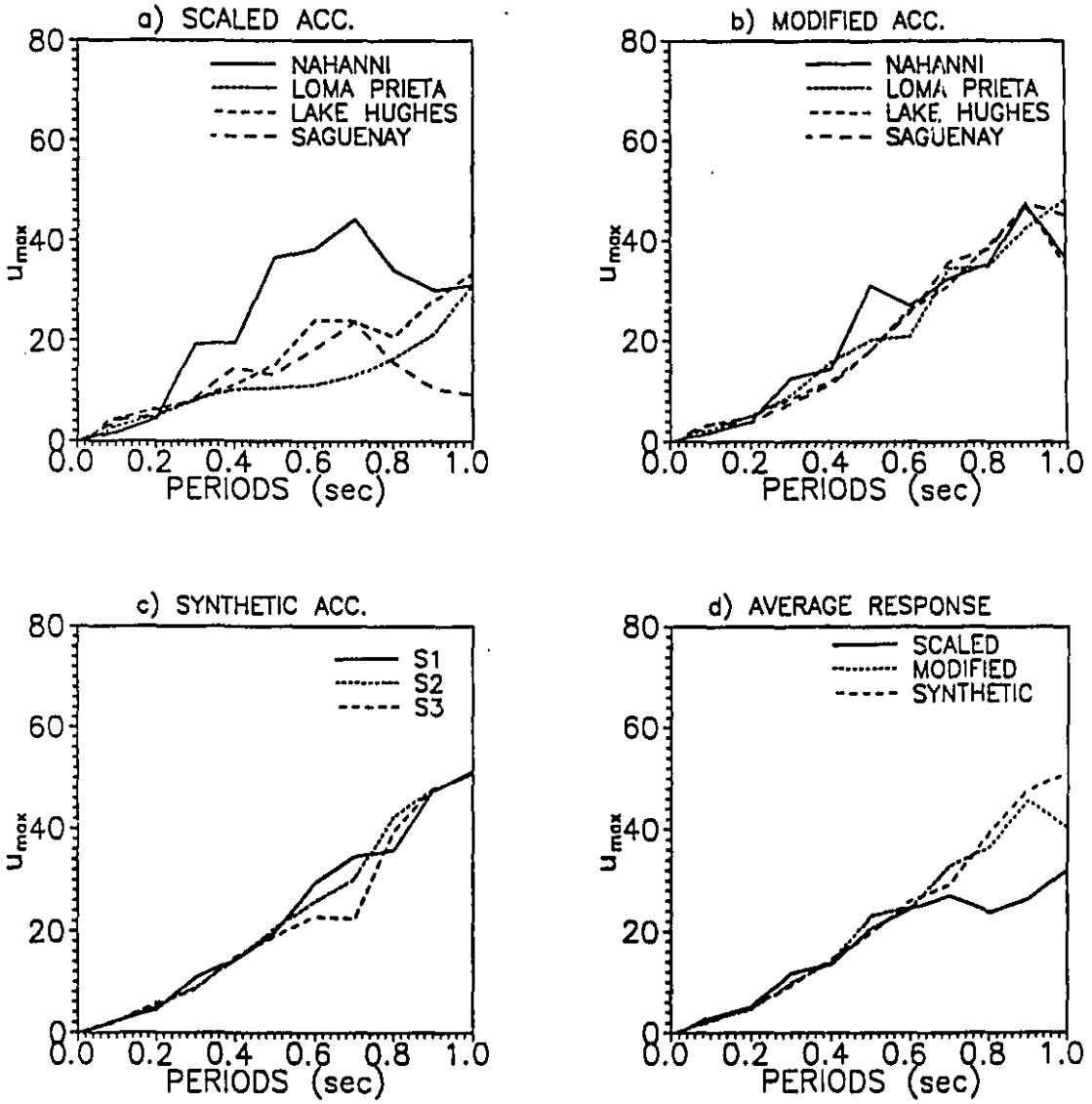

Figure 4.10: Effect of the type of accelerogram on maximum relative displacement, u_{max}.

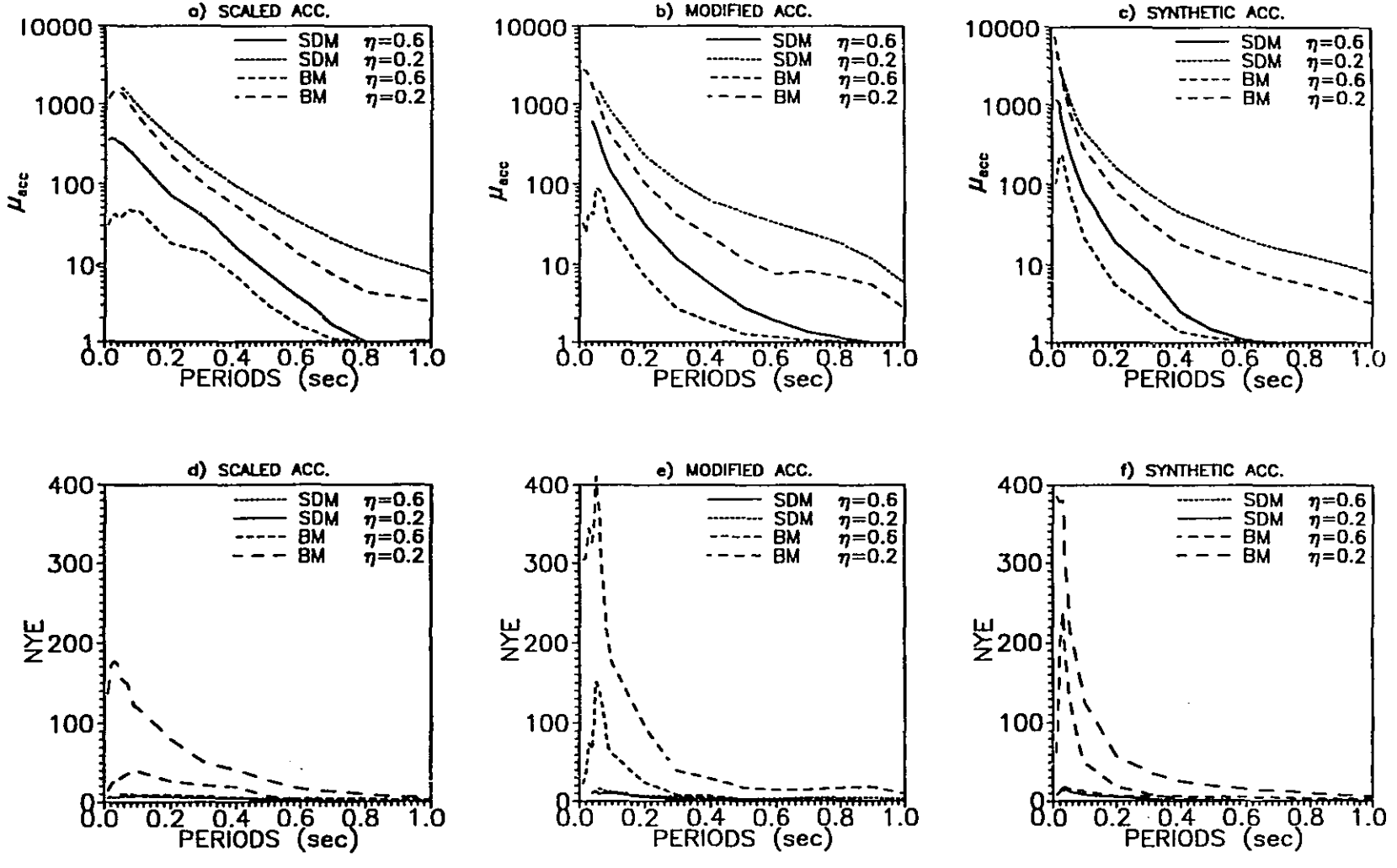

Figure 4.11 Effect of hysteresis models and strength on the NYE and μ_{acc}.

Chapter 5

Seismic Analysis of Dams

5.1 Introduction

After applying the studied design earthquakes to short period SDOF systems, these earthquakes are applied to a real multi-degree-of-freedom structure that is a concrete gravity dam shown in Fig. 5.1. The dam is excited in both the horizontal and vertical directions simultaneously. It is subjected to four scaled historical records, four modified records and three synthetic records. Table 5.1 shows the scaling factors (according to SM1 scaling method) of the historical records.

The vertical components of Nahanni site 2 and San Fernando Lake Hughes records were not available, and these two records were replaced by Nahanni site 1 and site 3 records. The modification process was applied to both the horizontal and vertical components of the historical records. However, as a general procedure, as recommended by the Offshore code (CSA S471-M1989. 1989) the vertical component was scaled such that its SI_a be 2/3 that of the horizontal component. The vertical component must be an independent component to insure statistical independence of the horizontal and vertical components. The two-dimensional synthetic accelerograms were obtained by combining any two different synthetic accelerograms discussed in chapter three, and scaling the vertical component by 2/3. Three of these combined accelerograms were retained. Figures 5.2-5.4 show the input accelerograms and their 5% damped spectra.

In a first step, a linear elastic seismic analysis of the dam-reservoir-foundation

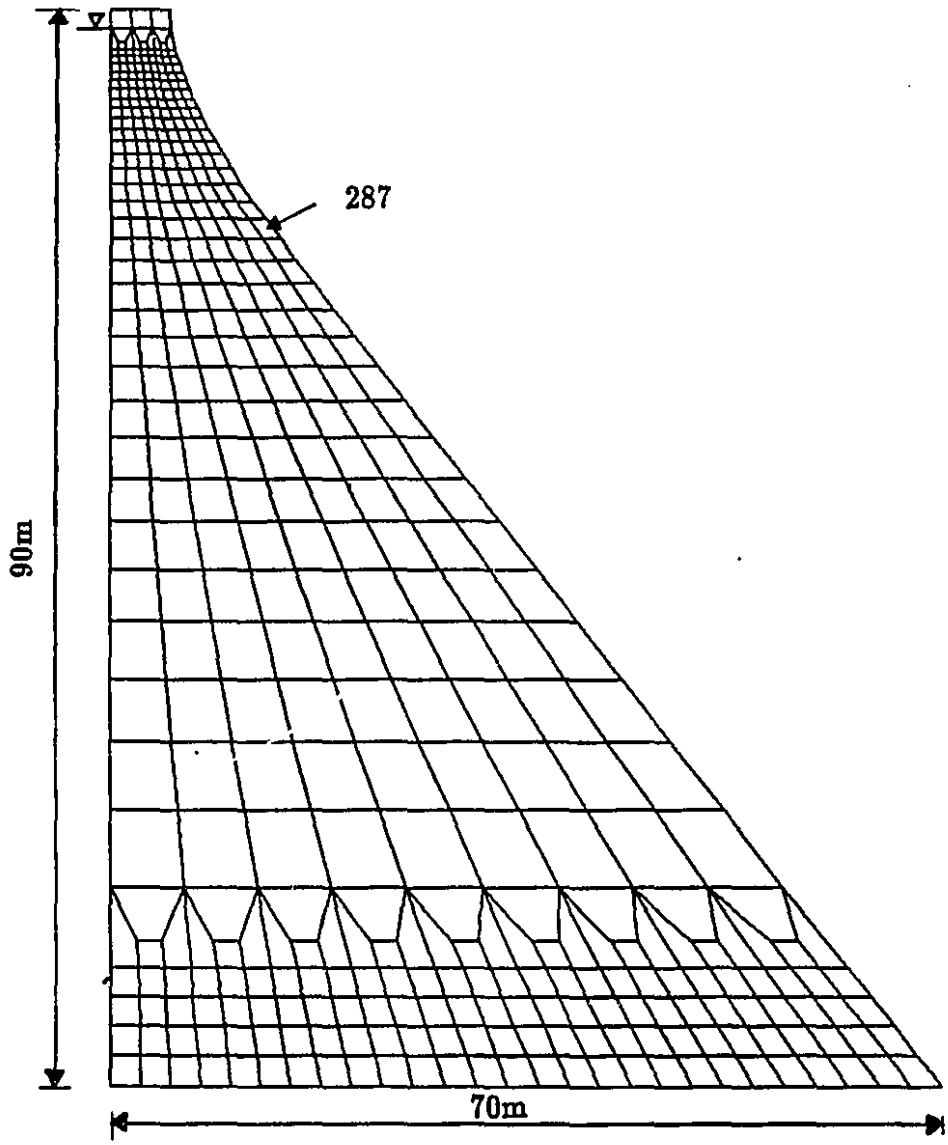

Figure 5.1: Dam geometry and mesh.

Figure 5.2: Time histories and spectra of scaled records

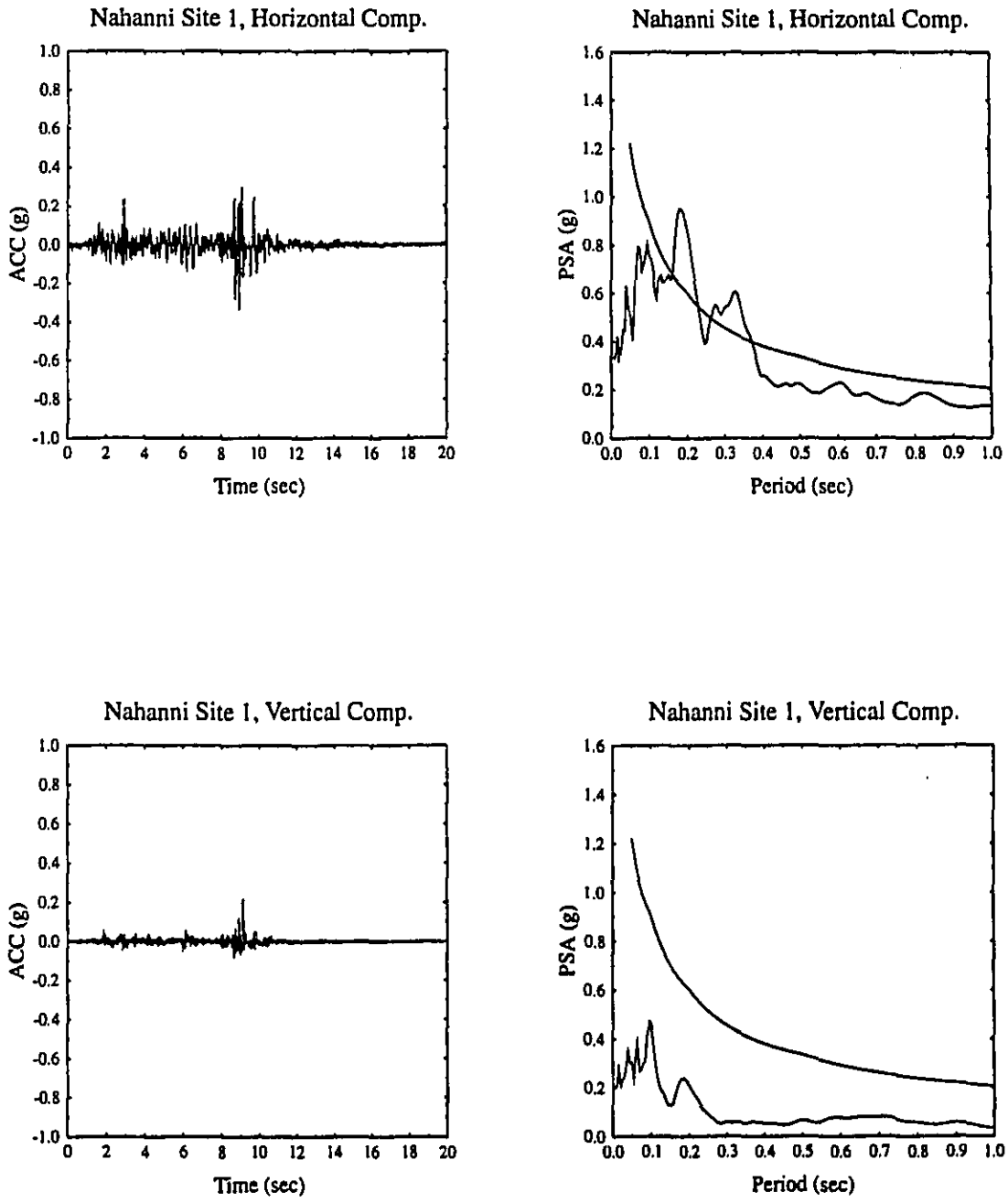

Figure 5.2a : Scaled Nahanni site 1 record.

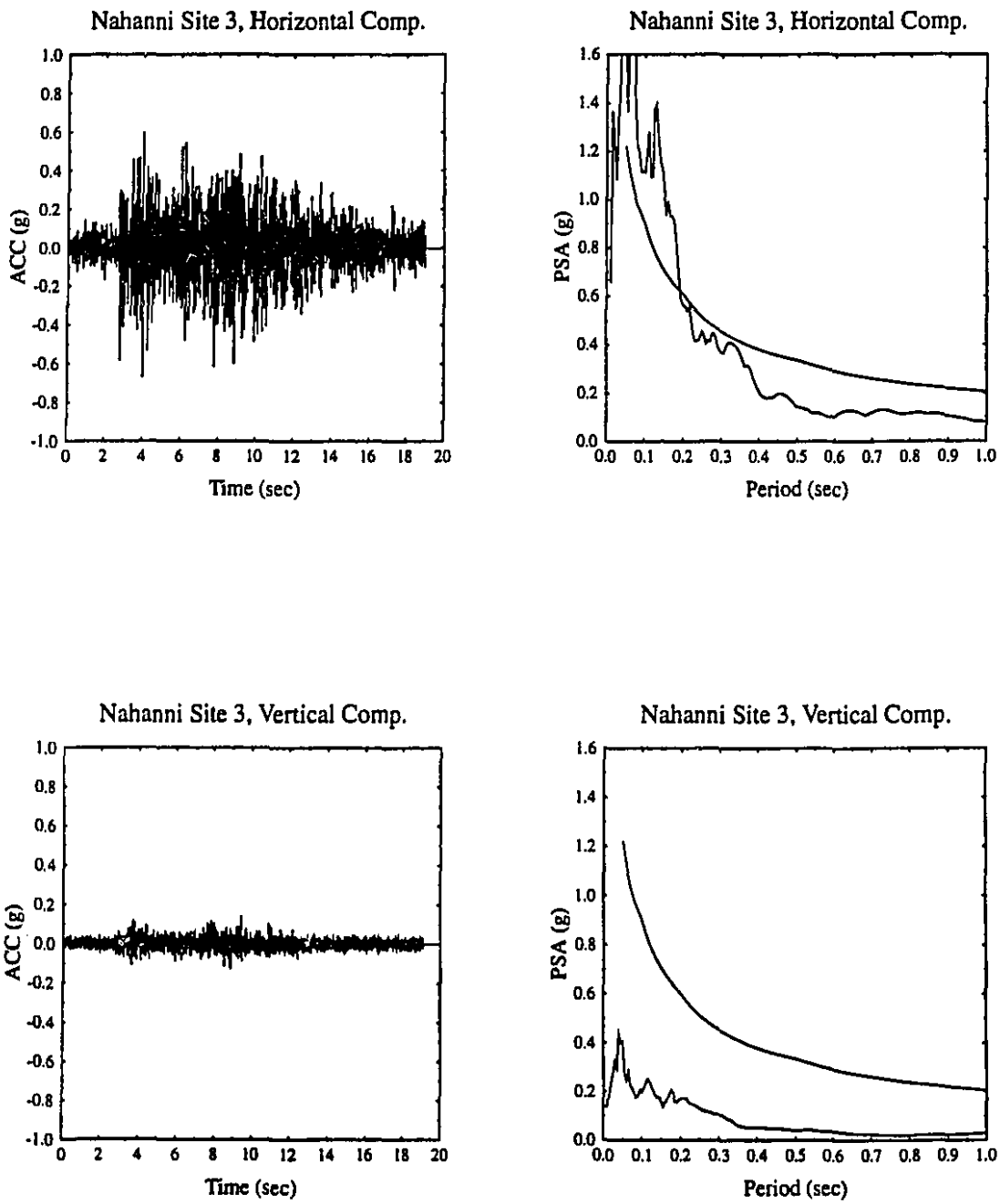

Figure 5.2b : Scaled Nahanni site 3 record.

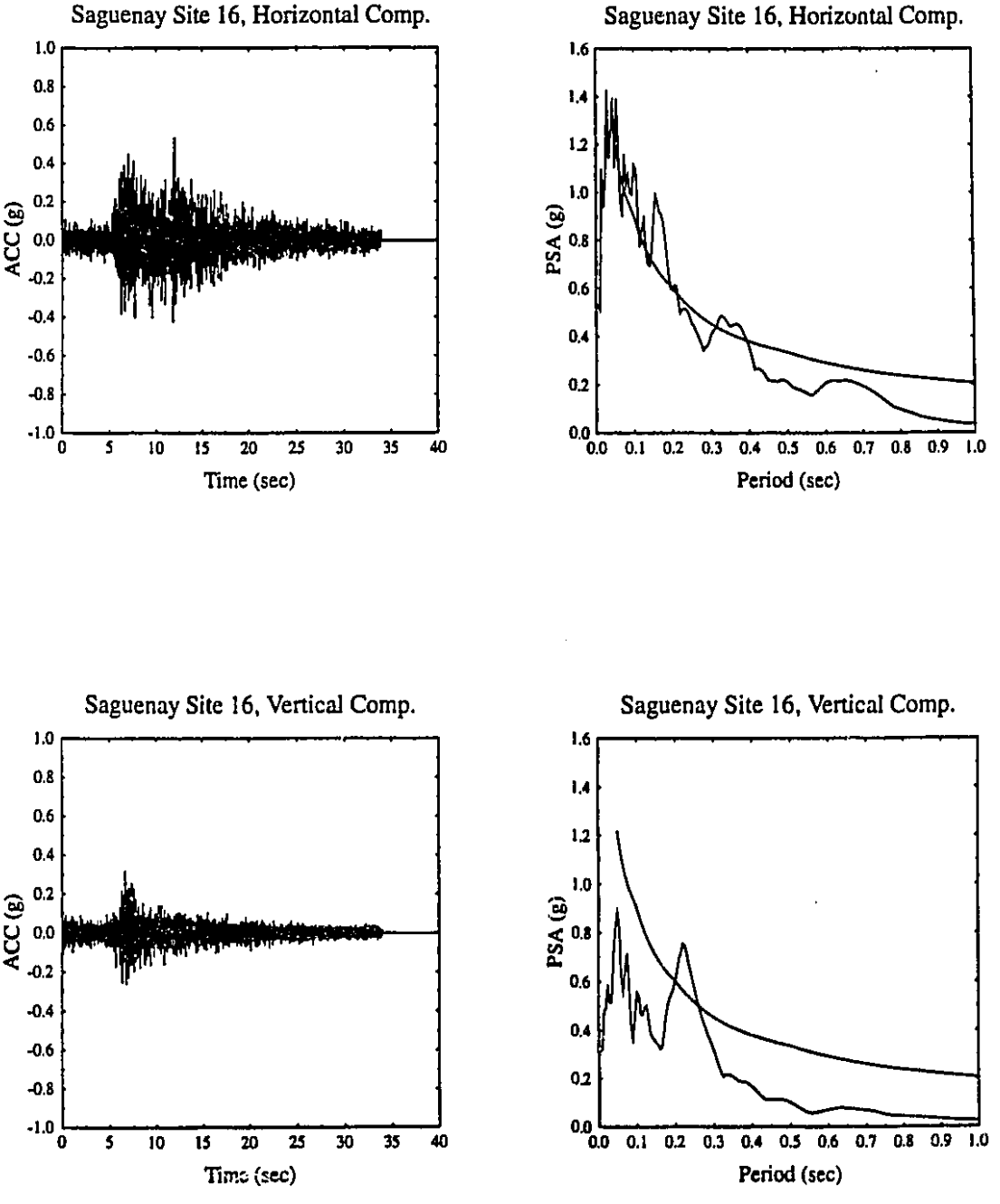

Figure 5.2c : Scaled Saguenay site 16 record.

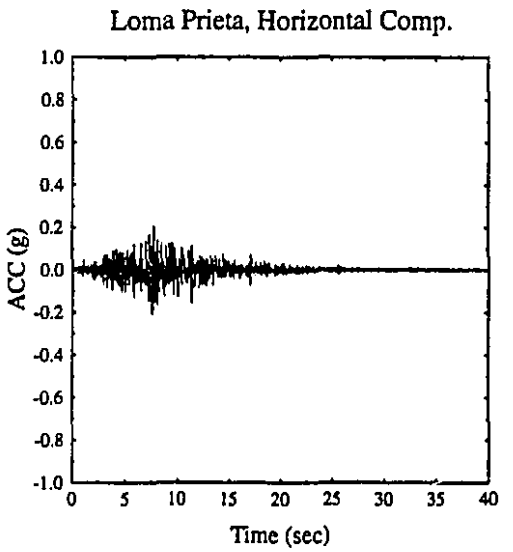

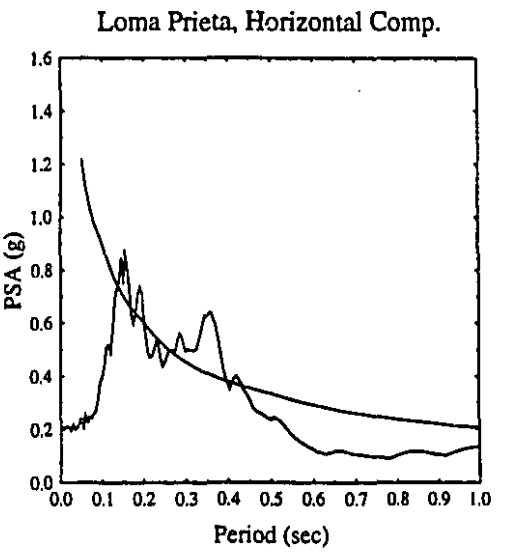

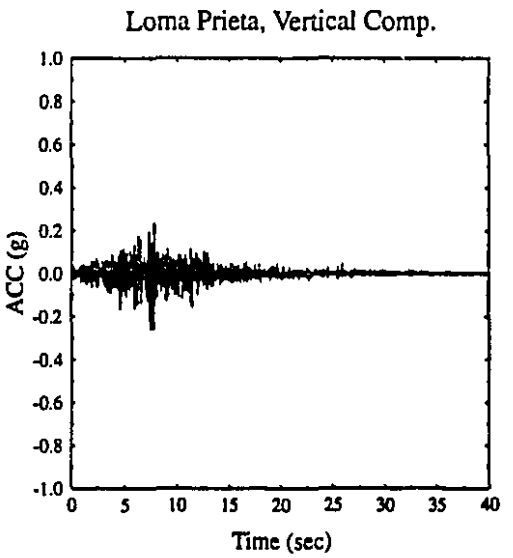

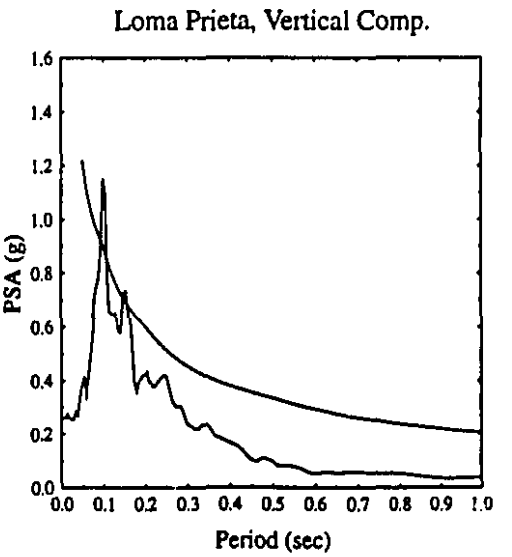

Figure 5.2d : Scaled Loma Prieta record.

Figure 5.3: Time histories and spectra of modified records

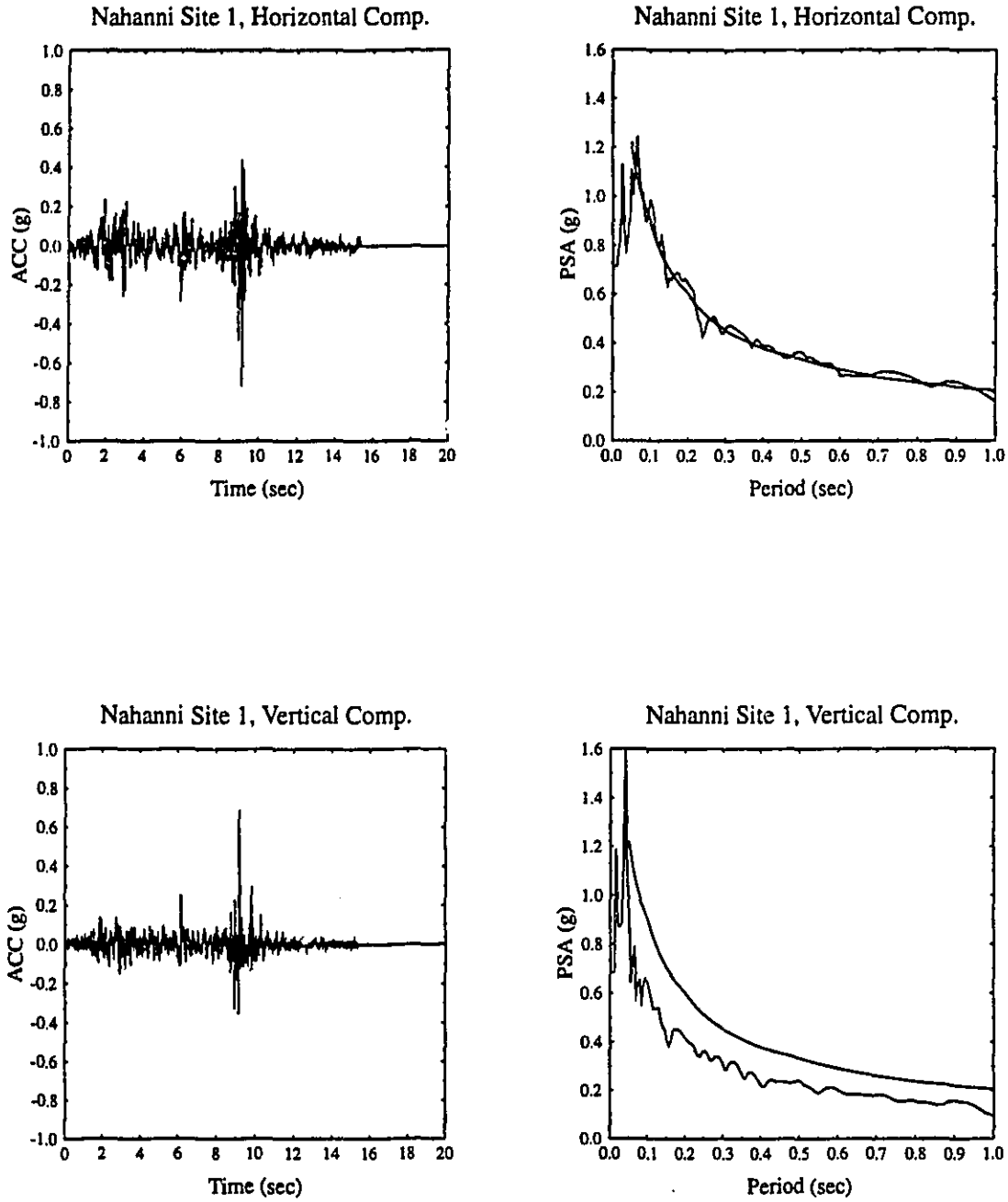

Figure 5.3a : Modified Nahanni site 1 record.

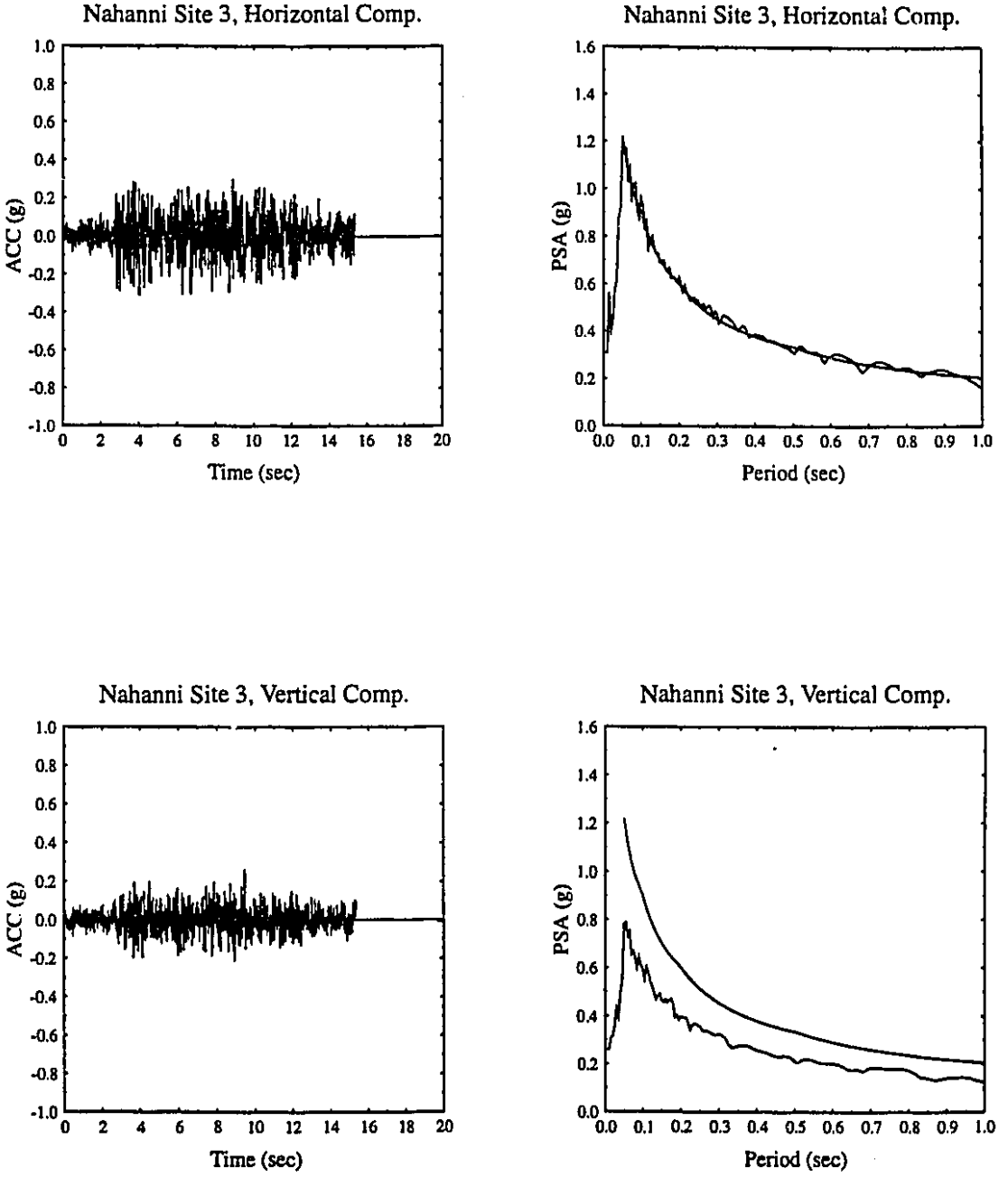

Figure 5.3b : Modified Nahanni site 3 record.

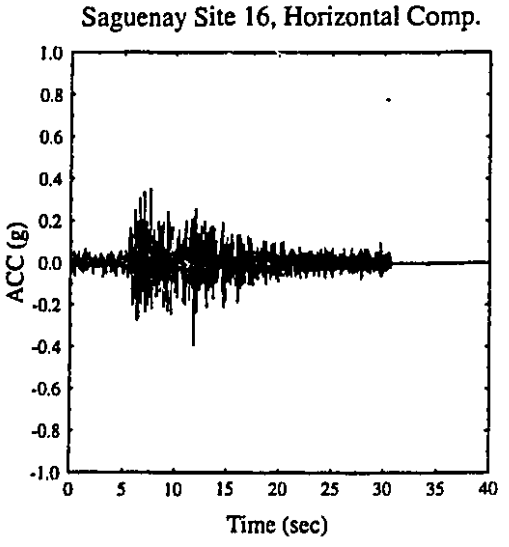

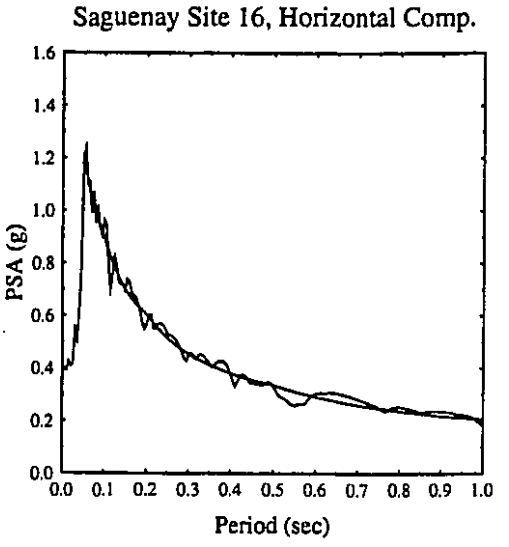

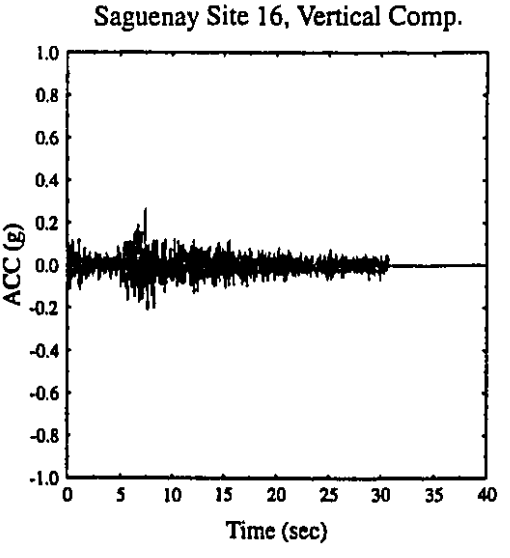

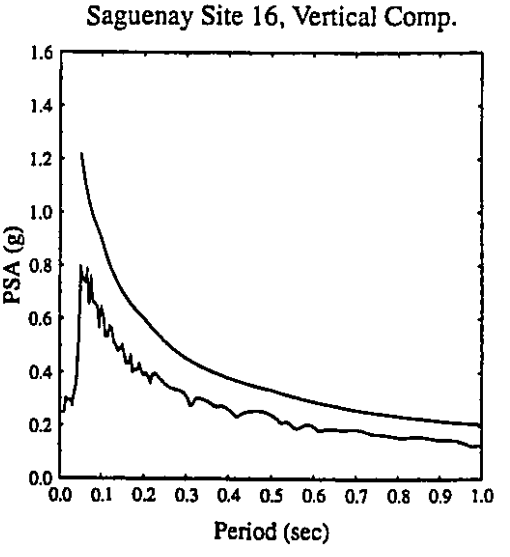

Figure 5.3c : Modified Saguenay site 16 record.

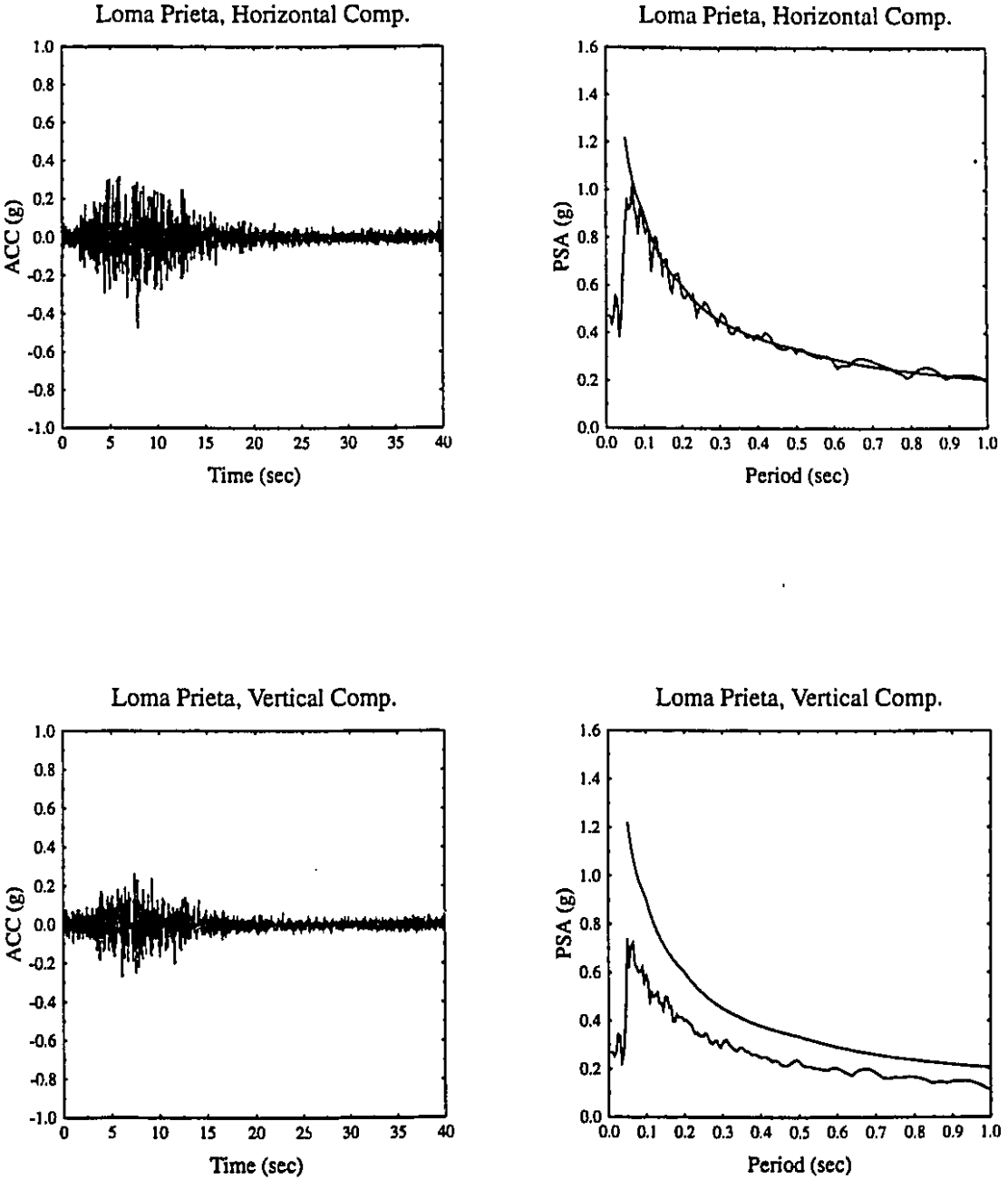

Figure 5.3d : Modified Loma Prieta record.

Figure 5.4: SIMQKE generated motions time histories and spectra

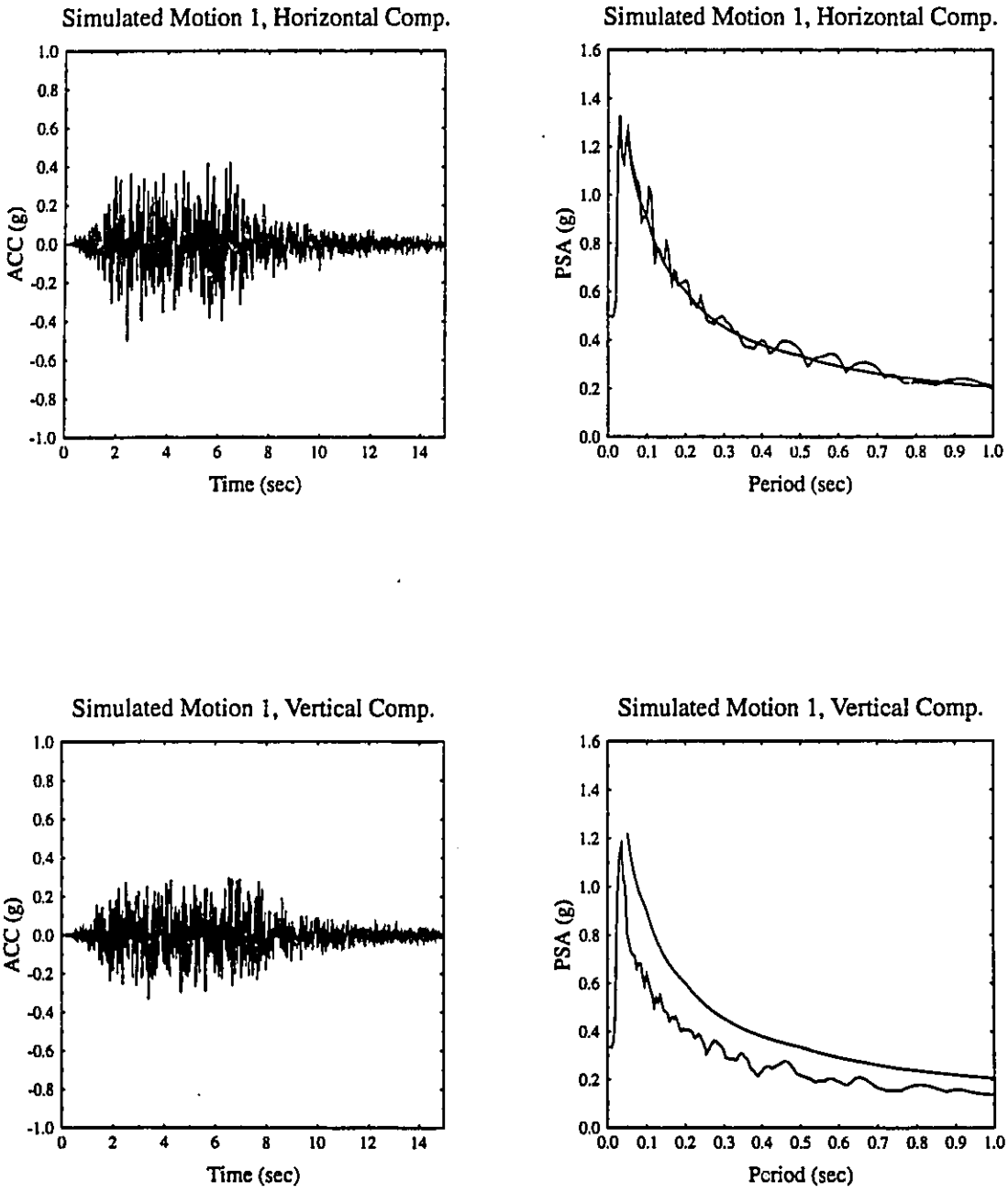

Figure 5.4a : Simulated motion 1.

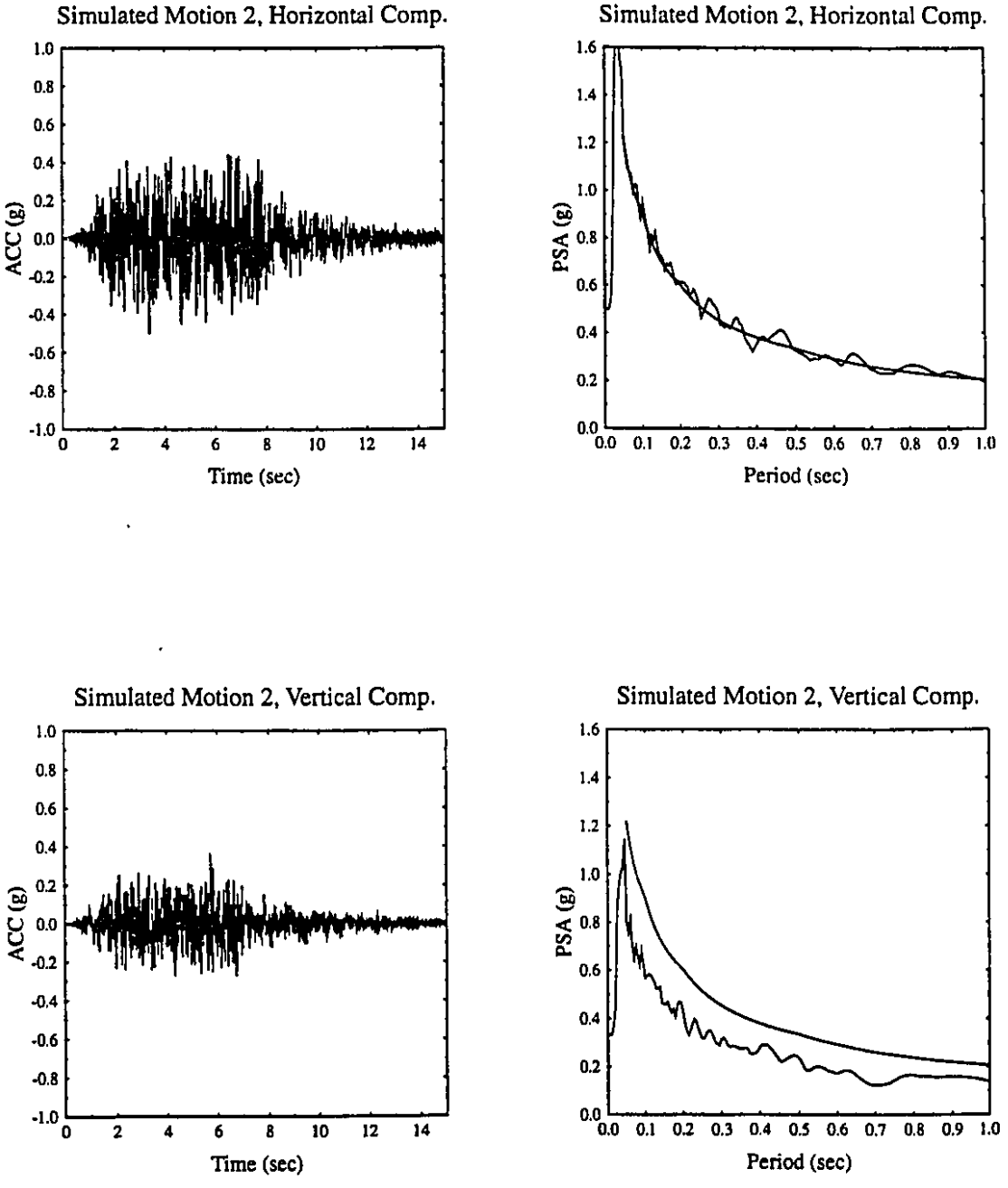

Figure 5.4b : Simulated motion 2.

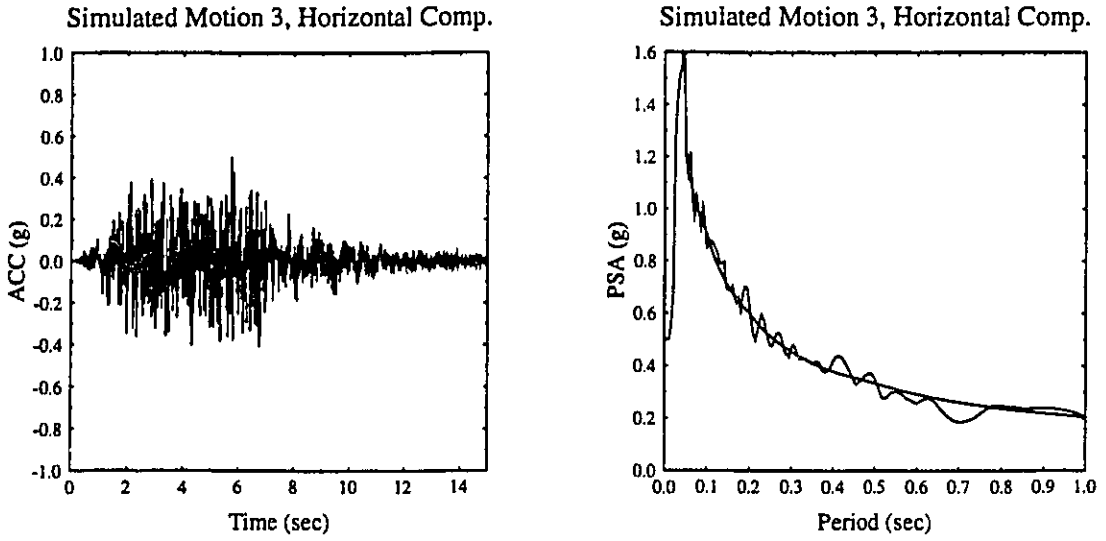

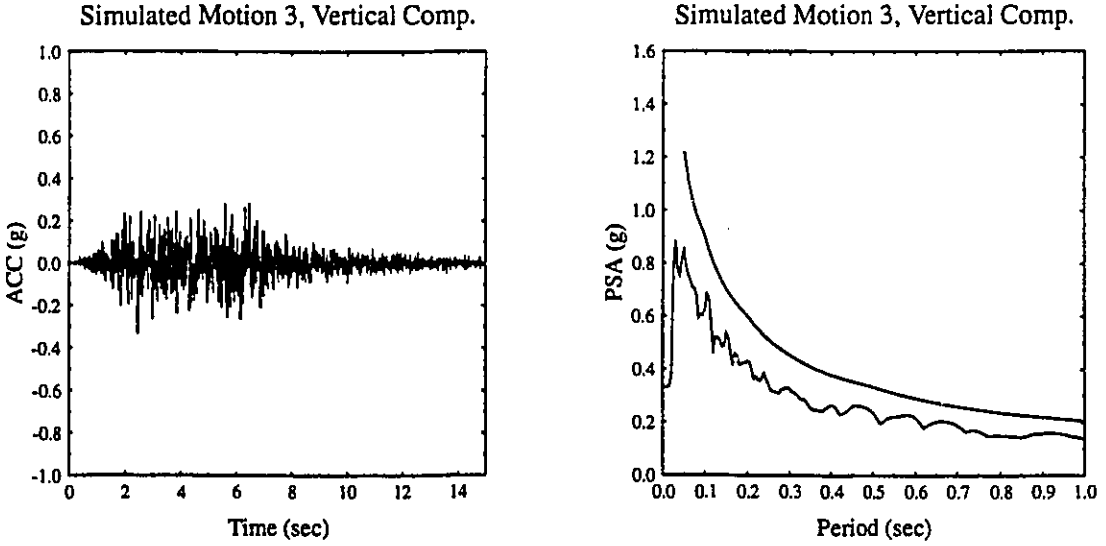

Figure 5.4c : Simulated motion 3.

Record	$Sla_{(0.10)}$(cm/sec)	SF
Loma Prieta Ver.	168.8	0.788
Saguenay site 16 Ver.	42.9	3.004
Nahanni site 1 Hor.	517.7	0.257
Nahanni site 1 Ver.	658.4	0.303
Nahanni site 3 Hor.	58.0	2.297
Nahanni site 3 Ver.	57.6	3.466

Table 5.1: Scaling factors for selected historical records.

system is performed, and in a second step, a nonlinear fracture mechanics seismic analysis of the fixed-to-the-base concrete block of the dam (no interaction with reservoir or foundation) is performed in order to have a preliminary idea of the influence of the type of earthquakes on the crack pattern.

5.2 Linear elastic seismic analysis

The analysis is performed in the frequency domain using the program EAGD-84 (Fenves and Chopra 1984). The foundation is assumed to be a homogenous visco-elastic half space, and the water impounded in the reservoir is idealized as a fluid of constant depth (86 m) and infinite length in the upstream direction. Energy dissipation in the concrete is modelled by a constant hysteretic damping factor of 10% which corresponds to a 5% viscous damping ratio in all vibration modes of the dam. The reservoir bottom absorption phenomenon is modelled by a wave reflection coefficient α taken as 0.7 in this study. The interaction with the foundation is taken into account through a Poisson's ratio of 1/3 and a hysteretic damping factor of 0.1. The analysis is based on substructuring techniques and a plane stress state is assumed. The first resonant frequency of the dam-foundation-reservoir system is approximately equal to 3.3 sec for all earthquake records considered. Since the goal of this section is to study the influence of the type of earthquakes on the system's response, four response parameters have been chosen to represent the main features of the system's response. These parameters are :

(i) The crest maximum horizontal displacement, D_{max} and corresponding time of occurrence (t_{max}).

(ii) The crest maximum horizontal acceleration, Acc_{max} and corresponding time of occurrence (t_{max}).

(iii) The crest horizontal acceleration response spectrum for zero damping (as a measure of the frequency content of the response and its intensity). This is represented by the respective maximum PSA (and its respective period of occurrence, T_{max}) and the $SI_{a(0.04)}$. This was defined for 5% damping but computed here for 0% damping.

(iv) The maximum principal tensile stress (sigma) at element number 287 as shown in Fig. 5.1 (this location was selected because usually cracks originate around it) and the corresponding time of occurrence.

The following earthquake input motions were considered in the parametric analysis:

(i)	Scaled Nahanni site 1 records	(Horiz. and Vert.)	: SNS1
(ii)	Scaled Nahanni site 3 records	(Horiz. and Vert.)	: SNS3
(iii)	Scaled Saguenay site 16 records	(Horiz. and Vert.)	: SSS16
(iv)	Scaled Loma Prieta records	(Horiz. and Vert.)	: SLP
(v)	Modified Nahanni site 1 records	(Horiz. and Vert.)	: MNS1
(vi)	Modified Nahanni site 3 records	(Horiz. and Vert.)	: MNS3
(vii)	Modified Saguenay site 16 records	(Horiz. and Vert.)	: MSS16
(viii)	Modified Loma Prieta records	(Horiz. and Vert.)	: MLP
(ix)	Simulated motion 1	(Horiz. and Vert.)	: SM1
(x)	Simulated motion 2	(Horiz. and Vert.)	: SM2
(xi)	Simulated motion 3	(Horiz. and Vert.)	: SM3

The results of these analyses are presented in Tables 5.2 to 5.5 (NZC being the number of zero crossings for the displacement time history at the crest) and in Figures 5.5 to 5.7. The influence of the dam size was studied by analyzing the half size (45 m)and double size (22.5 m) models of the dam subjected to scaled and modified Saguenay Site

16 and Loma Prieta records and a synthetic records. This led to the results displayed in Tables 5.4-5.5 and Figures 5.18 to 5.29.

Figures 5.5-5.6 and 5.9-5.10 show that when moving from the seismic response of the full size dam to the scaled records, SNS1, to that of the modified records, MNS1, the response parameters are amplified except D_{max}. There are more peaks of significant amplitude in the displacement time history of the MNS1. These peaks have the particularity to occur early in the history. The shape of the response time histories are also very dissimilar. Figures 5.7-5.8 and 5.11-5.12 show that a lesser shape dissimilarity is noticed in SNS3-MNS3, and even lesser in SSS16-MSS16 (where there is an almost perfect match between scaled and modified responses). In the contrary, SLP showed a decrease in the displacement and PSA response when moving from SLP to MLP. It is also noticed that important (not maximum) stress and acceleration peaks increased, in number and magnitude in the response to MLP. The simulated motions yielded responses of similar shape and maximum magnitude except for some details. Table 5.2 shows the typical drop in NZC for eastern records and increase for western records. It also shows that the time of occurrence of the maximum accelerations and stresses did not change from scaled to modified records, and only slight overall change was noticed in the displacements. To help assessing the differences and similarities in the response , a statistical analysis was made for each type of accelerograms (though the size of the sample is small, it gives some valuable information) as shown in Table 5.3.

It can be observed from Table 5.3 that as a general trend, the response to scaled records presents the maximum dispersion, then come the SR to the modified records, and lastly the response to synthetic accelerograms. In this analysis, the modification process had an effect of scaling down the Loma Prieta and Nahanni site 1 records, and scaling up the Saguenay site 16 and Nahanni site 3 records. This is expressed in the closeness of the response parameters of these two subgroups especially the scaled up records. This trend may mean that for a well grouped response, it is better to scale up (by modification) than to scale down. Overall, the response to modified records is better grouped than to the scaled records as was the case for SDOF systems. The almost perfect constancy and the small standard deviation (SD) and coefficient of variation (COV) in the response to synthetic motions emphasizes the conclusion made earlier (for SDOF systems) about

the representativity of a single simulated record. The only noticeable drawback of the synthetic motions is the low mean and individual stress values, as compared to other means and other individual values for scaled and modified records. This observation is of significant importance, since the failure criterion is based on reaching the maximum tensile stress or the crushing stress.

As a general trend, the mean values for the response to all three types of accelerograms are very close except for the PSA, but with distinctive COV's. This would suggest that it is better to rely on mean response (even of scaled records) than to individual accelerogram sensitive response.

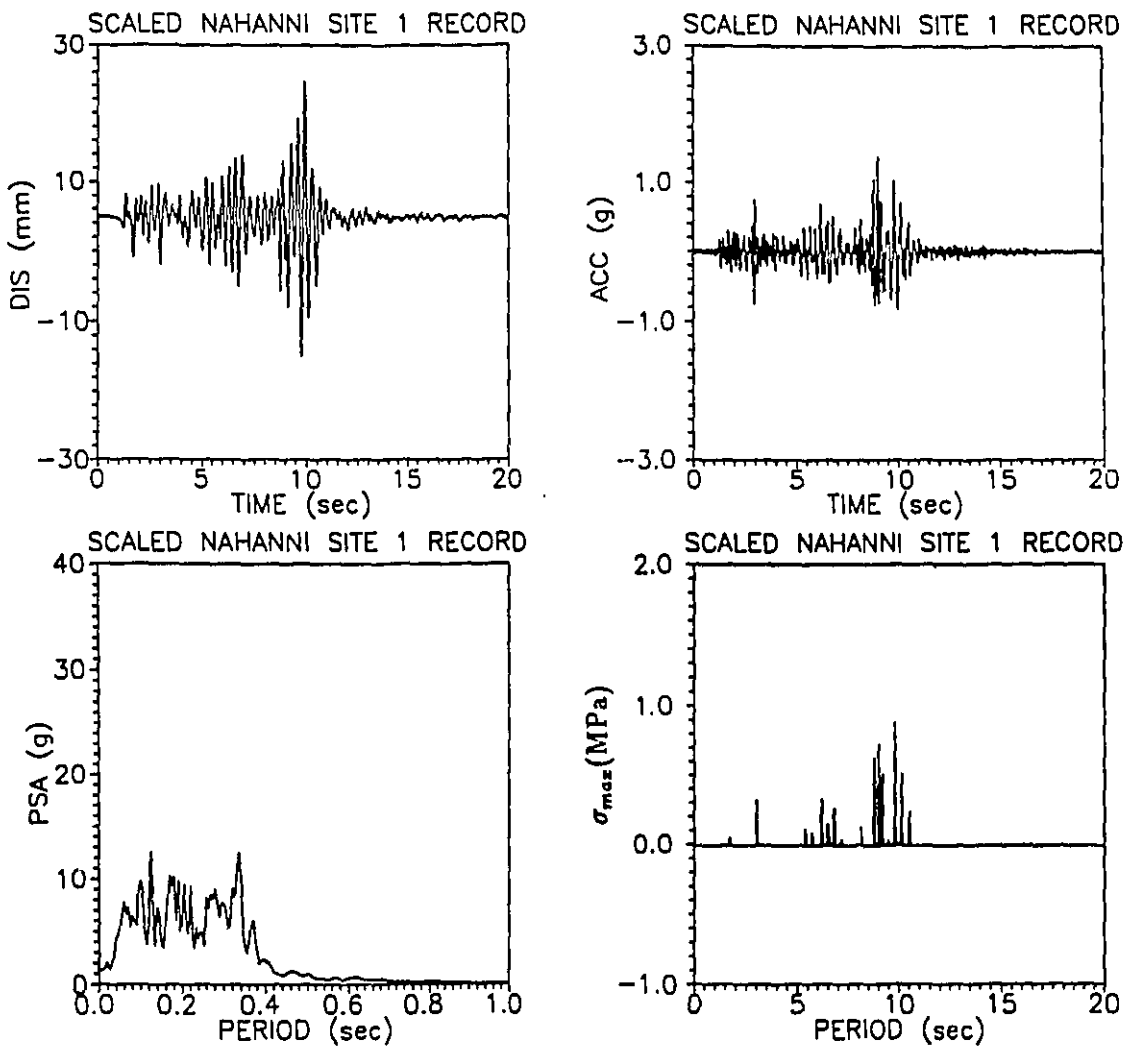

Figure 5.5: Seismic response to scaled Nahanni site 1 record (SNS1).

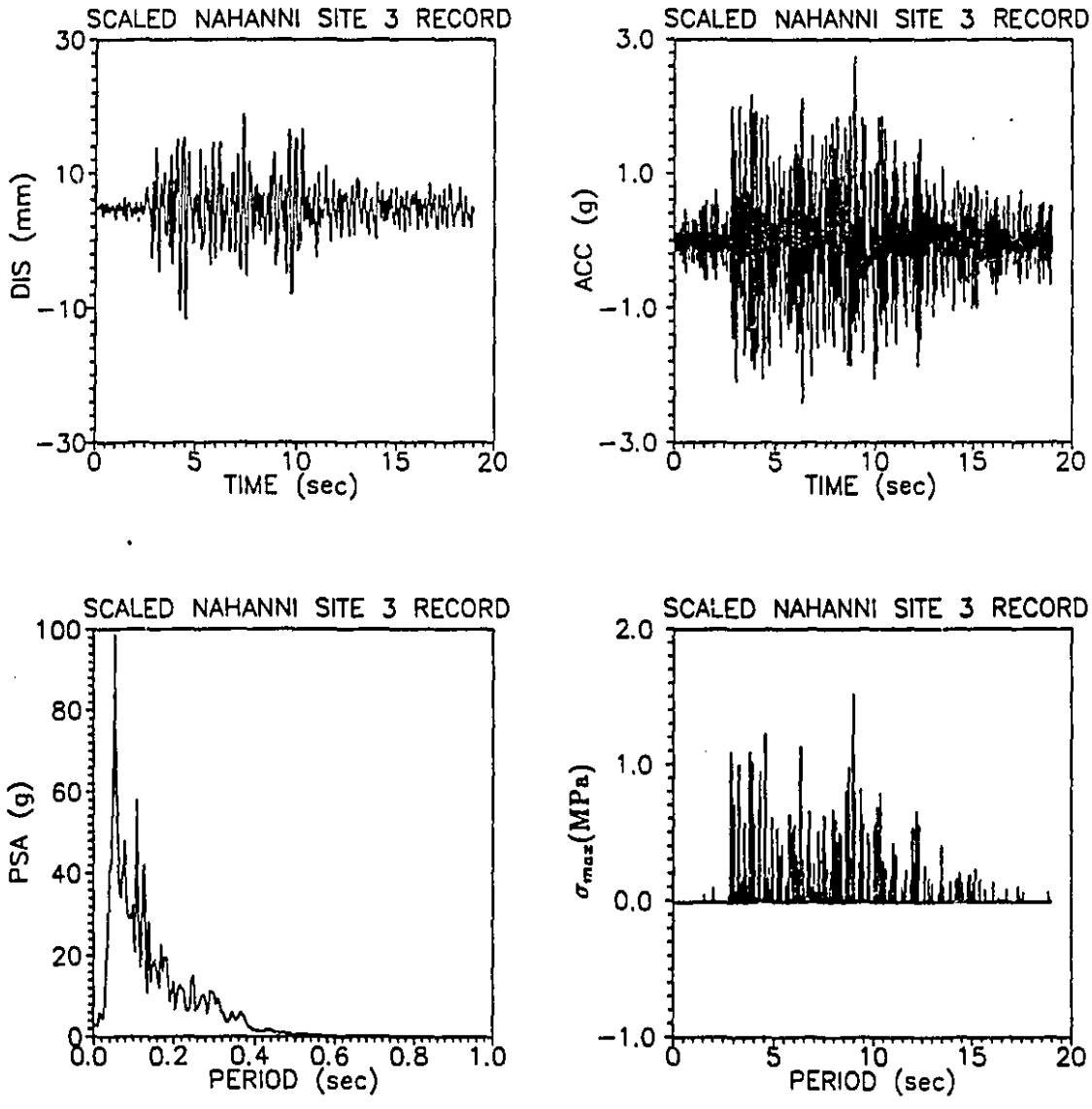

Figure 5.6: Seismic response to scaled Nahanni site 3 record (SNS3).

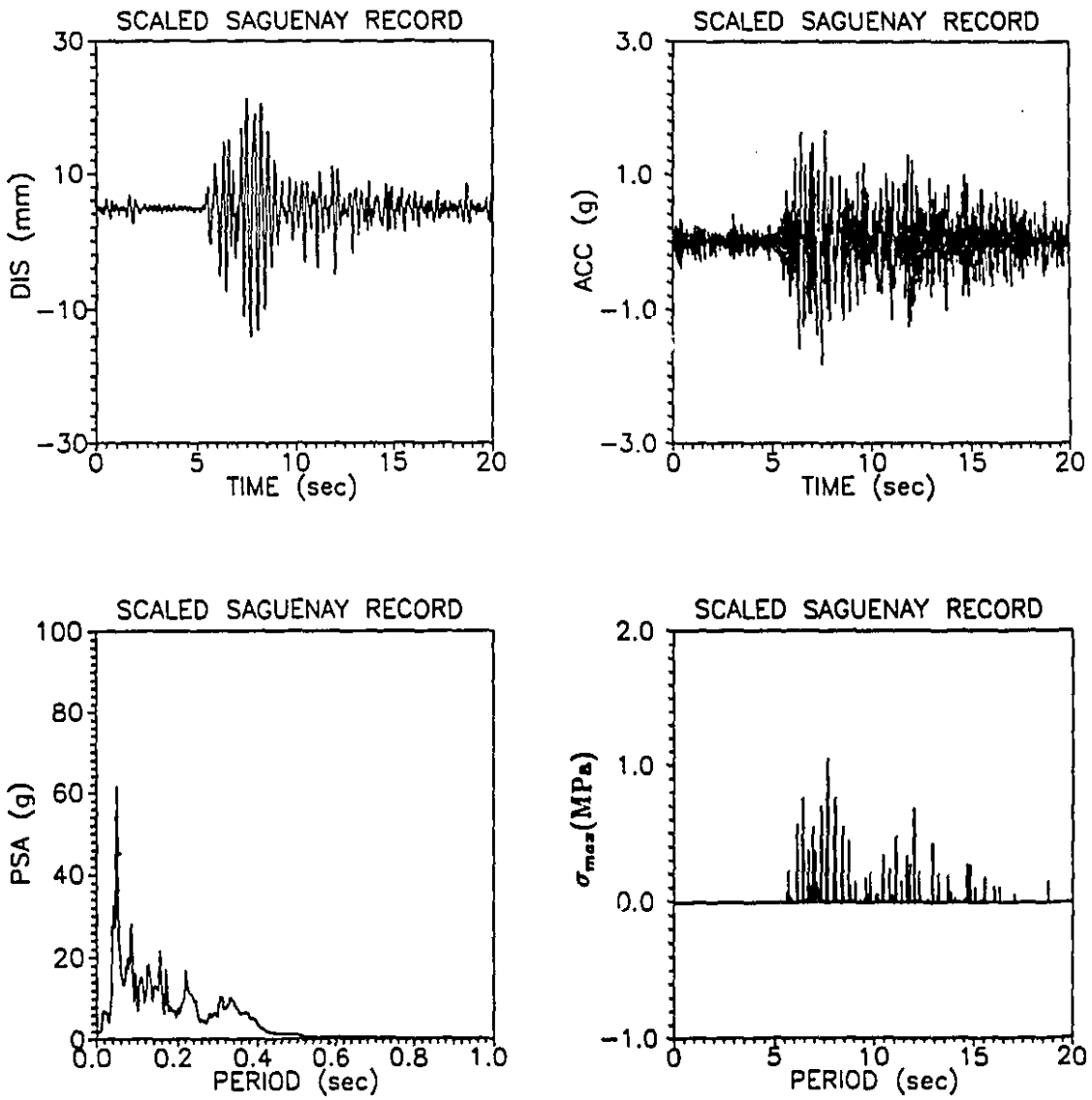

Figure 5.7: Seismic response to scaled Saguenay site 16 record (SSS16).

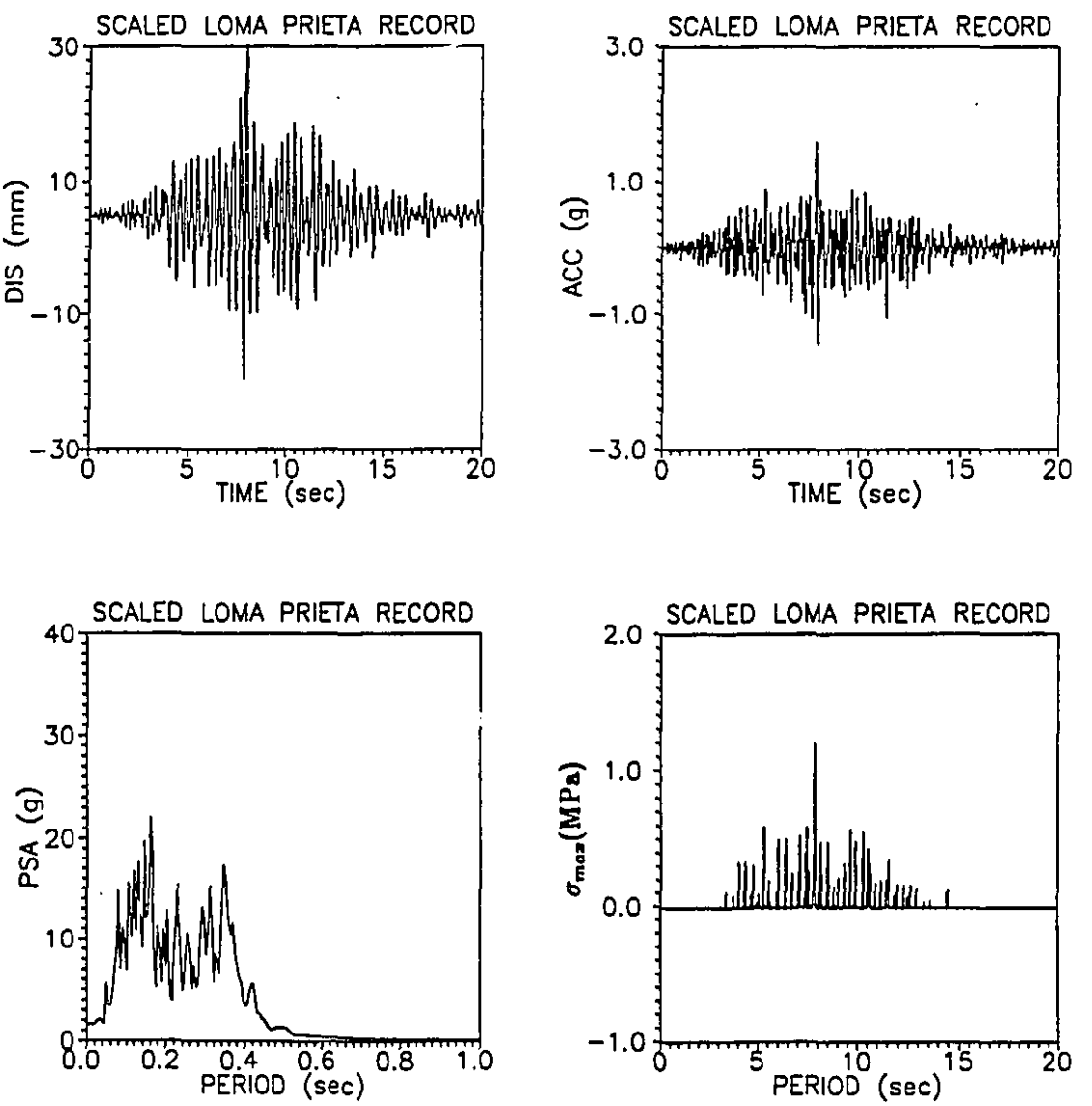

Figure 5.8: Seismic response to scaled Loma Prieta record (SLP).

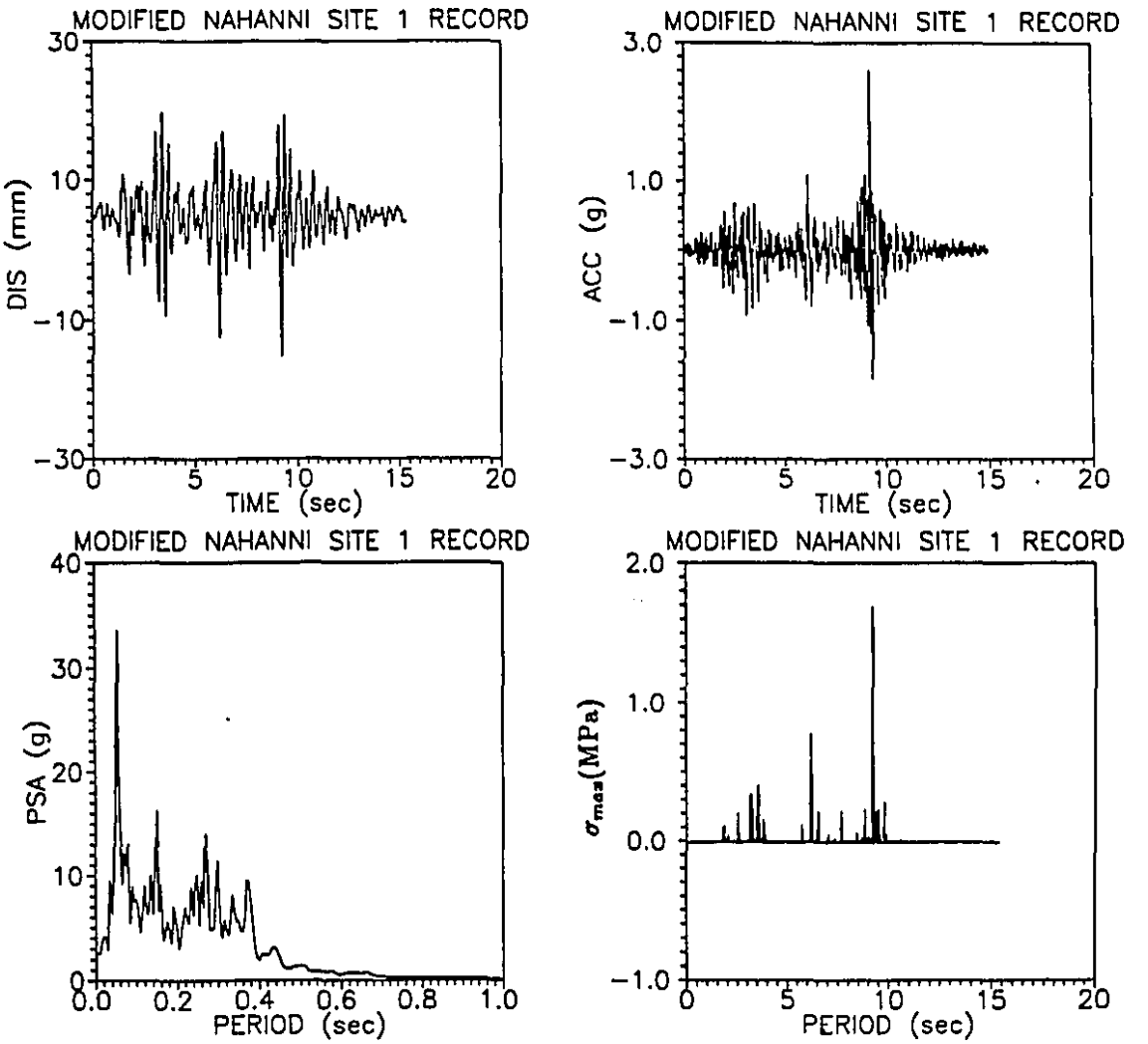

Figure 5.9: Seismic response to modified Nahanni site 1 record (MNS1).

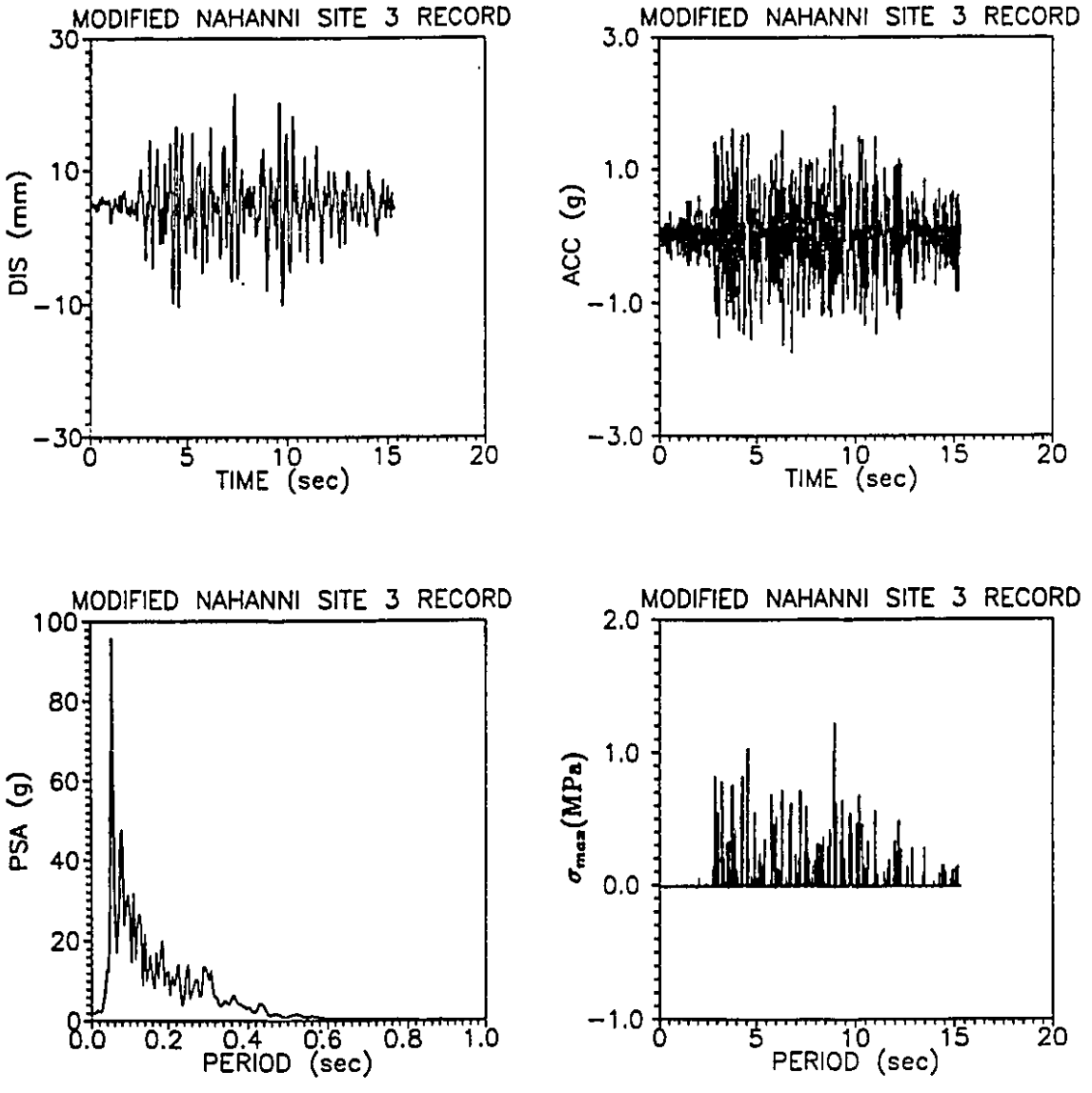

Figure 5.10: Seismic response to modified Nahanni site 3 record (MNS3).

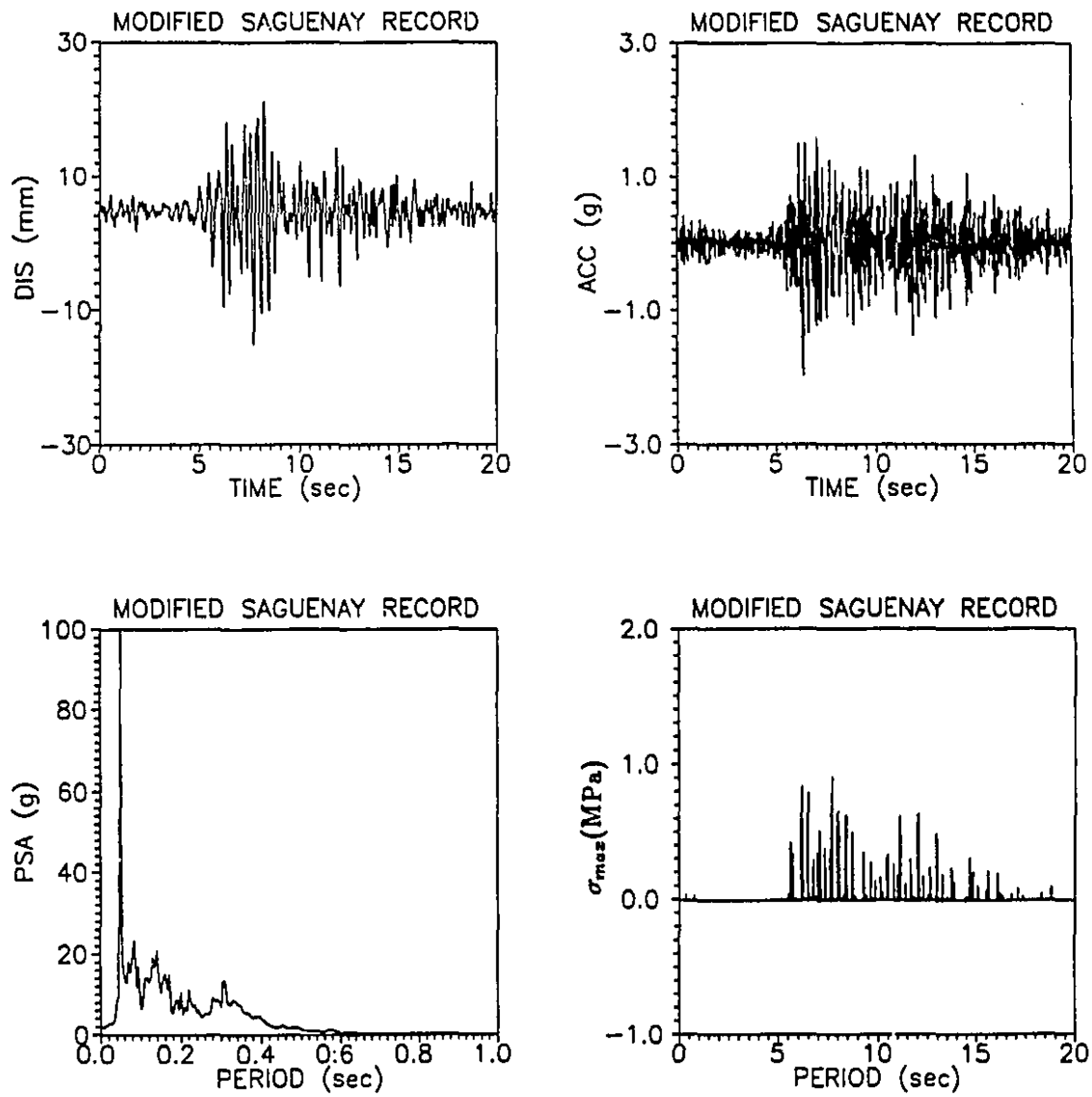

Figure 5.11: Seismic response to modified Saguenay site 16 record (MSS16).

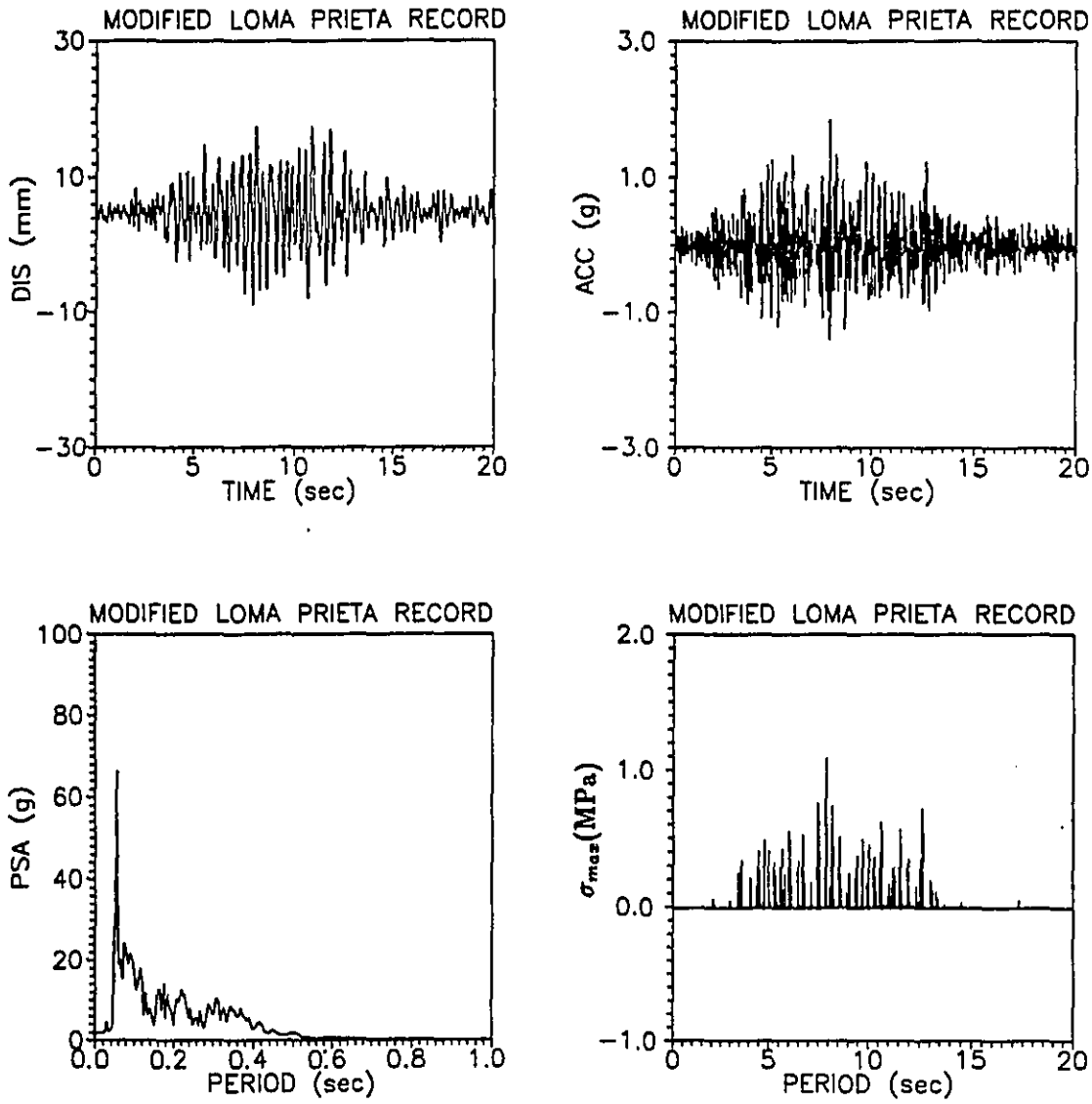

Figure 5.12: Seismic response to modified Loma Prieta record (MLP).

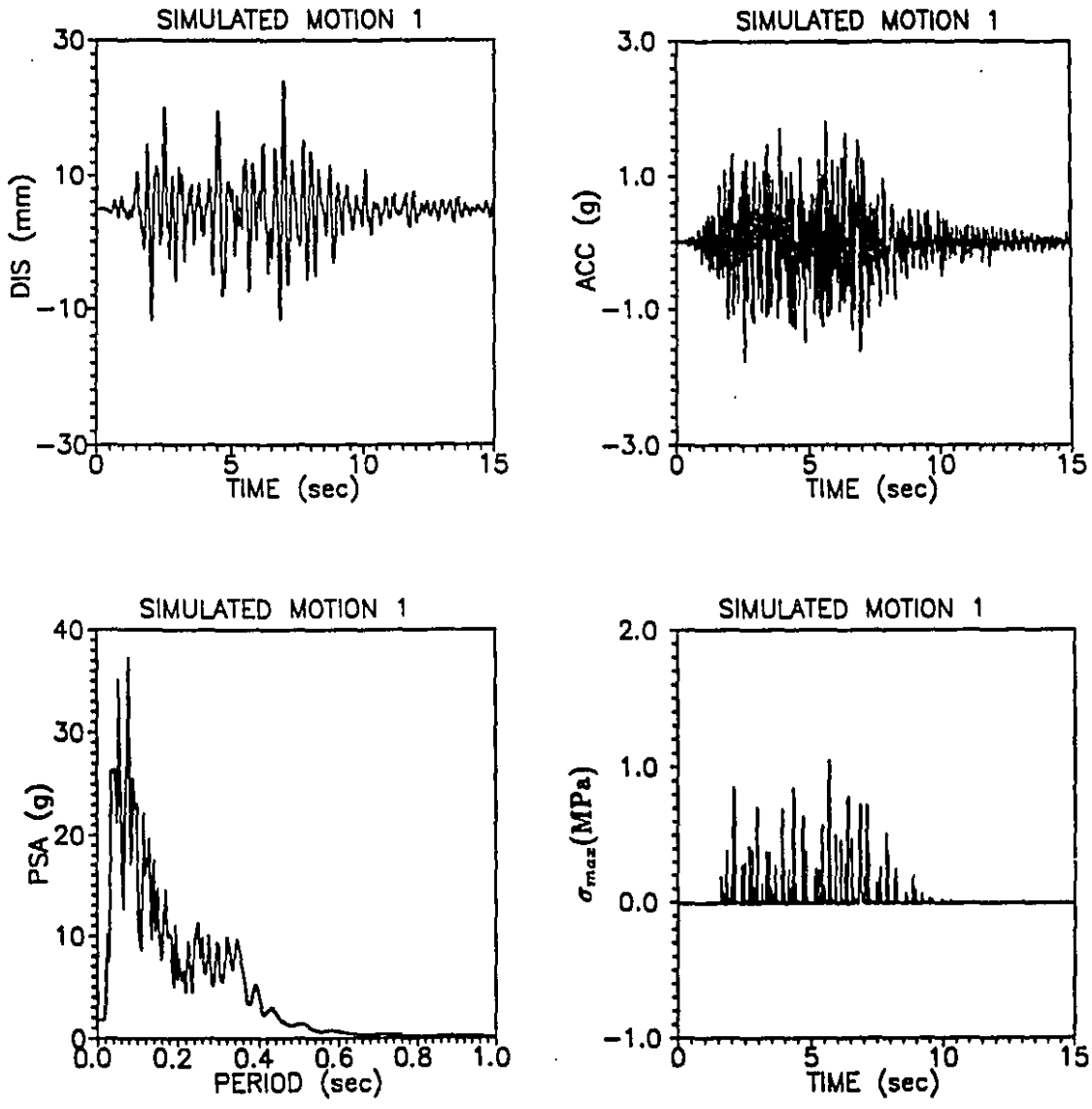

Figure 5.13: Seismic response to simulated motion 1 (SM1).

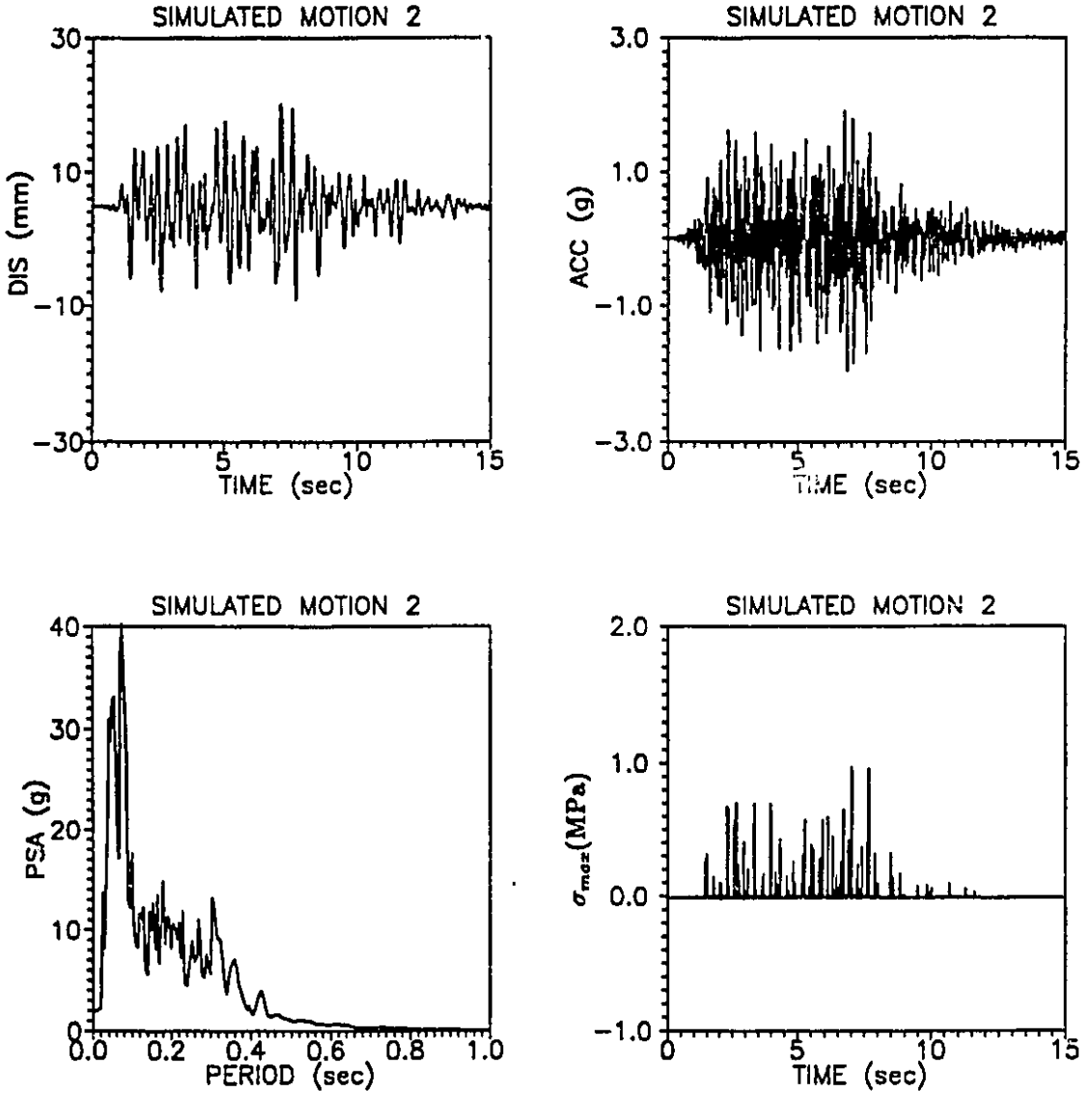

Figure 5.14: Seismic response to simulated motion 2 (SM2).

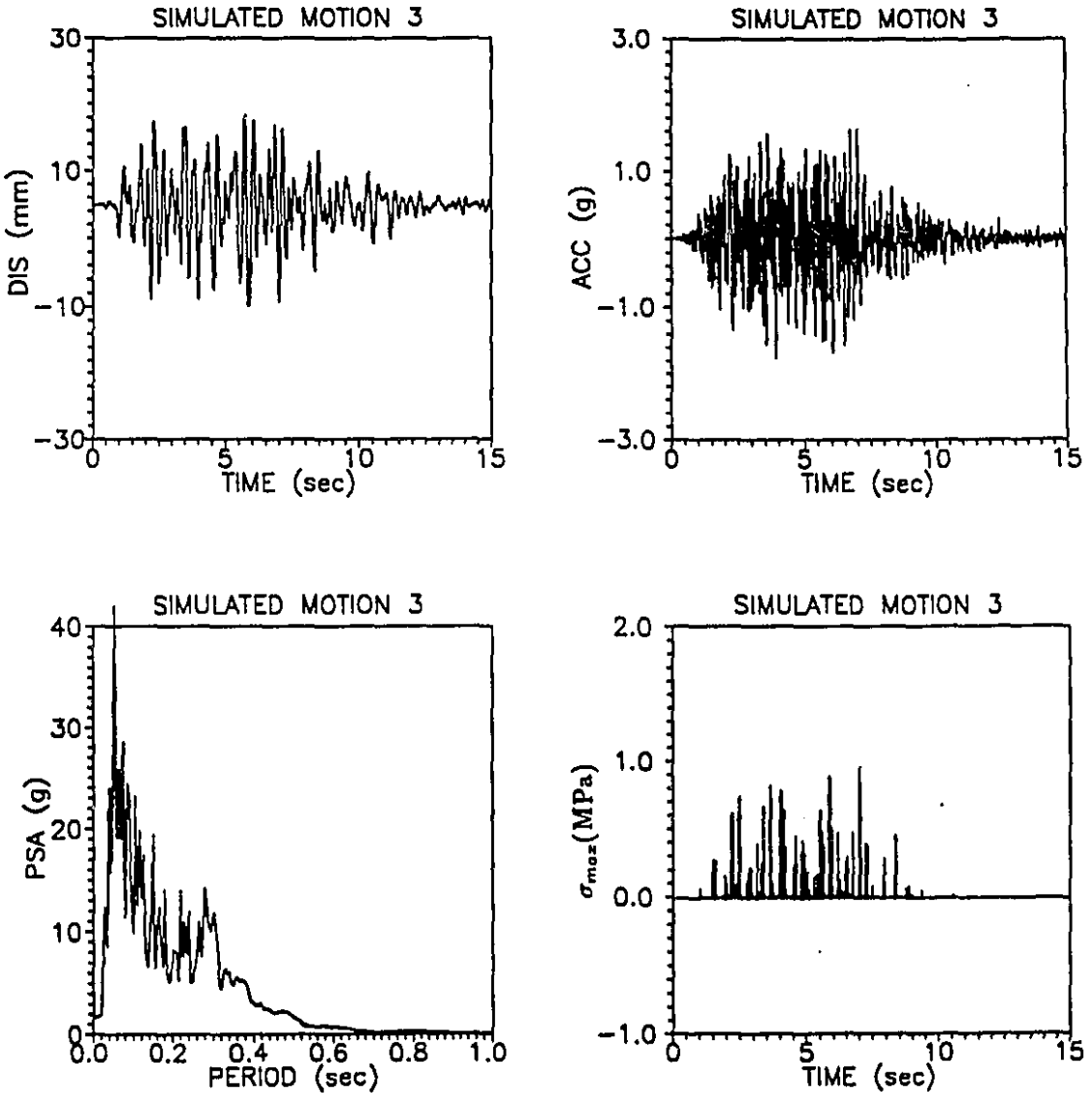

Figure 5.15: Seismic response to simulated motion 3 (SM3).

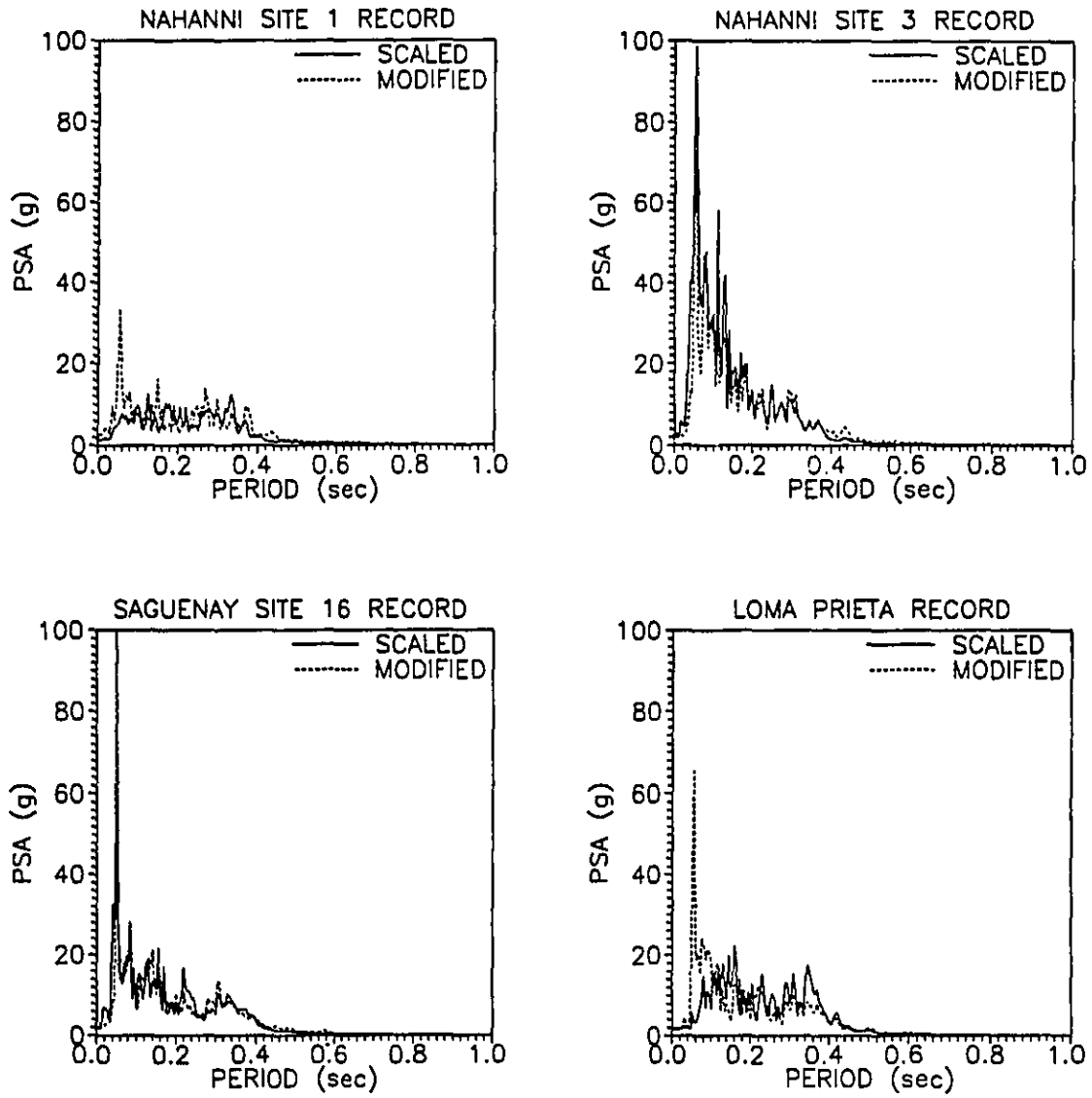

Figure 5.16: Comparative study, in terms of PSA, of the seismic response to scaled and modified records.

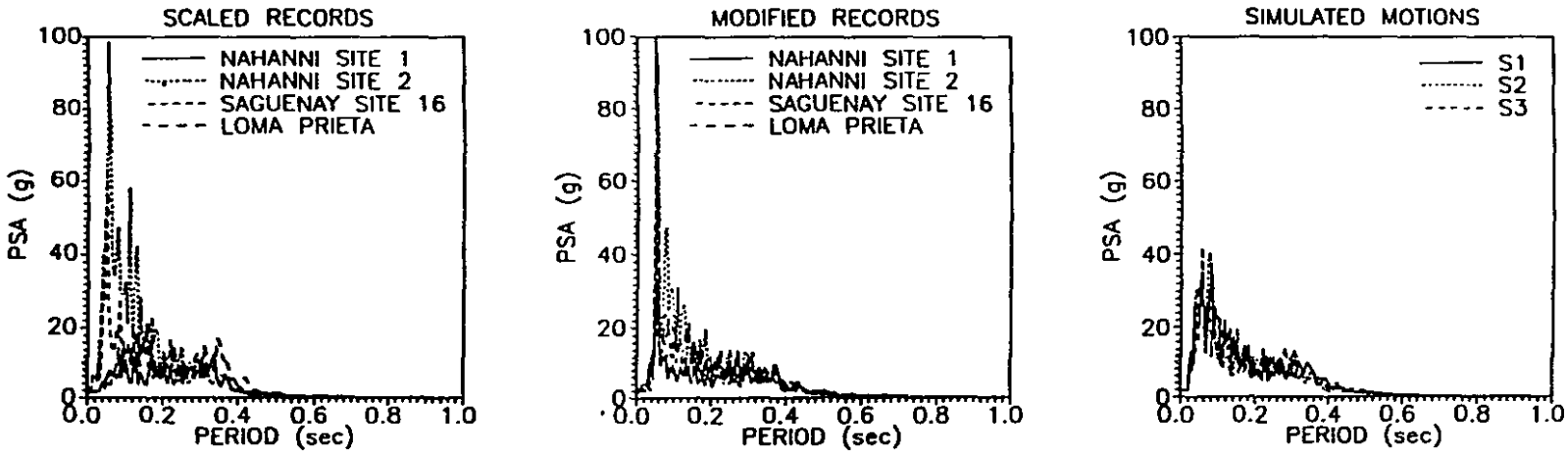

Figure 5.17: Comparative study, in terms of PSA, of the seismic response to scaled modified and simulated accelerograms.

To study the influence of the size of the dam on the response to different types of accelerograms, two smaller dams (45 m and 22.5 m) were analyzed for the scaled and modified Saguenay site 16 and Loma Prieta records, and the second simulated motion (SM2). A statistical analysis was performed here as well to assess the variability in the response for different sizes. As it would be expected, one of the smaller dams would fall in the very short period region where the amplification in the response spectrum is maximum. In this analysis it was the case of the half size model.

Figures 5.18, 5.21 show the response to scaled records for half size dam (45m). The displacement, acceleration and stress time histories due to SS16 are typical high frequency time histories of relatively small amplitude (almost same as for full scale model (90m)). The same conclusions can be drawn from the quarter scale model (22.5 m) (Fig. 5.19, 5.22)), except a noticeable drop in the stress amplitude. This may be explained by the fact that for the half scale model the fundamental mode period of vibration (around 0.16 sec) fell in the range of high frequency amplification of the response spectrum of a high frequency earthquake. Figure 5.20 shows the more intense response of the reduced scale models in terms of displacement and stresses, and the more intense response of the full scale model in terms of acceleration and its spectrum. The response to SLP shows different features in the stress time history characterized by larger amplitudes and longer stress "pulses". This means that a relatively large tensile stress will remain applied for a considerable time (one second), which may lead to excessive cracking or fast crack growth. This is due to the inherent low to medium frequency characteristic of the Californian earthquake. This observation is also shown in the response of the quarter scale model (22.5 m) (Fig. 5.22) where the same type of acceleration response is observed, but with a more sinusoidal type of displacement response. However, the stress response shows amplitudes similar magnitude to that of the half scale model (45 m), but of smaller number and of longer pulse duration (3 seconds) occurring much later in the history than those of the full (90 m) and half scale (45 m) models. When the 45 m and 22.5 m dams are subjected to the modified records, they display very common features. They lead to amplified displacement and stress response (compared to the 90 m dam response to modified records). The stress response having the particularity of showing important

	D_{max} (mm)	t_{max} (sec)	Acc_{max} (g)	t_{max} (sec)	NZC	sigma (MPa)	t_{max} (sec)	PSA (g)	T_{max} (sec)	$SI_{2s(0.04)}$ (g^{-2}*sec)
Scaled historical records SM1 ($SIe_{(0.1)}$)										
Nahanni site 1	24.5	9.9	1.37	9.0	340	0.88	9.8	12.5	0.12	2.5
Nahanni site 3	18.8	7.3	2.74	8.9	597	1.52	8.9	61.6	0.05	6.6
Saguenay S16	21.1	7.5	1.81	7.5	696	1.05	7.7	98.7	0.05	4.2
Loma Prieta	30.4	8.0	1.60	7.8	256	1.20	7.8	11.4	0.48	3.8
Historical records with modified Fourier amplitude spectra										
Nahanni site 1	19.7	3.4	2.60	9.2	341	1.68	9.2	33.5	0.05	3.0
Nahanni site 3	21.4	7.4	1.95	9.0	415	1.22	9.0	99.8	0.05	5.6
Saguenay S16	21.2	6.2	1.98	6.4	535	0.90	7.7	95.7	0.05	4.2
Loma Prieta	17.3	8.0	1.83	7.9	526	1.08	7.9	65.5	0.48	4.0
Synthetic time histories (white noise)										
S1	20.2	7.1	1.96	6.5	452	0.97	7.0	40.3	.07	4.4
S2	24.0	7.0	1.81	5.7	406	1.04	5.6	37.2	.08	4.5
S3	18.2	5.7	1.76	3.9	413	0.95	7.0	41.9	.05	4.3

Table 5.2: Maximum seismic response to different types of accelerograms.

	D_{max} (mm)			Acc_{max} (g)			NZC		
	Mean	SD	COV	Mean	SD	COV	Mean	SD	COV
Historical	23.7	4.4	0.19	1.88	0.52	0.28	472	180	0.38
Modified	19.9	1.6	0.08	2.09	0.30	0.14	454	81	0.18
Synthetic	20.8	2.4	0.11	1.84	0.09	0.05	423	20	0.05

	σ (MPa)			PSA(g)			$SI_a(0.04)$		
	Mean	SD	COV	Mean	SD	COV	Mean	SD	COV
Historical	1.16	0.23	0.20	46.0	36.5	0.79	4.3	1.50	0.35
Modified	1.22	0.29	0.24	73.6	26.7	0.36	4.2	0.93	0.22
Synthetic	0.98	0.04	0.04	39.8	1.9	0.05	4.4	0.08	0.02

Table 5.3: Statistical analysis on response parameters.

pulses. However, in a case by case study, the MSS16 leads to a higher frequency and higher amplitude displacement and stress responses than the MLP, hence reproducing the influence of the richness in high frequency of the exciting motion when the structure analyzed has a fundamental period in high frequency range. An amplification of as much as eight times can be noticed in the stress response to the MSS16 and of five times to the MLP, with a larger number of stress impulses of important magnitude and length (one second) for the MSS16. A similar amplification of the order of 1.6 is noticed in the displacement time history with a larger number of displacement peaks of large amplitudes for the MSS16. The acceleration response remained low compared to the full scale model (90 m). The response of the smallest dam was very low in all parameters. It yielded an almost constant displacement of around 9 mm (with 13.5 mm as a maximum), and an insignificant amount of stress of around 0.2 Mpa. The acceleration responses remained almost the same as for the 45 m dam. These observations are better seen in Table 5.4 that summarizes the maximum responses for the three different sizes of dams subject to the SSS16, MSS16 and a simulated motion, as well as in the comparative plots of Fig. 5.20. These data show that the displacements and stresses are amplified (maximum stresses occurring later in the history for the 45 m dam), and that the acceleration of the crest was

reduced (this has an implication on the floor spectra for which instruments and machines are designed). The response to simulated motions led to results similar to those of modified records except that the maximum responses in terms of displacements and stresses were much higher, as shown in Fig. 5.28 for the 45 m dam. However, it is worth noticing that the displacement time history does not display as much high frequency as in the response to modified records. Moreover, the large stress pulses occur earlier in the history and are of higher amplitude and longer duration (around 1.5 seconds). Ratio of 4.4 and 1.2 can be obtained between the stress responses to simulated accelerograms and scaled and modified records respectively. Similar ratios of ratios of 2.0 and 1.2 are obtained for displacements.

Another interesting feature in the response to simulated motion is the relatively important response of the 22.5 m dam in terms of displacement and stress as shown in Fig. 5.29. It is clear that these responses are much higher than in the case of modified and scaled records, especially in terms of stress where ratios of maximum stress reach 11.0 for scaled records (simulated/scaled) and 17.7 for modified records (simulated/modified). However, the stresses impulses are very small in number (two in this specific case). Beside these few pulses, the stresses are almost zero as in the case of scaled and modified records. The maximum displacement is not very high, but the number of amplitudes having large peaks of magnitude close to the maximum are more noticeable. These two observations are of importance as of the adequacy of using simulated motion in the seismic analysis of small dams. The possible reason behind this is the presence of a variety of high motion in the simulated motion, that are not present in the modified and scaled records, and that excites some important vibrational modes of the small dam which has very small fundamental period (around 0.08 sec). Therefore, more study of this type of motion on small dams is required before reaching any general conclusion. To study the general sensitivity of the response to the dam size for the three types of earthquakes (considered in the analysis of the 45 m and 22.5 m dams, namely Saguenay site 16 (SSS16 and MSS16), Loma Prieta (SLP and MLP) and SM1), a statistical analysis on the response to each size was performed and is presented in Table 5.5. This analysis shows that the mean values support the conclusions made earlier. The COV's obtained suggest that reduced size dams reflect more scatter than full scale ones, which requires more seismic analyses and study of small dams subjected to high frequency ground motion.

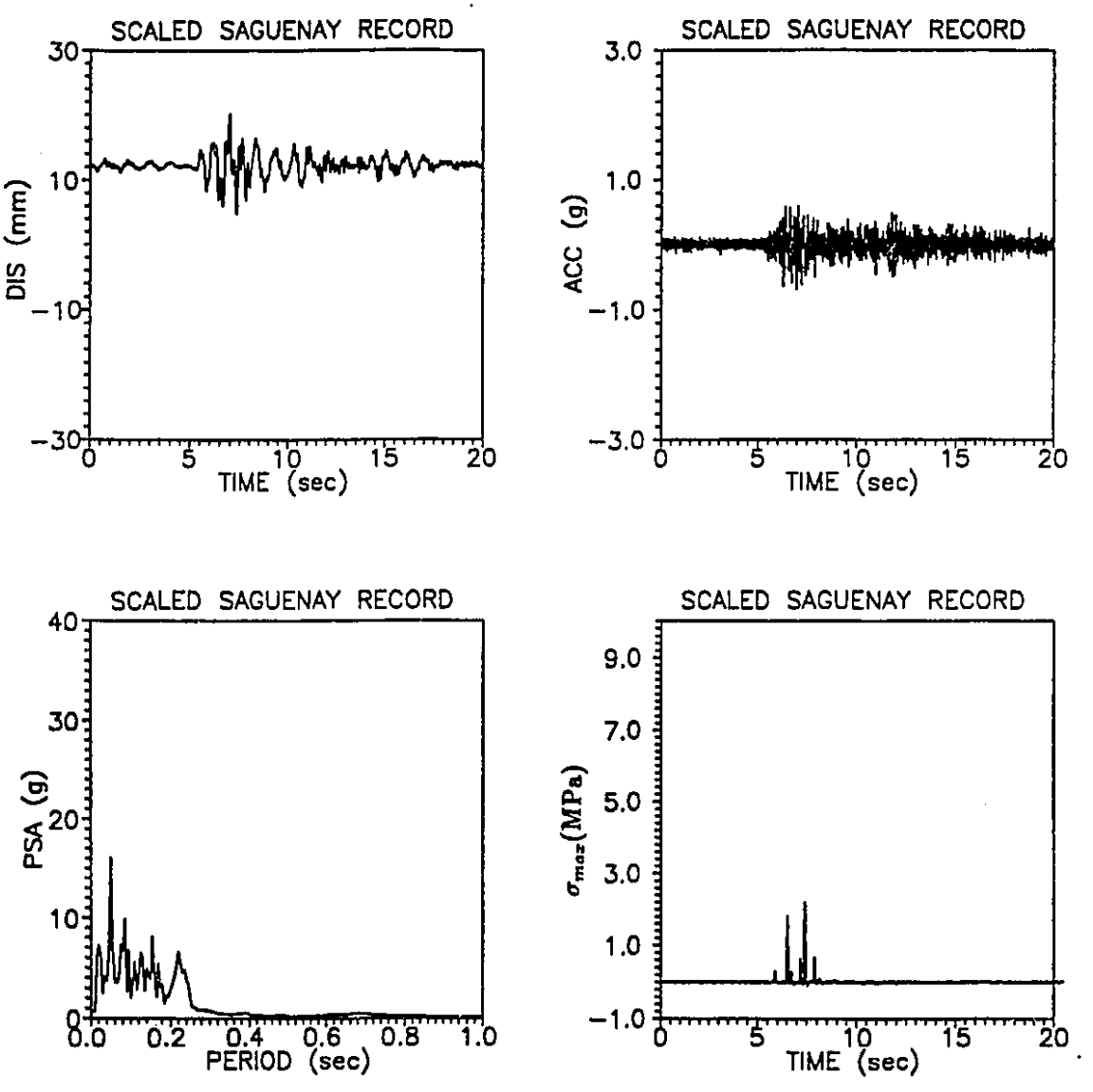

Figure 5.18: Seismic response to SS16, half-size model (45 m).

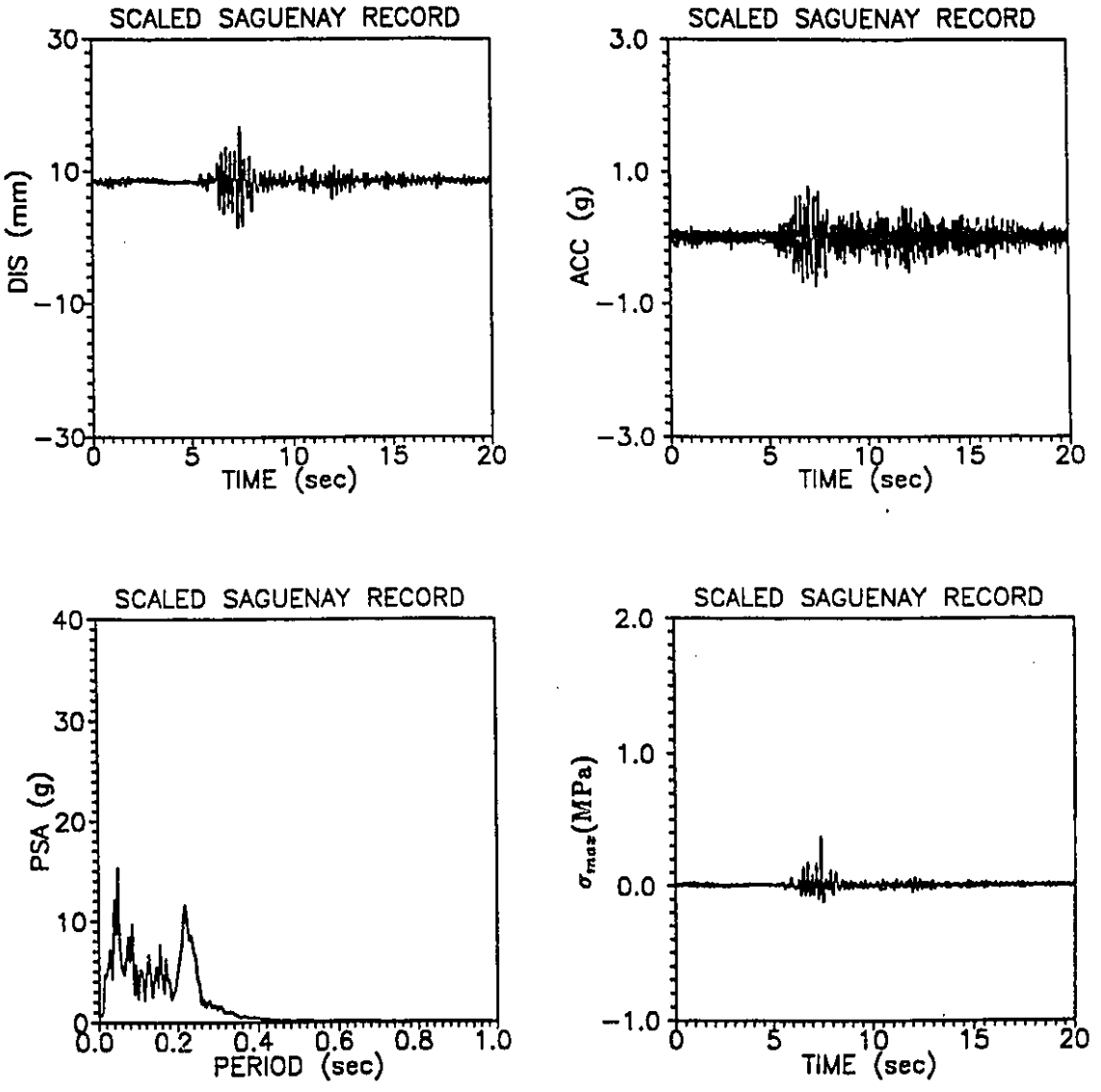

Figure 5.19: Seismic response to SS16, quarter-size model (22.5 m).

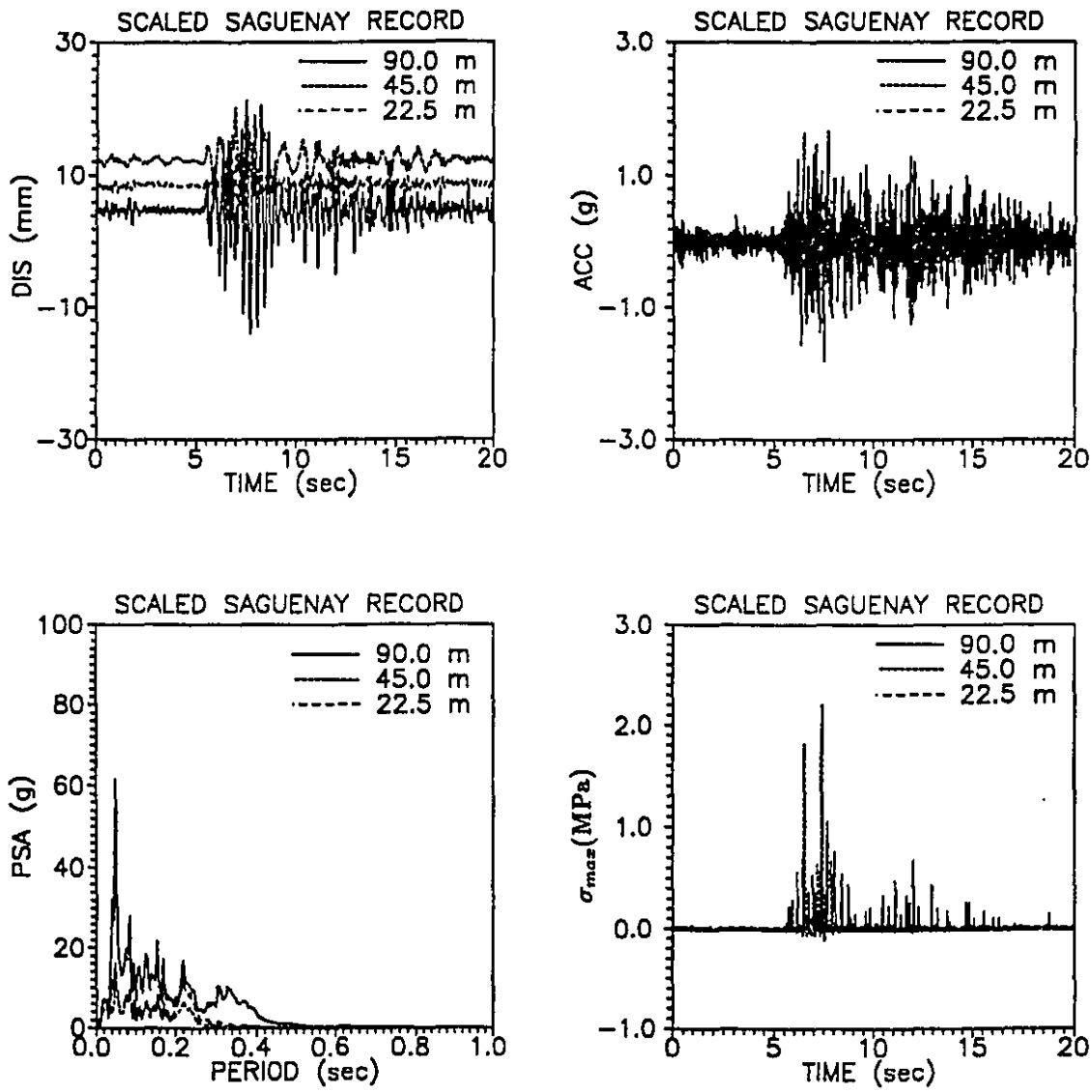

Figure 5.20: Seismic response to SS16, comparative plots.

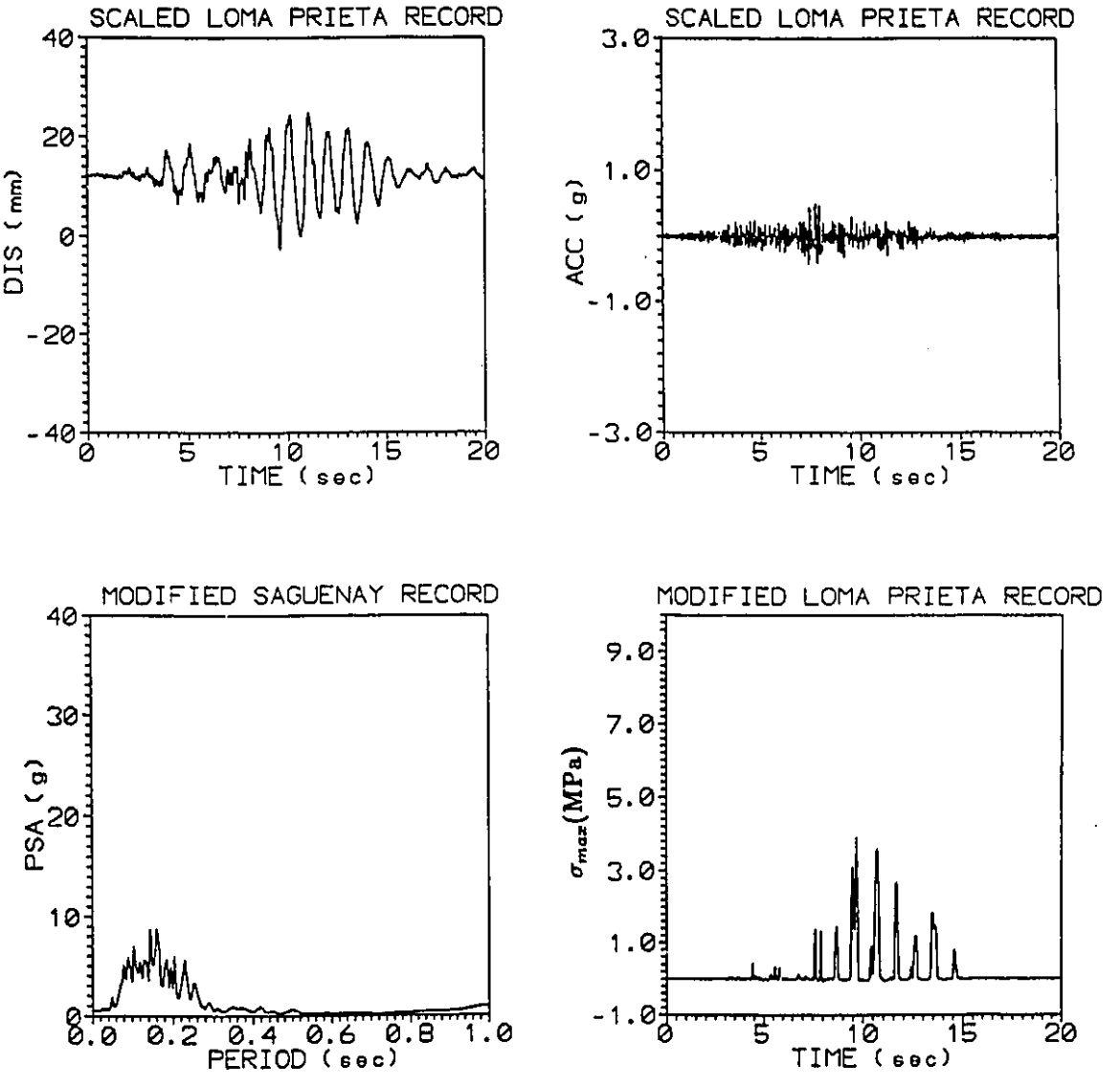

Figure 5.21: Seismic response to SLP, half-size model (45 m).

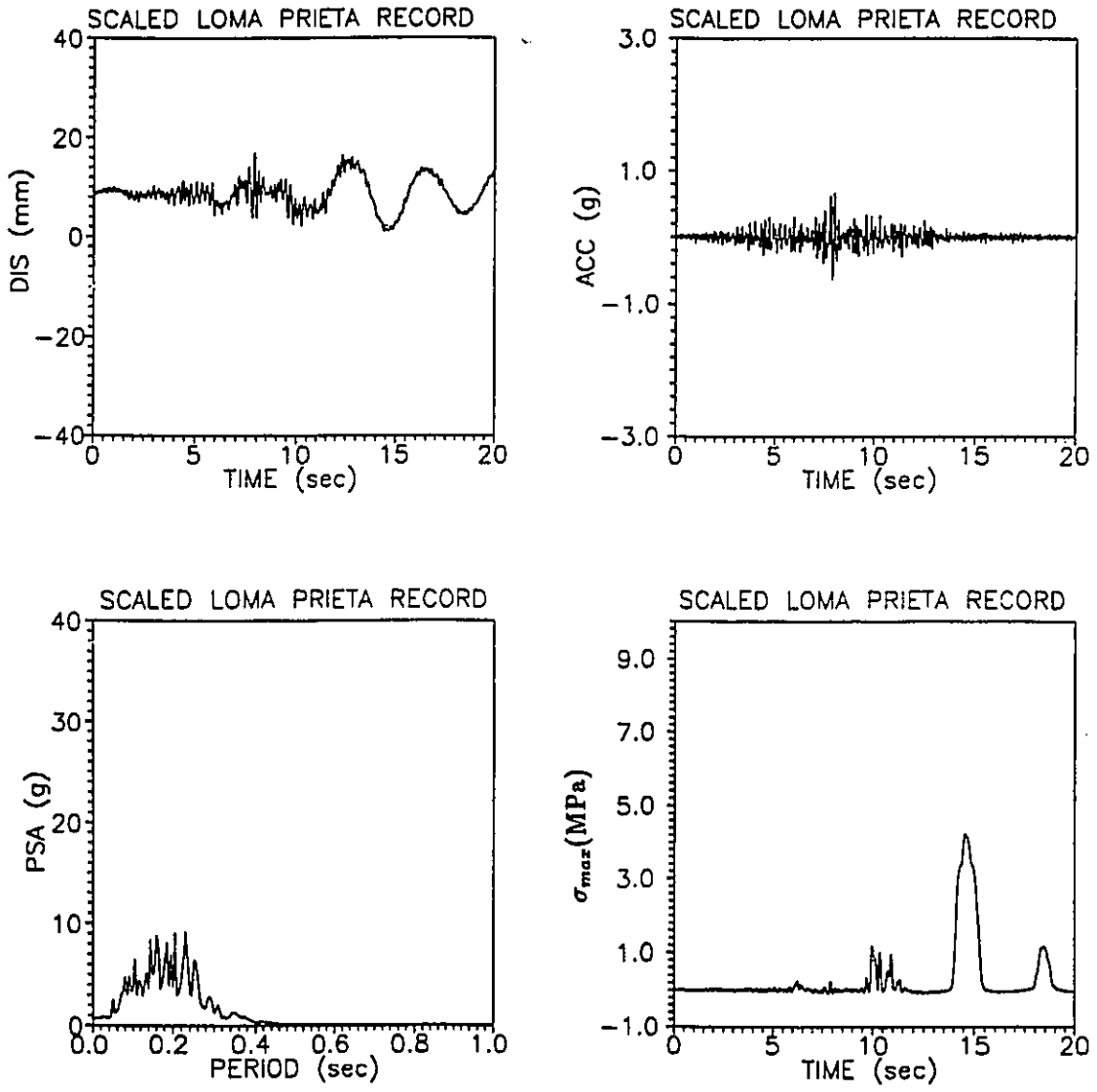

Figure 5.22: Seismic response to SLP, quarter-size model (22.5 m).

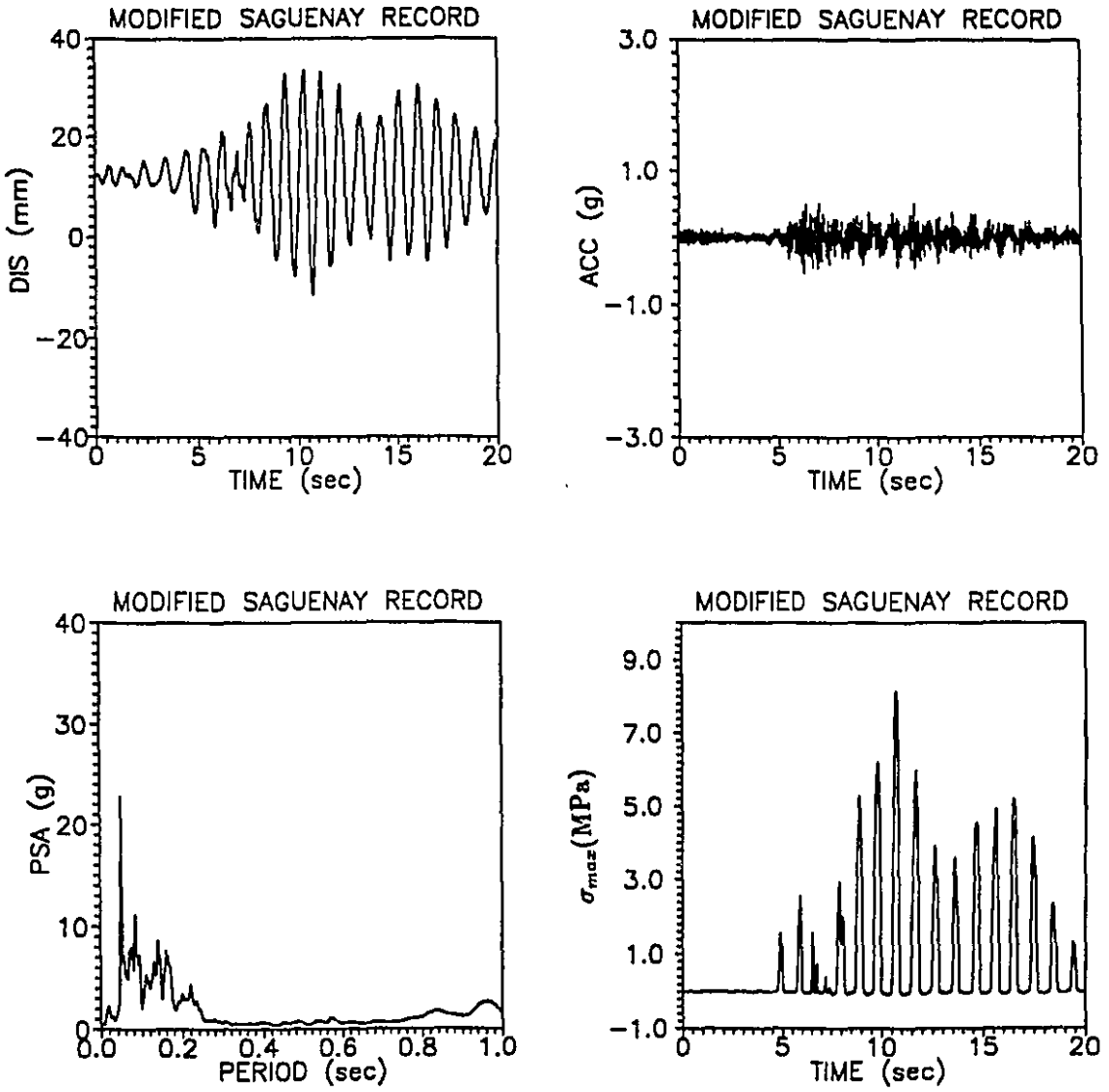

Figure 5.23: Seismic response to MS16, half-size model (45 m).

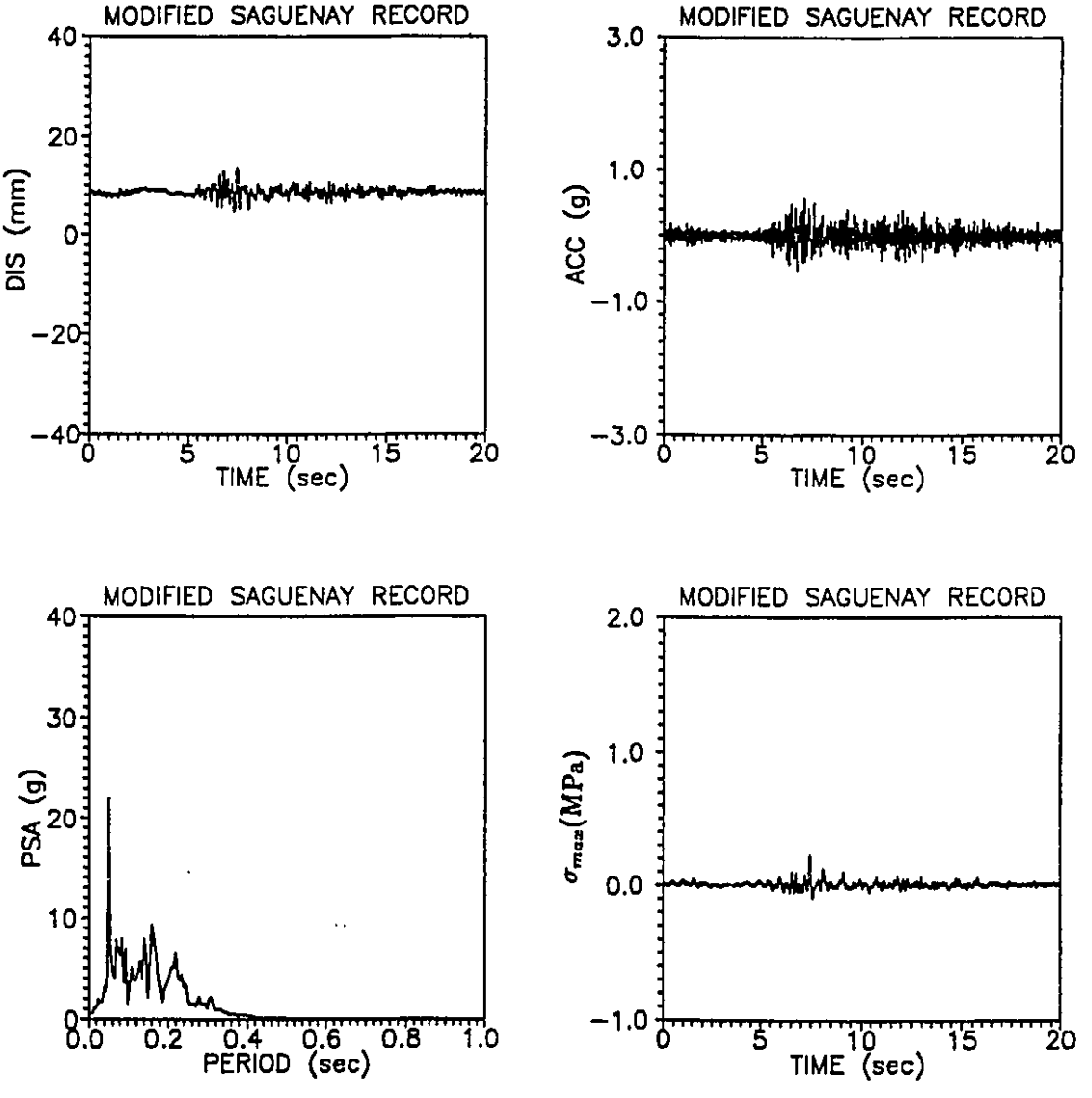

Figure 5.24: Seismic response to MS16, quarter-size model (22.5 m).

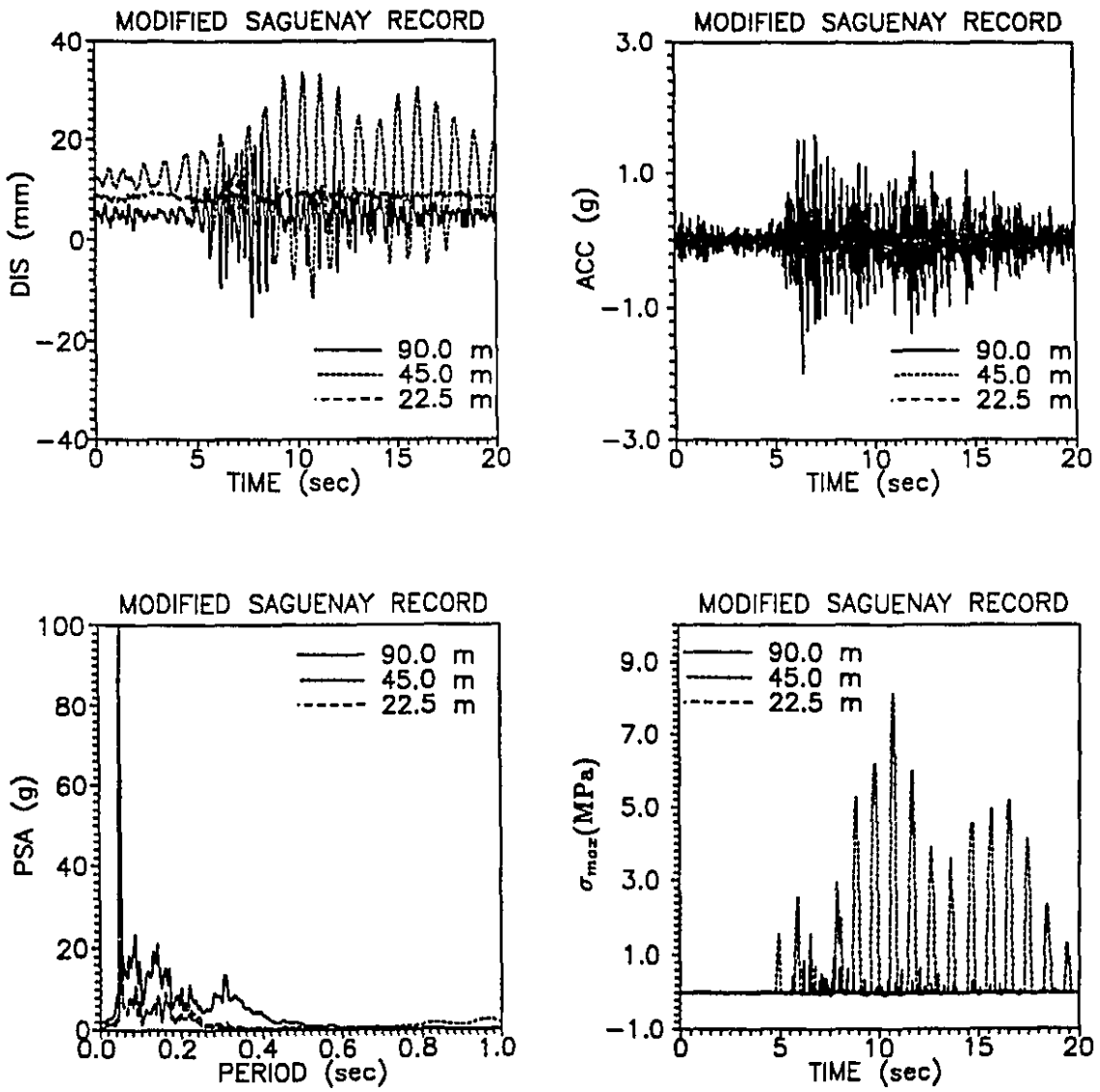

Figure 5.25: Seismic response to MS16, comparative plots.

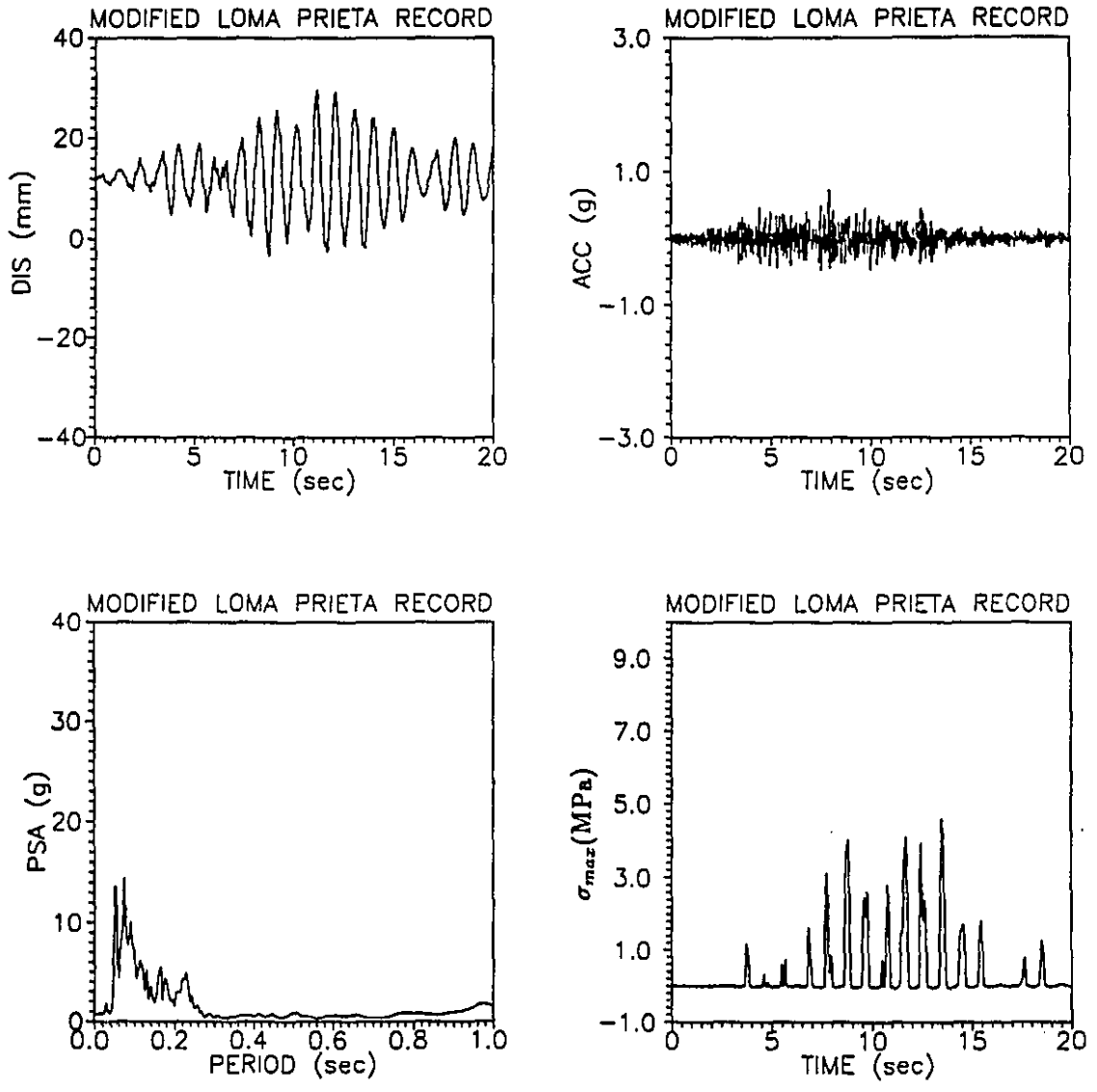

Figure 5.26: Seismic response to MLP, half-size model (45 m).

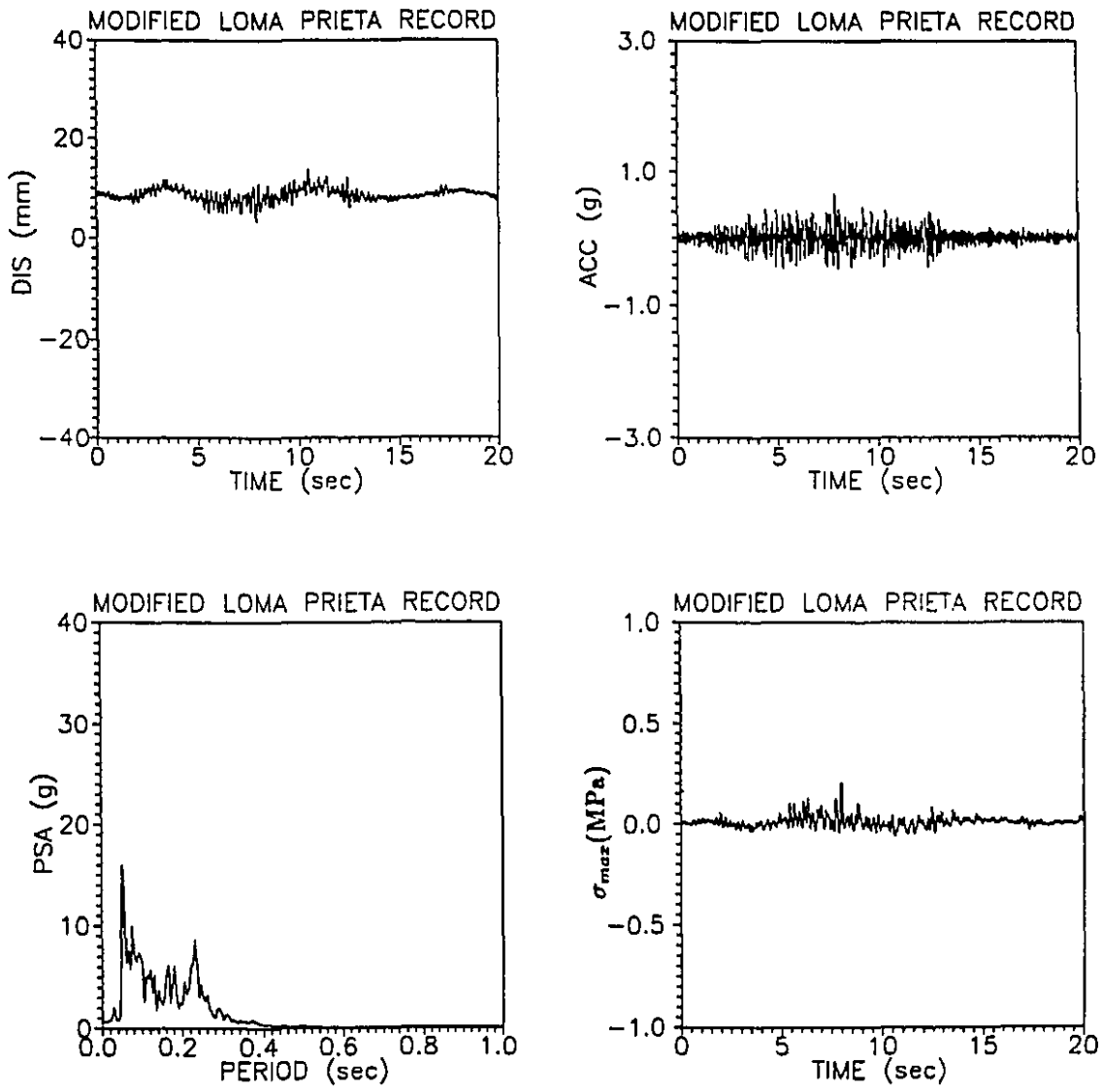

Figure 5.27: Seismic response to MLP, quarter-size model (22.5 m).

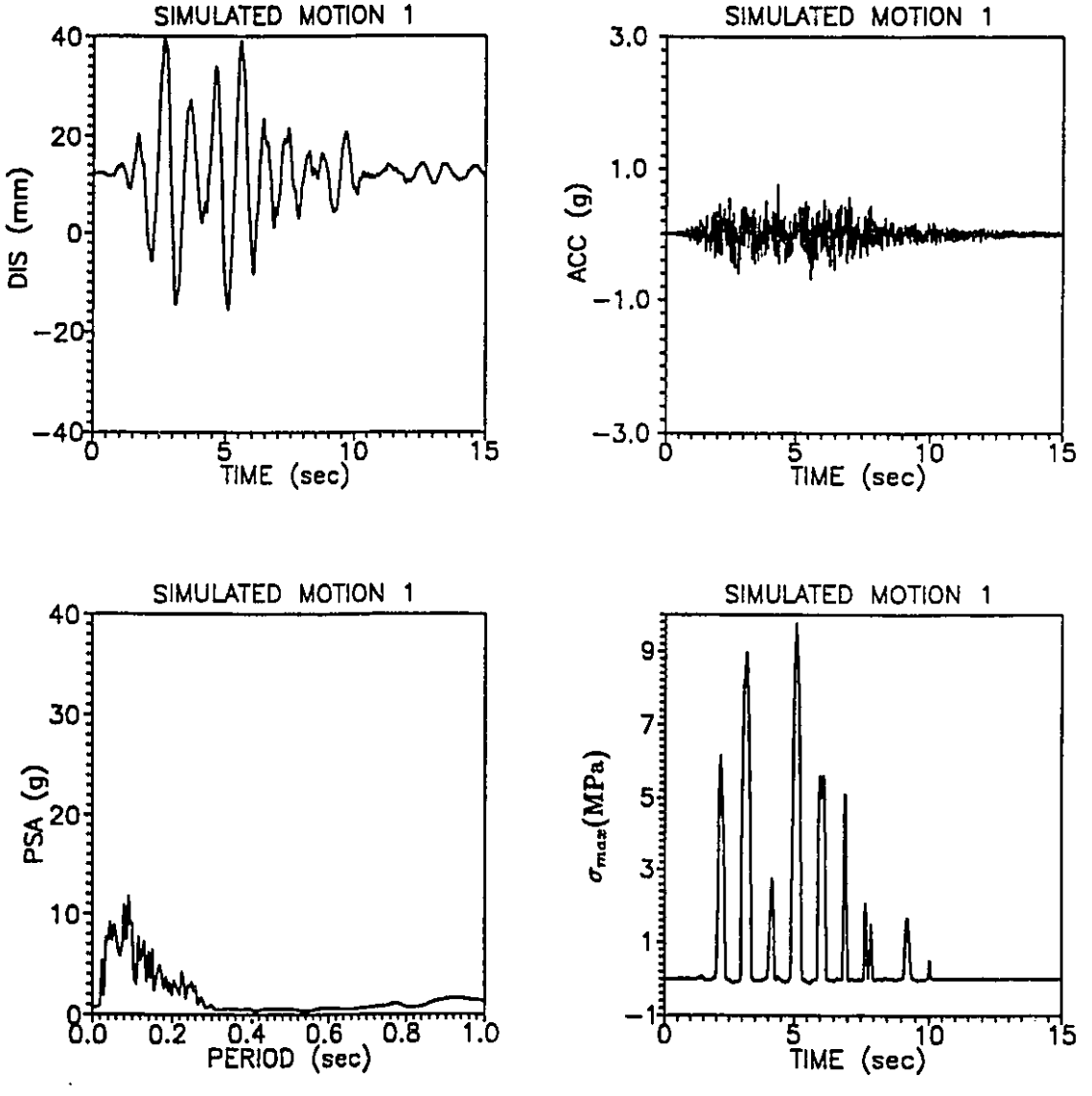

Figure 5.28: Seismic response to SM2, half-size model (45 m).

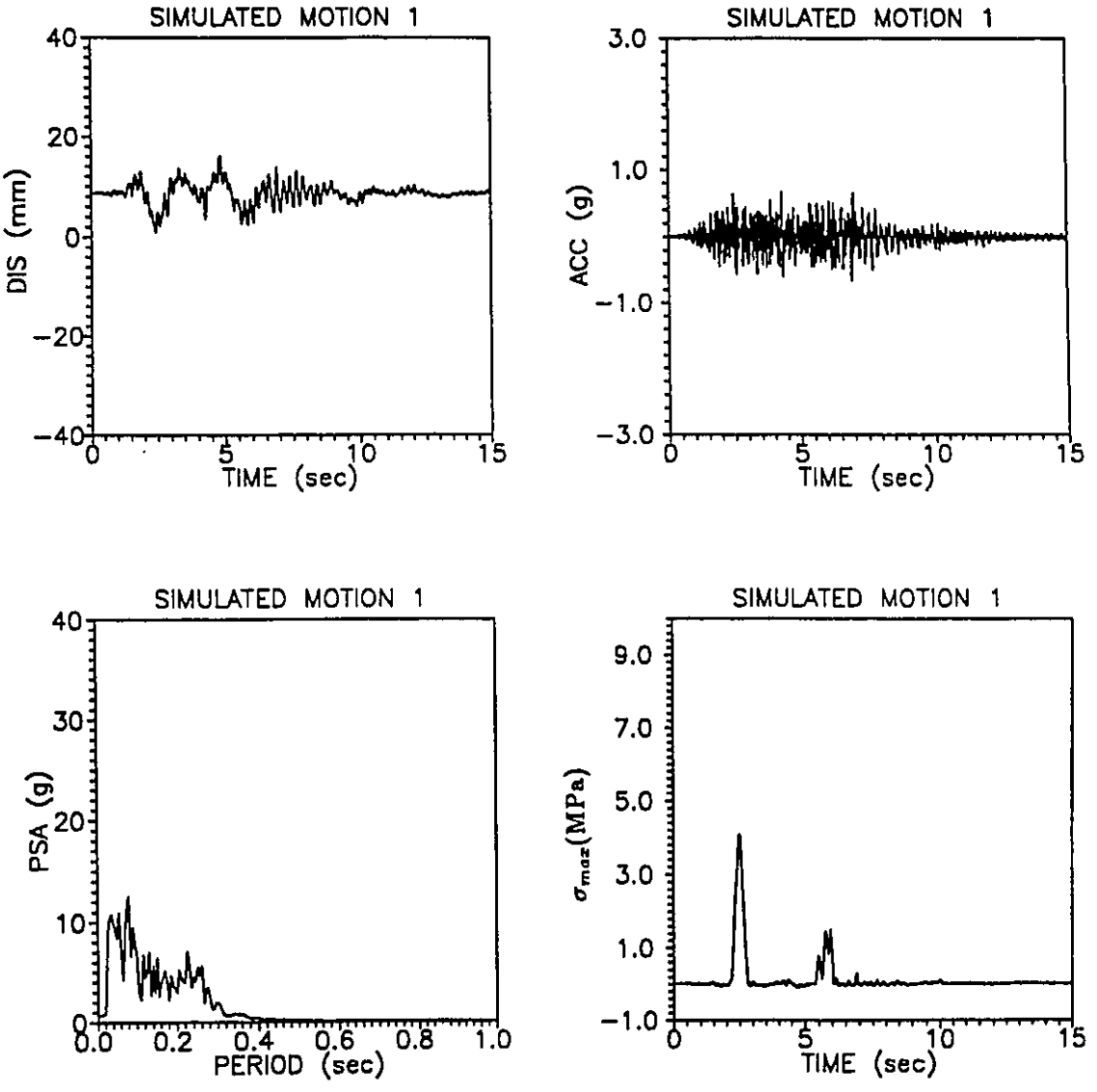

Figure 5.29: Seismic response to SM2, quarter-size model (22.5 m).

	D_{max} (mm)	t_{max} (sec)	Acc_{max} (g)	t_{max} (sec)	NZC	sigma (MPa)	t_{max} (sec)	PSA (g)	T_{max} (sec)	$SI_{a(0.04)}$ (g^2*sec)
Scaled Saguenay record (SSS16)										
Full size dam (90 m)	21.1	7.5	1.81	7.5	696	1.05	7.7	98.7	0.05	4.2
Half size dam (45 m)	20.0	7.0	0.68	7.0	789	2.20	7.4	16.1	0.05	1.1
Quarter size dam (22.5 m)	16.8	7.4	0.76	7.0	859	0.37	7.4	15.3	0.05	1.5
Modified Saguenay record (MSS16)										
Full size dam (90 m)	21.2	8.2	1.98	6.4	535	0.90	7.7	95.7	0.05	4.2
Half size dam (45 m)	33.4	10.3	0.52	6.3	511	8.14	10.7	22.8	0.05	1.2
Quarter size dam (22.5 m)	13.5	7.5	0.56	7.1	527	0.23	7.4	22.0	0.05	1.3
Synthetic accelerogram (SM2)										
Full size dam (90 m)	24.0	7.0	1.81	5.7	406	1.04	5.7	37.3	0.08	4.5
Half size dam (45 m)	39.9	2.7	0.75	4.3	403	9.77	5.1	11.7	0.09	1.3
Quarter size dam (22.5 m)	16.0	4.3	0.66	4.3	460	4.07	2.5	12.5	0.08	1.5

Table 5.4 : Maximum seismic response for different sizes of the dam.

	D_{max} (mm)			Acc_{max} (g)			NZC		
	Mean	SD	COV	Mean	SD	COV	Mean	SD	COV
90 m dam	22.1	1.34	0.06	1.86	0.08	0.04	546	119	0.22
45 m dam	31.1	8.28	0.26	0.65	0.10	0.15	568	163	0.29
22.5 m dam	15.4	1.40	0.09	0.66	0.08	0.12	615	174	0.28

	σ (MPa)			PSA(g)			$SI_a(0.04)$		
	Mean	SD	COV	Mean	SD	COV	Mean	SD	COV
90 m dam	1.00	0.07	0.07	72.23	28.26	0.37	4.30	0.14	0.03
45 m dam	6.70	3.25	0.48	16.87	4.50	0.27	1.20	0.08	0.07
22.5 m dam	1.55	1.77	1.14	16.60	3.98	0.24	1.43	0.09	0.06

Table 5.5: Statistical analysis on response parameters for different heights (seismic responses to SSS16, MSS16, SLP, MLP, and SM2 are considered).

5.3 Nonlinear fracture mechanics seismic analysis

To understand more about the influence of the type of input accelerograms, a nonlinear fracture mechanics seismic analysis of the 90 m dam was performed under the previously described motions. The dam was assumed to be fixed at the base and not retaining any water (i.e. the dam was subjected to only its weight and the earthquake motion). This analysis is done using the computer program FRAC-DAM developed at McGill University by S.S. Bhattacharjee (S.S. Bhattacharjee, P. Léger and J. Venturelli, 1992). The program uses a smeared crack approach with a new strain softening model. According to the mentioned reference the following concrete parameters were used :

(i) E = 27960 MPa (elastic modulus)

(ii) $\nu = 0.2$ (Poisson's ratio)

(iii) $\rho = 2400$ kg/m^3 (mass density)

(iv) $\sigma_t = 2$ MPa (tensile strength)

(v) $G_f = 250$ N/m (fracture energy)

A 10% dynamic magnification of tensile strength and fracture energy were used in the seismic analysis, and 5% stiffness proportional damping in the first mode. The Newmark integration method was used with a time step $\Delta t = 0.0025$ sec.

Figures 5.30 to 5.32 show the obtained crack profiles for the different types of earthquake motions. It is clear from these figures that the crack profile is seriously influences by the input details. At this stage it is worth mentioning that the vertical component of the input motion has an important role in the crack profile, and tends to make the cracks horizontal and straight. Indeed, as a trial, a scaling factor of 2.0 instead of 2/3 was used for the vertical motion. It resulted in a clean straight horizontal crack that crossed the entire top section of the dam. Almost all cracks initiate at the downstream face, they start straight and then curve. Other cracks occur on the upstream face and have the particularity of being horizontal and straight. SNS3 and SS16 being records of similar "intensity" in

terms of relatively small initial PGA, and scaling factors, they displayed cracks initiating at the same location on the downstream face. The difference between these two motions is in the upstream face where horizontal crack developed, mainly because of the influence of the vertical component. SNS1 crack profiles did not show similarity with the previous two. SLP did not produce any crack. At this stage, and given that SLP was scaled down, it is though that the absence of cracks is due to the Western nature of SLP, where the high frequency motion that would damage the dam is very low if not absent.

The most interesting part of this analysis is that of the modified records. They all exhibit two initial horizontal cracks from each face of the dam. For MNS3 the downstream crack curved significantly, but for MLP the degree of curvature was very minor. The remaining two did not show curvature at all. The cracks initiated from similar location in each case with little (negligible) variation due to the details of the input motion. For MNS1 and MSS16 the cracks are almost similar in shape and location. MNS3 displayed a curving crack as well as the MLP at a lesser degree. The MLP crack had the same location as other motions for the upstream face, but different for the downstream face. This may be due to the western nature of the MFLP. As for the simulated motion, only little can be said. SM1 and SM2 exhibited exactly similar (in location and shape) downstream cracks, but SM2 displayed some typical upstream horizontal cracks that were not as severe as the downstream crack. Cracks due to SM3 were completely different (in shape and location) and were mainly upstream cracks. Since only three simulated motions were tested, it is not possible to give a decisive conclusion on the efficiency of the simulated motions.

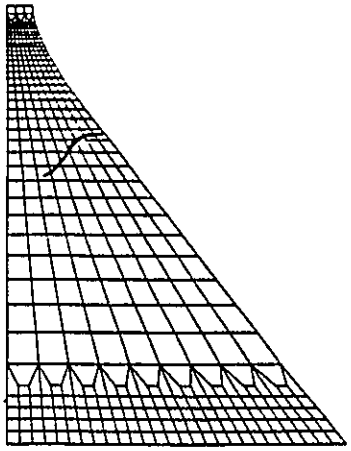

SNS1

Scaled Nahanni Site 1

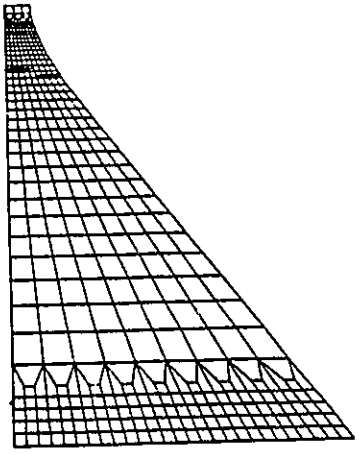

SNS3

Scaled Nahanni Site 3

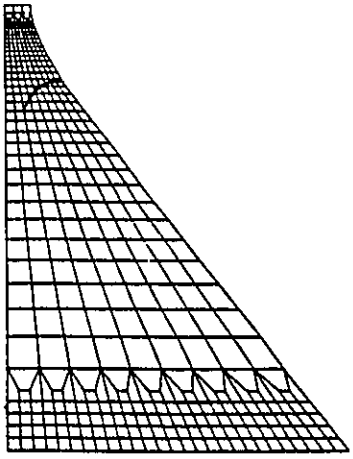

SSS16

Scaled Saguenay Site 16

Figure 5.30: Crack Patterns due to scaled accelerograms

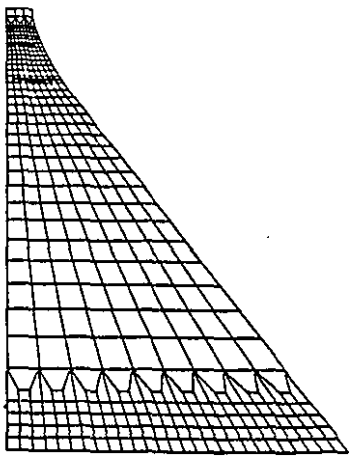

MNS1

Modified Nahanni Site 1

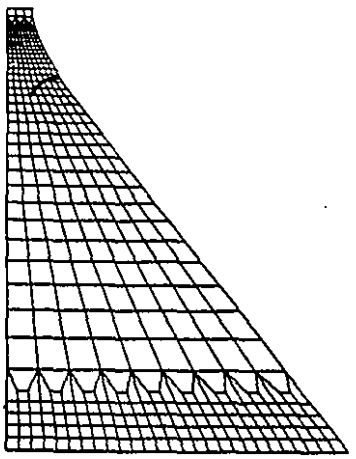

MNS3

Modified Nahanni Site 3

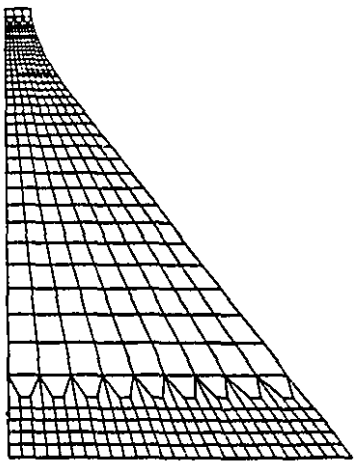

MSS16

Modified Saguenay Site 16

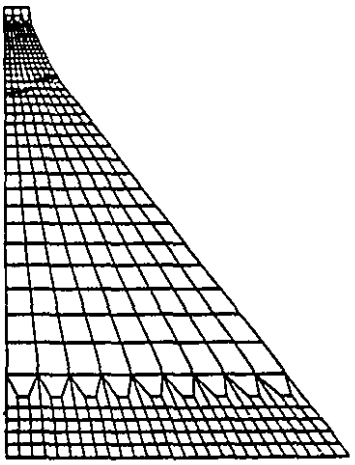

MLP

Modified Loma Prieta

Figure 5.31: Crack Patterns due to modified accelerograms

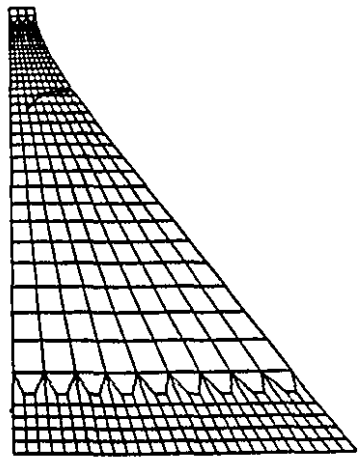

SM1

Simulated motion 1

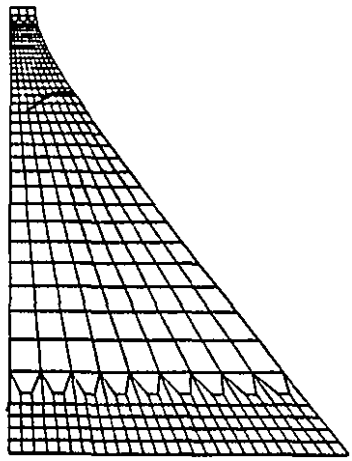

SM2

Simulated motion 2

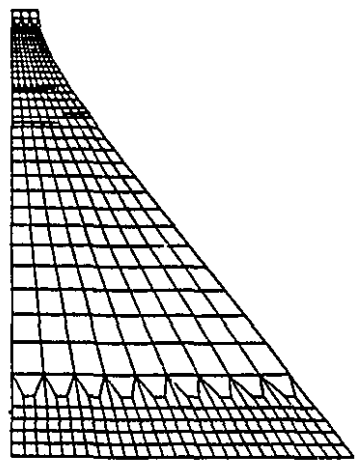

SM3

Simulated motion 3

Figure 5.32: Crack Patterns due to simulated accelerograms (90 m dam).

Chapter 6

Conclusions

Ideally, a series of real earthquakes scaled to cover the target spectra in the range of important structural periods should be used in seismic safety evaluation of critical facilities. However, the worldwide database is deficient in large magnitude near source record with seismotectonic environment compatible with the Eastern Canadian conditions. Moreover, the computational and engineering effort to carry out and interpret inelastic time-history seismic analysis is very significant. To reduce the computational effort, and provide input ground motion suitable for seismic safety evaluation able to yield dynamic response amplification corresponding to the target design spectrum over the frequency range of interest, spectrum-compatible accelerograms can be used.

In this study the response of SDOF systems with different hysteresis models and strengths, to three types of accelerograms; (i) scaled historical records, (ii) historical records with modified Fourier amplitude spectra, and (iii) synthetic accelerograms, has been examined. Moreover the seismic ground motion parameters and pulses characteristics of the selected accelerograms have been investigated. Finally, exploratory linear and fracture earthquake response analysis of short period concrete gravity dams (90m, 45 m and 22.5 m) subjected to the three types of accelerograms have been carried out.

The following conclusions can be made:

(i) ENA earthquakes are very rich in high frequency motion and have initially a large number of zero crossings and acceleration pulses, compared to their Western counterparts, and this is reflected in the structural response.

(ii) The Atkinson and Boore (1990) attenuation relationships are compatible with ENA records, and may be used successfully to generate high frequency spectrum-compatible accelerograms for ENA environment.

(iii) The deficiency of WNA records is inherent and cannot be compensated by the modification of their Fourier amplitude spectrum. However, a good spectrum-compatibility to ENA spectra may be achieved for periods longer than 0.10 sec.

(iv) The process of modification of the Fourier spectra of historical records increases the NZC and number of pulses for WNA records, and decreases them for ENA records. The Fourier modification of low magnitude records, such as those of the Saguenay earthquake, to achieve compatibility with a larger near-source event is possible and appears to give acceptable results.

(v) Synthetic accelerograms do not have a number of pulses necessarily larger than historical records, they tend to exhibit a smaller amplitude of the largest pulse as compared to scaled historical records.

(vi) The scaling of historical records to $SI_{a(.10)}$ is a good procedure for the seismic response of short-period structures. If ENA records are used exclusively, the scaling to $SI_{a(.04)}$ is recommended. Scaling to PGA is not recommended especially if WNA records are used. Scaling procedures do not affect the frequency content. However, some definitions of the duration of strong shaking are not linearly affected by the application of the scaling factor.

(vii) The scaling of the M=5.9 at 42 km Saguenay record to the $SI_{a(0.10)}$ of an M=7 at 20 km event, is not recommended since it requires a scaling factor approximately equal to 4. The SDOF responses, particularly for the bilinear hysteresis model in terms of NYE and NZC, presents very significant differences with the other records.

(viii) Artificial accelerograms (modified or synthetic) have larger RMSA and AI than scaled historical records.

(ix) Synthetic accelerograms give excellent spectrum-compatibility compared to modified historical records.

(x) The short period range may be divided in two parts; the very short-period (VSP, $T_1 < 0.20$ sec), and moderate short-period range (MSP, $0.20 \leq T_1 \leq 0.50$ sec). In the VSP, some response parameters such as μ_{max}, $\frac{E_h}{E_i}$, NZC, and NYE are particularly sensitive to the details of input motions considered.

(xi) If synthetic accelerograms are used, a single record appear to be adequate to produce a representative structural response. If modified records are used, more than one should be used.

(xii) Spectrum-compatible accelerograms should reproduce, as far as possible, the essential ground motion characteristics inherent in historical records. For linear seismic response analysis, either historical record with modified Fourier spectra or synthetic accelerograms can be used to evaluate the structural response. For nonlinear analysis, Fourier modified records tend to be closer to the responses of the scaled records than that obtained from the synthetic accelerograms. Historical records with modified Fourier amplitude spectra tend to minimize the variation in $\frac{E_h}{E_i}$, μ_{max}, μ_{acc}, NZC, and NYE as compared to the results obtained from synthetic accelerograms for these indexes. The parameters E_i and u_{max} computed from modified or synthetic records are very similar.

(xiii) The seismic analyses of dams (90 m, 45 m and 22.5 m) revealed other important properties of artificial earthquakes and that are the intensity, duration and time of occurrence of stress pulses which need to be carefully studied based on more data and better correlation between artificial and historical records. The eastern earthquakes being rich in high frequency motion had more influence on small dams (having relatively small fundamental period), especially in terms of displacements and stresses.

(xiv) The nonlinear seismic fracture analyses of the 90 m dam showed that high intensity vertical motion had a tendency to produce horizontal crack profile,

and showed how different input motions of same type lead to a relatively similar crack patterns.

Most investigations on the use of artificial accelerogram for nonlinear seismic analysis of critical facilities located in North America, have been based on US West coast seismic events. This study has examined the use of artificial accelerograms for ENA environment that is rich in high frequency motion. Western records should not be used to investigate the seismic safety of ENA structures with important periods of vibration shorter than 0.10 sec. As the important periods lengthens, Western records become more acceptable to represent ENA conditions.

Recommendations for future work

This report is far from covering all aspects of design earthquakes for Eastern Canada. Therefore, it is suggested that more attention be given to the variability of attenuation laws, as well as the synthetic accelerograms generation. The use of nonstationnary white noise and the addition of more parameters that better represent the randomness of earthquakes is also recommended. As for the seismic response, it is suggested to test more accelerograms of the three types in the nonlinear analysis of real multi-degree-of-freedom structures such as buildings, dams, offshore structures, and other lifeline structures, and to observe the variability of damage indexes with these different accelerograms. There is a lot of work that can be done with respect to seismic dam analysis, especially the response to modified and simulated motions. Special attention should be given to small dams and other structures having relatively very short fundamental period. The dam fracture analyses are restricted to empty reservoir, whereas the reality is otherwise. Therefore, it is recommended to study the real case with full interaction, keeping in mind the points raised in this study.

References

1. ADAMS, J., and BASHAM, P. 1989. Seismicity and seismotectonics of Canada east of the Cordillera. Geoscience Canada, 16(1) :3-16.

2. ATKINSON, G.M., and BOORE, D.M. 1990. Recent trends in ground motion and spectral response relations for North America. Earthquake Spectra, 6(1): 15- 35.

3. ATKINSON, G.M. 1992. Personal communication.

4. BARENBERG, M.E. 1989. Inelastic response of a spectrum-compatible artificial accelerogram. Earthquake Spectra, 5(3): 477-493.

5. BASHAM, P.W., WEICHERT, D.H., ANGLIN, F.M., and BERRY, M.J. 1985. New probabilistic strong seismic ground motion maps of Canada. Bulletin of the Seismological Society of America, 75: 563-595.

6. BHATTARCHARJEE, S.S., LÉGER, P. and VENTURELLI, J. 1992. Thermo-seismic analysis of concrete dams. Fracture Mechanics of Concrete Structures. Z.P. Bazant Ed., Elsevier Pub., Proc. Int. Conf. on Fracture Mech. of concrete Struct. Breckenridge, Colorado, USA, pp 361-366

   ACI conference on fracture mechanics, Colorado.

7. BERTERO, V.V. 1979. Seismic performance of reinforced concrete structures. Anal. Acad. Ci. Ex. Fis. Nat. Buenos Aires, (31) : 75-95.

8. BOLT, B.A. 1973. Duration of strong ground motion. Proceedings of the Fifth World Conference on Earthquake Engineering, Roma. 1, 6-D, paper No. 292.

9. CAN3-N289.2-M81. 1981. Ground motion determination for seismic qualification of CANDU nuclear power plants. Canadian Standards Association, Rexdale, Ontario, Canada.

10. CAN3-N289.3-M81. 1981. Design procedures for seismic qualification of CANDU nuclear power plants. Canadian Standards Association, Rexdale, Ontario, Canada.

11. CEA, Canadian Electrical Association 1990. Safety assessment of existing dams for earthquake conditions, report No. 420 G 547, Vol. A, B, and C-2, Montreal, Quebec.

12. CHOPRA, A.K., and LOPEZ, O.A. 1979. Evaluation of simulated ground motions for predicting elastic response of long period structures and inelastic response of structures. Earthquake Engineering and Structural Dynamics, 7: 383-402.

13. CHRISTIAN, J.T. 1988. Developing design ground motions in practice. Earthquake Engineering and Soil Dynamics II - Recent advances in ground motion evaluation. ASCE Geotechnical Special Publication No.20, pp. 405-429.

14. CSA S471-M1989. 1989. General requirements, Design criteria, the Environment and loads. Part 1 of the code for the design, construction and installation of fixed offshore structures. Canadian Standards Association, Rexdale, Ontario, Canada.

15. DOBRY, R., IDRISS, I.M. and NG, E. 1978. Duration characteristics of horizontal components of strong-motion earthquake records. Bulletin of the Seismological Society of America, 68(5): 1487-1520.

16. DUNBAR, W.S. 1991. Safety assessment of existing dams for earthquake conditions: part 2 - Ground motion estimation methodology. Canadian dam

safety seminar. BiTech Publishers LTD, Vancouver, pp. 21-33.

17. DUNBAR, W.S. and CHARLWOOD, R.G. 1991. Empirical methods for the prediction of response spectra. Earthquake spectra. 7(3): 333-353.

18. EERI Committee on seismic risk. 1989. The basics of seismic risk analysis. Earthquake Spectra 5(4): 675-702.

19. ELLIS, G.W., SRINIVASAN, M., and CAKMAK, A.S. 1990. A program to generate site dependent time histories: EQGEN. Technical report NCEER-90-0009, National Center for Earthquake Engineering, Buffalo, USA.

20. FEMA, FEDERAL EMERGENCY MANAGEMENT AGENCY. 1985. Federal guidelines for earthquake analyses and design of dams. U.S. Government printing office : 1985 0-527-114/30411.

21. FENVES, G. and CHOPRA A.K. 1984. EAGD-84 a computer program for earthquake analysis of concrete gravity dams. Report No. UCB/EERC-84/11, University of California, Berkeley.

22. HASEGAWA, H.S, BASHAM, P.W., and BERRY, M.J. 1981. Attenuation relations for strong seismic ground motion in Canada. Bulletin of the Seismological Society of America, 71(6): 1943-1962.

23. HEIDEBRECHT, A.C., BASHAM, P.W., RAINER, J.H., and BERRY, M.J. 1983. Engineering applications of new probabilistic seismic ground-motion maps. Canadian Journal of Civil Engineering, 10: 670-680.

24. HERMANN, R.B. and NUTTLI, O.W. 1984. Scaling and attenuation relations for strong ground motion in eastern north America. 8th world conf. Earthquake Eng., San Francisco 1984 vol II, pp. 305-309.

25. JOYNER, W.B. and BOORE, D.M. 1988. Measurement, characterization, and prediction of strong ground motion. Earthquake Engineering and Soil Dynamics II - Recent advances in ground motion evaluation. ASCE Geotechnical Special Publication (20) : 43-102.

26. LIOU, G., PENZIEN, J., and YEUNG, R.W. 1988. Response of tension-leg platforms to vertical seismic excitations. Earthquake Engineering and Structural Dynamics, 16: 157-182.

27. MAHIN, S.A. and LIN, J. 1983. Construction of inelastic response spectra for single-degree-of-freedom-systems. Report No. UCB/EERC-83/17. Earthquake Engineering Research center, University of California, Berkeley.

28. McCANN, M.W. and SHAH, H.C. 1979. Determining strong-motion duration of earthquakes. Bulletin of the Seismological Society of America, 69(4): 1253-1265.

29. McGUIRE, R.K. 1988 . Engineering model of earthquake ground motion for eastern north America. Electrical Power Research Institute NP-6074, Research project 2556-16.

30. National Building Code of Canada. 1990. National Research Council of Canada, Ottawa, Ontario.

31. NAU, J.M., and HALL, W.J. 1984. Scaling methods for earthquake response spectra. ASCE Journal of Structural Engineering, 110(7): 1533-1548.

32. NUTTLI, O.W. 1981. Similarities and differences between Western and Eastern United States earthquakes, and their consequences for earthquake engineering. Proceedings of earthquakes and earthquake engineering : the Eastern United States. Sept 14-16, 1981, Knoxville, Tennessee : 25-51.

33. NUTTLI, O.W., and HERMANN, R.B. 1987. Ground motion relations for eastern north American earthquakes. Developments in geotechnical engineering 44. Ground motion and engineering seismology. pp. 231-241. Edited by A.S. CAKMAK, Department of Civil Engineering, Princeton University.

34. PAL, S., DASAKA, S.S., and JAIN, A.K. 1987. Inelastic response spectra. Computers and Structures, 25 (3) : 335-344.

35. RAINER, J.H. 1986. Applications of the fourier transform to the processing of vibrational signals. Institute for Research in Construction, National Research Council.

36. RUIZ, P. and PENZIEN, J. 1969. PSEQGN. Artificial generation of earthquake accelerograms. Report No. UCB/EERC-69/3, University of California, Berkeley.

37. SEED H.B., IDRISS I.M. and KIEFER F.W. 1968. Characteristics of rock motions during earthquakes. Report No. UCB/EERC-68/5, University of California, Berkeley.

38. SHAW, D.E., RIZZO, P.C., and SHUKLA, D.K. 1975. Proposed guidelines for synthetic accelerogram generation methods. Proceedings of the 3rd SMIRT conference, LONDON 1975, k1/4, pp. 1-11.

39. SCHIFF, S.D. 1988. Seismic design studies of low-rise steel frames. Ph.D. thesis, Department of Civil Engineering, University of Illinois at Urbana-Champaign.

40. SIMQKE. 1976. A program for artificial motion generation. User's manual. Department of Civil Engineering, Massashusetts Institute of Technology.

41. TARBOX, G.S., DREHER, K.J., and CARPENTER, L.R. 1979. Seismic analysis of concrete dams. Third ICOLD conference New Delhi, Q. 51, R. 11, pp. 963-994.

42. TINAWI R. et al. 1990. Les dommages dus au tremblement de terre du Saguenay du 25 Novembre 1988. Canadian Journal of Civil Eng. 17(3): 366-394..

43. TRIFUNAC, M.D. and BRADY, A.G. 1975. A study of the duration of strong earthquake ground motion. Bulletin of the Seismological Society of America, 65(3): 581-626.

44. TSAI, Y.B., BRADY, F.W, and CLUFF, L.S. 1990. An integrated approach for characterization of ground motions in PG&E's long term seismic program

for Diablo canyon. Proceedings of fourth U.S.National conference on earthquake engineering, May 20-24, 1990, Palm Springs, California, 1 : 597-606.

45. USCOLD 1985. Guidelines for selecting seismic parameters for dam projects. National Science Foundation, Grant No. CEE-8218049. C/O CHAS, T. MAIN, INC. PRUDENTIAL CENTER, BOSTON, MA 02199

46. UANG, C. and BERTERO, V.V. 1990. Evaluation of seismic energy in structures. Earthquake Engineering and Structural Dynamics, 19: 77-90.

47. VANMARCKE, E.H. and LAI, S.P. 1980. Strong-motion duration and RMS amplitude of earthquake records. Bulletin of the Seismological Society of America, 70(4): 1293-1307.

48. VON THUN, J.L., ROEHM, L.H., SCOTT, G.A., and WILSON, J.A. 1988. Earthquake ground motions for design and analysis of dams. Earthquake Engineering and Soil Dynamics II- Recent advances in ground-motion evaluation. ASCE Geotechnical Special Publication 20 : 463-481.

49. WALD, D.J., BURDICK, L.J., and SOMERVILLE, P.G. 1988. Simulation of acceleration time histories close to large earthquakes. Earthquake Engineering and Soil Dynamics II- Recent advances in ground-motion evaluation. ASCE Geotechnical Special Publication No.20, pp. 430-444.

50. WALD, D.J., BURDICK, L.J., and SOMERVILLE, P.G. 1988. The Whittier Narrow California Earthquake of October 1, 1987- Simulation of recorded accelerations. Earthquake Spectra 4(1): 139-156

51. WANG, P.C., and YUN, C.B. 1979. Site-dependent critical design spectra. Earthquake Engineering and Structural Dynamics, 7: 569-578.

Appendix A

DEFINITION AND APPLICATION OF MAGNITUDE SCALES

When attenuation laws are used, one must be careful regarding the magnitude definition used in that law, the misuse of the right definition will lead to erroneous results (NUTTLI, O.W., and HERMANN, R.B. 1982), the following is a summary of most important definitions of magnitude scales.

Local magnitude, M_L : Corresponds to the logarithm of peak amplitude, in microns, measured on Wood-Anderson seismograph at a distance of 100 km from source and on firm ground. In practice, some corrections are made to this definition to account for the type of instrument, the distance and the site conditions. It is used to represent the size of moderate earthquakes, and it is more closely related to the damaging ground motion than any other magnitude scale. M_L has been used extensively in California, and in general, do not exceed 6.5

Surface wave magnitude, M_S : Corresponds to the logarithm of maximum amplitude of surface waves with 20 sec period. This definition is used to represent the size of large earthquakes. The Richter magnitude is often mixed between M_L and M_S.

Body wave magnitude, M_b : Corresponds to the logarithm of maximum amplitude of P-waves (compressional waves) with 1 sec period. However if the P-waves, in their way to the seismograph, pass through a region of inelastic attenuation, they will be attenuated, and will give a distorted information about the size of the earthquake. To remediate to this problem the body wave magnitude is calculated through the use of the amplitude of 1 sec period higher- mode Rayleigh, L_g, surface waves, that do not penetrate the attenuation

zone, the magnitude is then called m_{bLg}, and is commonly used in ENA.

Moment magnitude, M or M_w : This definition is based on the total elastic strain energy released by the fault rupture, which is directly related to the seismic moment, $M_0 = GAD$, where G is the modulus of rigidity of rock, A the area of fault rupture surface, and D the fault displacement. This magnitude scale definition overcomes the shortcoming of the M_S magnitude to accurately measure the size of very large earthquakes. The M_L magnitude saturates at around 7.0, and the M_S magnitude saturates at around 8.0.

Some empirical relationships exist between these definitions, but should be used with great care. The following are some of these relationships :

1-Hanks and Kanamori (1979, CEA vol. C2, 1990)

2-Purcaru and Berckhemer (1978, CEA vol. C2, 1990)

3-Thatcher and Hanks (1973, CEA vol. C2, 1990)

4-Boore and Atkinson (1987, CEA vol. C2, 1990)

5-Atkinson (1984)

References :

1. ATKINSON, G.M. 1984. Attenuation of strong ground motion in Canada from a random vibrations approach. Bulletin of the Seismological Society of America, 74: 2629-2653.

2. NUTTLI, O.W., and HERMANN, R.B. 1982. Earthquake magnitude scales. ASCE Journal of geotechnical Engineering, vol 108, No GT5, May 1982: 783-786.

Appendix B

DEFINITIONS OF DURATION OF STRONG MOTION

Bracketed Duration

Time between first and last excursions of absolute value of acceleration above some prescribed value (usually 0.05g) (BOLT, B.A. 1973. Duration of strong ground motion. Proceedings of the Fifth World Conference on Earthquake Engineering, Roma. 1, 6-D, paper No. 292).

Fractional Duration

Time between first and last excursions of absolute value of acceleration above some prescribed fraction of peak acceleration (KAWASHIMA, K., and AIZAWA, K. 1989. Bracketed and normalized durations of earthquake ground acceleration. Earthquake Engineering and Structural Dynamics, 18: 1041-1051).

Trifunac-Brady Duration

Time span between arrival of 5% and 95% of the total energy of ground shaking, where the energy is defined as the integral of the squared acceleration for the component of motion of interest (TRIFUNAC, M.D. and BRADY, A.G. 1975. A study of the duration

of strong earthquake ground motion. Bulletin of the Seismological Society of America, 65(3): 581-626).

Vanmarcke-Lai Duration

Time span (D_{VL}) within ground shaking that satisfies the following two conditions:
(i) The computed mean-square acceleration ${\sigma_a}^2$ during D_{VL}, times D_{VL}, equals the total energy for ground shaking.
(ii) The observed PGA is a value calculated to occur once, on the average, for stationary random Gaussian motion with mean-square acceleration ${\sigma_a}^2$ and duration D_{VL} (VANMARCKE, E.H. and LAI, S.P. 1980. Strong-motion duration and RMS amplitude of earthquake records. Bulletin of the Seismological Society of America, 70(4): 1293-1307).

McCann-Shah Duration

Time span bounded by :
(i) upper cutoff time beyond which the derivative of the cumulative root mean square acceleration (RMSA) of the ground motion record is always decreasing; and
(ii) lower cutoff time beyond which the derivative of the cumulative RMSA of the reversed ground motion record is always decreasing (McCANN, M.W. and SHAH, H.C. 1979. Determining strong-motion duration of earthquakes. Bulletin of the Seismological Society of America, 69(4): 1253-1265).

Appendix C

ZERO MEAN VELOCITY BASE LINE CORRECTION COEFFICIENTS

This base line correction technique was proposed by Newmark (1973). The acceleration correction is parabolic over any number of time intervals during the event:

$$a_0(t) = C_1 + C_2(\frac{t - T_1}{T_2}) + C_3(\frac{t - T_1}{T_2})^2, \qquad T_1 < t < T_2 \tag{C.1}$$

where T_1 and T_2, denote the limits of a time interval and $C_k, k = 1, 2, 3$, are constants obtained from the velocity minimization:

$$\frac{\partial}{\partial C_k} \int_{T_1}^{T_2} [v_c(t)]^2 dt = 0 \tag{C.2}$$

where $v_c(t)$ is the corrected velocity record obtained by integrating the corrected record $a_c(t)$.

The last equation leads to the following system of equations:

$$\begin{Bmatrix} C_1 \\ C_2 \\ C_3 \end{Bmatrix} = \begin{bmatrix} -300. & 900. & -630. \\ 1800./\xi & -5760./\xi & 4200./\xi \\ -1890./\xi^2 & 6300./\xi^2 & -4725./\xi^2 \end{bmatrix} \begin{Bmatrix} A_1 + (v_c(T_1) - v(T_1))/(2\Delta T) \\ A_2 + (v_c(T_1) - v(T_1))/(3\Delta T) \\ A_3 + (v_c(T_1) - v(T_1))/(4\Delta T) \end{Bmatrix} \tag{C.3}$$

where $\xi = \frac{\Delta T}{T_2}; \Delta T = T_2 - T_1$; and A_1, A_2, and A_3 are defined as

$$A_1 = \frac{1}{(\Delta T)^3}\int_0^{\Delta T} v(\tau + T_1)\tau\, d\tau$$
$$A_2 = \frac{1}{(\Delta T)^4}\int_0^{\Delta T} v(\tau + T_1)\tau^2\, d\tau \qquad \text{(C.4)}$$
$$A_3 = \frac{1}{(\Delta T)^5}\int_0^{\Delta T} v(\tau + T_1)\tau^3\, d\tau$$

In these equations $v(t)$ is the uncorrected velocity record obtained by direct integration of the uncorrected acceleration record $a(t)$. It is assumed that both the corrected and uncorrected acceleration, vary linearly over each time step of the original acceleration record. This is not exact for the corrected acceleration record (because of the parabolic variation of the correction in time), but it is assumed that the time step of the acceleration history is small enough for the error to be insignificant.

Reference : Base line correction. ABAQUS user's manual, Vol. V. pp 4.8. 1992. Hibbitt, Karlsson, and Sorensen, Inc.